

Founded 1925

Incorporated
by Royal Charter 1961*To promote the advancement
of radio, electronics and kindred
subjects by the exchange of
information in these branches
of engineering*

The Radio and Electronic Engineer

The Journal of the Institution of Electronic and Radio Engineers

The Future of Broadcasting

IN April 1970, the British Government proposed to set up a Committee under the Chairmanship of Lord Annan to enquire into the future of broadcasting, but because of a change of Government, the Committee was not appointed. A Committee has now been formed under the Chairmanship of Lord Annan and has invited, by public advertisements, '... views on present and future broadcasting services in the United Kingdom'.

The terms of the request are presumed to encourage expression of opinion on (1) programme content, (2) political control of broadcasting services and, hopefully, (3) appraisal of the technical facilities which would give viewers and listeners freedom to see or hear 'on the spot' events which concern and influence our world.

Public comment will probably concentrate on aesthetic considerations associated with programme content; the National Electronics Council will, no doubt, focus attention on the desirability of meeting and indeed anticipating consumer needs by providing visual displays on domestic buying, metering services and facilities for easy switching of audio and visual communication and broadcasting—in short, the maximum use of radio and electronics for the benefit of the public at large.

Control of broadcasting services is largely a matter for empirical decision. The 1974 Labour Party document 'The People and the Media' evokes wider arguments: the radio and electronic engineer will however deplore that the sections proposing a 'Communications Council', a 'Broadcasting Commission' and control of transmission facilities, reveal an absence of competent technical advice. Just thirty years ago the Institution advocated the permanent appointment of a Communications Commission with special responsibility for allocating radio frequencies. The Institution's Post-war report also urged greater use of cable systems which is only cautiously touched on in the Labour Party report.

The Annan Committee comprises fourteen members who can be expected to comment with varying degrees of authority on the programme and political aspects, but only one member qualified to express opinion on the technical possibilities which will greatly affect the whole future of broadcasting. Just as 'the man who never made a mistake never made anything', so too do we not expect infallibility from this new Committee: we hope however that sight will not be lost of the wider horizons made possible by present and future technical innovations. For example, post-war decisions on the technical development of broadcasting based on recommendations of the 1943 Television Committee were controversial to say the least. The retention of pre-war television standards may have facilitated earlier resumption of transmissions but the delay that immediate adoption of higher definition standards would have caused, could surely have been borne by both the public and industry. Hence higher definition did not arrive until 1964.

A certain reluctance to grasp the possibilities of cable television was seen in the report of the Pilkington Committee in 1962, and this is now clearly one of the most important current political/technical issues in television. The experience gained in cable television over the past decade has been in spite of 'Pilkington' discouragement and some of its potentialities have been examined in this and other journals over the past decade.

Engineers have responsibilities which extend beyond their technical expertise. The pattern of broadcasting in this country in the future—perhaps for the remainder of this century or even longer—will depend to a great extent on the technical facilities that engineers can make. The consumer has the right to know about such present and possible future services even if for good economic or political reasons he is denied the opportunity to support innovations and wider choice of broadcasting services.

For this reason it would seem that a frank examination by experts of the present and future means of broadcasting and receiving precedes any review of how these services are to be used or controlled.

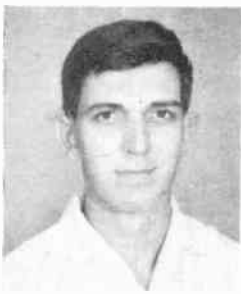
G. D. C.

Contributors to this issue



Professor Peter N. Robson received the B.A. degree in mechanical sciences from the University of Cambridge in 1953 and the Ph. D. in electrical engineering from the University of Sheffield in 1963. He worked from 1949 to 1951 and from 1953 to 1957 with Metropolitan Vickers Ltd., Manchester, latterly on the design of their microwave linear electron accelerators. Between 1957 and 1966 he was a Lecturer and later Senior

Lecturer and Reader in the Department of Electronic and Electrical Engineering, University of Sheffield. He spent a sabbatical year, 1966-67, as Research Associate at the Microwave Laboratory, Stanford University, California, from 1967 to 1968 he was Reader in Electronics at University College London, and he returned to Sheffield as Professor in 1968.



Mr. Michel Passot prepared for his examinations for Engineer Schools at the Lycée St. Louis in Paris and in 1965 entered the Ecole Centrale Lyonnaise. As a finalist in 1968 he submitted a thesis on a d.c. linear motor with variable reluctance. He continued his academic studies with Department of Electronic and Electrical Engineering at Loughborough University of Technology and after his first year obtained a

grant from the British Post Office to carry out research on the subject: 'Study of delta modulation by Hermite polynomials' towards a Master's degree. Mr. Passot left Loughborough in 1970 to do his military service and submitted his thesis in May 1973. Since May 1972 he has been with Compagnie Electro-Mécanique.



Mr. Raymond Steele completed his Higher National Certificate in electrical engineering and an apprenticeship in radio engineering at E. K. Cole Ltd., Southend-on-Sea in 1955 and for the next four years studied at King's College, University of Durham, where he obtained a degree in electrical engineering. He returned to E. K. Cole for two years as a research engineer, and then joined Cossor Radar and

Electronics of Harlow, Essex as a development engineer on radar displays. In 1962 he went to the Aeronautical Division of the Marconi Company at Basildon, Essex, as a research and development engineer. Mr. Steele entered the teaching profession in 1965 as a Lecturer at the Royal Naval College, Greenwich and since 1968 he has been at Loughborough University where he is a Senior Lecturer in the Department of Electronic and Electrical Engineering and a member of the Department's digital communications research group. His research activities in delta modulation systems started in 1966 and he has been the author or co-author of 10 papers on this subject. A book entitled 'Delta Modulation Systems' has just been published.



Mr. Alban Harrison (Fellow 1964, Member 1959) graduated with a B.Sc. degree from London University in 1939 and in 1940 joined the wartime Scientific Civil Service at the Establishment at Christchurch which moved later to Malvern and is now the Royal Radar Establishment. He spent the next seven years on development and field testing of military radar. In 1947 Mr. Harrison became Deputy Chief Engineer of the newly

formed radar development department of Henry Hughes and Son, now the Kelvin Hughes Division of Smiths Industries Limited; his present position is Chief Scientist (Radar) with the company. He has numerous published papers and patents concerned with radar and radar beacons to his credit. Mr. Harrison has served on the IERE Aerospace, Maritime and Military Systems Group Committee since its formation in 1960 as well as on organizing committees of several joint conferences in the field of ocean technology and marine navigational aids. He has been a member of various U.K. Government committees and working groups for marine radar and of working groups of IMCO Sub-committee on Safety of Navigation,



Professor Branko D. Rakovich received his bachelor's and doctor's degrees from the University of Belgrade in 1948 and 1955 respectively. From 1948 to 1951 he served as a research assistant at the Institute for Telecommunications of the Serbian Academy of Science, Belgrade. He then joined the Faculty of Electrical Engineering at the University of Belgrade as a teaching assistant until 1954 when he became an

assistant professor. From 1954 to 1955 he held a National Education and Research Council of Yugoslavia Fellowship at Marconi College, Chelmsford. In 1959 he was appointed an associate professor of electronics and later a full professor of electrical engineering. Currently he is also the Head of the Department of Electronics of the Faculty of Electrical Engineering, University of Belgrade. His research interests lie in the field of active and passive network synthesis particularly in wide-band amplifier theory and design.



Mr. Vidosav Stojanovich received the Dipl. Eng. and M.S. degrees from the University of Nish in 1965 and 1972 respectively. He is at present studying for his Ph. D. in the Department of Electronics of the Faculty of Electrical Engineering, University of Belgrade. Since 1962 he has been a Teaching Assistant in the Department of Electronics, University of Nish.

See also page 532.

Waveform shaping techniques for the design of signal sources

C. J. PAULL, B.Sc.(Eng.), Ph.D.*

and

W. A. EVANS, M.Sc., M.Inst.P., C.Eng., M.I.E.E. †

SUMMARY

A new circuit technique is described for the generation of a sinusoid from a triangle waveform based on the addition of suitably proportioned current trapezoids. Undesirable operating characteristics, particularly peak and crossover distortion associated with previously reported methods, are reduced to more tolerable levels in a fully temperature-compensated design. An optimum breakpoint and distortion analysis is developed for establishing the design method and estimating the performance of the circuit. Measurements made on the prototypes indicate that a total harmonic distortion of better than 0.2% is readily attainable, whilst the non-saturating transistor circuit design offers considerable potential at high frequencies. The technique is readily amenable to the thick-film process with the modest spread of resistor values, and the absence of any tedious setting-up procedure makes the circuit particularly attractive to the user.

* Department of Electrical and Electronic Engineering, University of Nottingham, Nottingham NG7 2RD.

† Department of Electrical and Electronic Engineering, University College of Swansea, University of Wales, Singleton Park, Swansea SA2 8PP.

List of Principal Symbols

| | |
|------------------|---|
| $V_{n1,2}$ | source voltages (d.c.) |
| V_i, V_o | peak amplitudes of input triangle and output sinusoidal waves respectively |
| v_i, v_o | instantaneous values of input and output signals |
| $V_{0(k)}^s$ | peak signal output from the k th trapezoidal waveform generator |
| $v_{0(k)}^s$ | instantaneous value as above |
| $R_{c(k)}$ | current source resistor as above |
| $R_{e(k)}$ | emitter resistor as above |
| $\alpha_{(k)}^s$ | slope of the k th trapezoid |
| $a_{(k)}^s$ | amplitude of k th trapezoid |
| r | number of segments in approximation |
| s | number of trapezoids or number of parallel branches in the diode-resistor array |

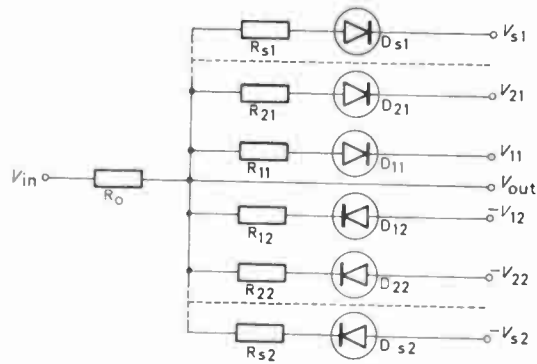
1 Introduction

In the last decade signal source design has made rapid advances reflecting the enormous strides that have taken place in the component technologies and associated electronic disciplines. The laboratory or bench oscillator based on simple, but effective, RC or LC circuits has given way to the more sophisticated function generator supplying at least sine, square and triangle waveforms over many decades of frequency (from 10^{-4} to 10^7 Hz). Remote programming may be included allowing the generator to be readily controlled from a computer. This necessitates a form of anti-bounce circuitry to maintain amplitude integrity under programmed frequency control, which essentially precludes the use of bridge or phase shift networks. It is only in those specialist areas requiring, for example, low distortion outputs of better than 0.1% total harmonic distortion that the bridge oscillator has maintained its supremacy, and even here there are indications that the function generator with an integral tracking filter is beginning to compete on not unfavourable terms. This latter development is likely to hasten the demise of the bridge oscillator for many applications, since in other departments the function generator is acknowledged as a superior instrument.

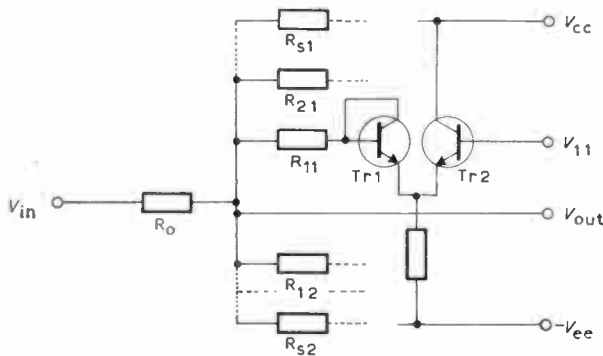
This paper concentrates on one aspect of function generator design indispensable to the performance of the instrument as a source of sinewaves, i.e. the generation of sinusoids from triangle waves using piecewise linear approximation techniques. A new method is described whose performance is analysed and assessed in relation to other known methods. The results obtained demonstrate that the new method based on the summation of current trapezoids compares very favourably with diode shapers currently in popular use.

2 Diode Shaping Networks

The basic network structure for a multiple segment approximation to a sinusoid is shown in Fig. 1(a). Diodes D_{11} to D_{s1} shape the positive, and D_{12} to D_{s2} shape the negative half cycle. It is clear that for waveform symmetry about zero the following relationships must be established: $R_{11} = R_{12}$; $R_{21} = R_{22}$ etc., and $|V_{11}| = |V_{12}|$; $|V_{21}| = |V_{22}|$ etc. The transfer characteristic of



(a) Basic diode shaping network



(b) Possible method for temperature compensation

Fig. 1

the network will be dependent on the number of diodes conducting and this may, in turn, be related to the source voltage. Where the slope of the triangular input waveform is normalized to unity, the conducting diodes and their associated resistors reduce the slope of the output in the ratio $Y_0/(Y_n + Y_0)$ where

$$Y_n = 1/R_{11} + 1/R_{21} + \dots + 1/R_{n1}$$

and

$$Y_0 = 1/R_0 \quad n \text{ diodes conducting.}$$

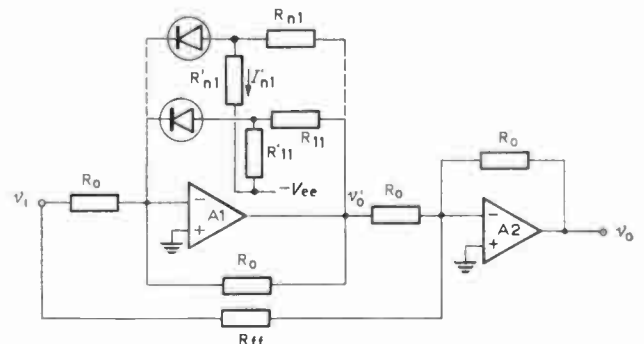
Adjustment of Y_n at each breakpoint, or the point at which a diode just begins to conduct, allows the total waveshape to be synthesized. The optimum location of the breakpoints has been the subject of a number of papers by Burt and Lange,¹ Aird and Court² and others. Appendix 1 details one method based on the work published by Barnes³ which has been shown to yield near optimum distortion figures. A particularly economical method of calculating distortion for a linear segment approximation waveform is developed in Appendix 2 and the results are summarized in Table 1 along with the abscissae and ordinates of the breakpoints to which they apply.

In practice, where the physical circuit fails to give the expected performance, it is usually the imperfectly matched $I-V$ characteristics of the individual diodes which are suspect. Silicon diodes have a typical forward voltage drop of 0.75 V with a temperature coefficient of -2.2 mV/degC . This offset voltage and the current dependent internal resistance of each diode may be

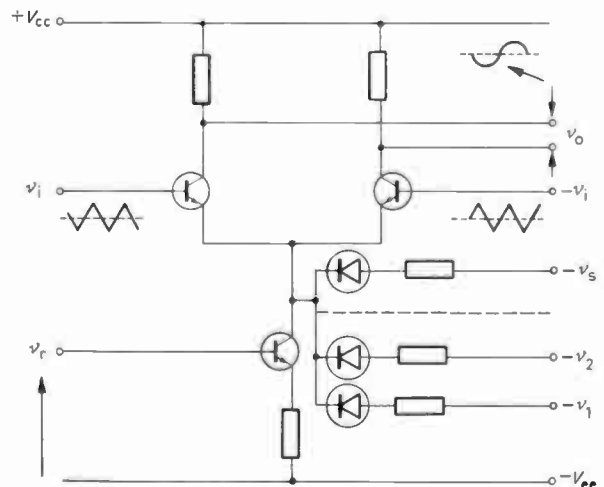
allowed for in the basic design, but individual variations can be expected to be troublesome. The negative temperature coefficient results in some increase in distortion, principally third harmonic, with the output becoming slightly 'peaked' or 'flattened'. Figure 1(b) shows how temperature effects may be compensated by replacing the diode in each series arm with a transistor. The V_{be} drop in Tr2 is now compensated by that of the corresponding transistor Tr2 in the voltage reference determining circuit. Temperature compensation is thus achieved, but incurs the penalty of increased circuit complexity.

In addition to the above, diode shapers are also known to be deficient in the following respects:

- (i) 'Spiking' at the output due to diode charge storage. This effect, which is most noticeable at the higher frequencies, can only be reduced by using faster, lower capacitance devices. Moderately low-cost Schottky diodes are now generally available, and these are becoming accepted as one solution to this problem, since they exhibit significantly lower capacitances and charge storage for a given forward current rating.
- (ii) Second-harmonic distortion arising from a lack of symmetry in the two halves of the shaper. The problem



(a) Diode feedback network



(b) Modified shaping system

Fig. 2

Table 1. Quarter cycle linear segment approximation (unrestricted)

| Number of Segments <i>r</i> | Maximum Departure <i>0</i> | Harmonic Content % of fundamental | Segment Number <i>k</i> | Abscissa of Breakpoint x^r_k | Ordinate of Breakpoint y^r_k |
|--------------------------------|-------------------------------|-----------------------------------|---|--|--|
| 1 | 0.1382 | 11.18 | 1 | 1.5708 | 1.138 |
| 2 | 0.0274 | 2.35 | 1 | 0.8846 1.5708 | 0.8011 1.0275 |
| 3 | 0.0114 | 0.98 | 1 2 3 | 0.6546 1.1383 1.5708 | 0.6202 0.9193 1.0114 |
| 4 | 0.0061 | 0.525 | 1 2 3 4 | 0.5326 0.9191 1.2539 1.5708 | 0.5140 0.8013 0.9564 1.0062 |
| 5 | 0.0039 | 0.33 | 1 2 3 4 5 | 0.4552 0.7825 1.0618 1.3205 1.5708 | 0.4435 0.7089 0.8771 0.9727 1.0039 |
| 6 | 0.0027 | 0.22 | 1 2 3 4 5 6 | 0.4010 0.6876 0.9302 1.1524 1.3639 1.5708 | 0.3929 0.6374 0.8044 0.9164 0.9814 1.0027 |
| 7 | 0.0019 | 0.12 | 1 2 3 4 5 6 7 | 0.3604 0.6172 0.8333 1.0298 1.2152 1.3944 1.5708 | 0.3546 0.5807 0.7421 0.8591 0.9394 0.9864 1.0019 |
| 8 | 0.0015 | 0.08 | 1 2 3 4 5 6 7 8 | 0.3288 0.5625 0.7584 0.9357 1.1020 1.2616 1.4172 1.5708 | 0.3244 0.5347 0.6892 0.8064 0.8936 0.9540 0.9897 1.0015 |
| 9 | 0.0012 | 0.06 | 1 2 3 4 5 6 7 8 9 | 0.3034 0.5185 0.6984 0.8607 1.0122 1.1569 1.2971 1.4346 1.5708 | 0.3000 0.4968 0.6442 0.7595 0.8492 0.9168 0.9640 0.9919 1.0012 |

is again one of matching of components or, alternatively, the inclusion of variable elements to compensate the naturally arising degree of unbalance. Some interaction between the variables is to be expected, and this complicates the adoption of any formalized adjustment procedure in a production or service environment.

(iii) An abrupt discontinuity in slope at the peak of the sinusoid. Using the basic resistor-diode network, the particular diode associated with the uppermost breakpoint must have nearly infinite conductance if a 'flat top' is to be realized. Whilst this is not practically feasible, the injection of a small anti-phase triangular signal at a later stage can substantially correct for this defect.

This latter aspect of function generation is well illustrated by the circuit of Fig. 2(a). In this arrangement the resistor-diode array is included within the feedback loop of an operational amplifier such that the positive

half wave response at v'_0 will be similar to that of the basic circuit Fig. 1(a), provided that:

$$R'_{n1} = \frac{(V_{ec} + V_d)R_{n1}}{V_{n1}} \quad \text{where } n = 1, 2, \dots, s$$

$V_d = \text{diode voltage}$

Clearly this eliminates the necessity for a chain of voltage sources V_{n1} but it equally ensures that the slope at v'_0 cannot realistically approach zero without I'_{n1} becoming excessive. The feed forward of the anti-phase triangle wave to A_2 via R_{ff} can, however, be so arranged as to provide the requisite degree of slope cancellation at v_0 .

2.1 Modified Diode Shaping System

In an attempt to overcome some of the disadvantages alluded to above, Klein and Hagenbeuk⁴ have proposed an alternative scheme shown in somewhat simplified form in Fig. 2(b). In this circuit, the resistor-diode array and

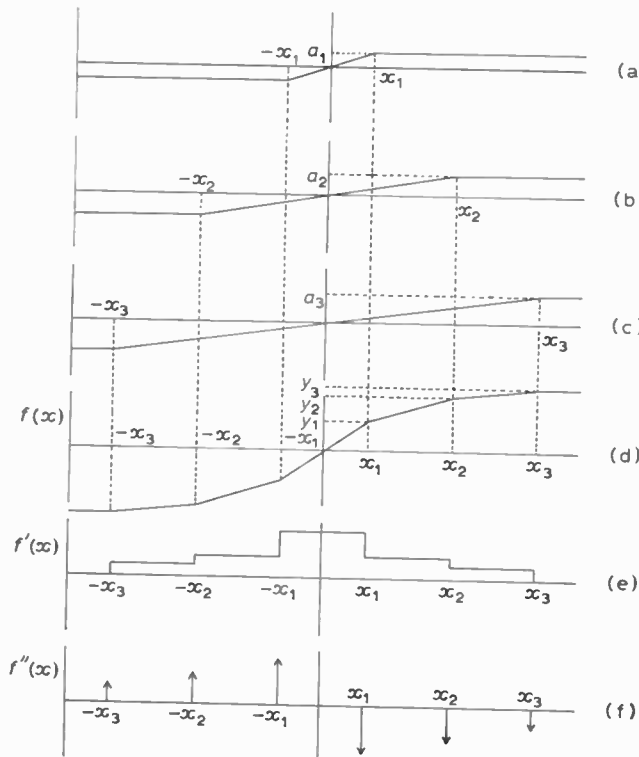


Fig. 3. Schematic of synthesis of linear approximation waveform from three trapezoids.

the differential pair of transistors together supply the demand of the current sink transistor. The triangle waveforms injected in anti-phase into the base inputs of the differential pair of transistors are of the order of a few volts, so that only one device will conduct during the greater part of each half cycle. Essentially, the circuit behaves as a switched emitter follower. Assuming the emitter follows the base perfectly and, further, that the conductance in the emitter lead can be varied as $\cos(\pi v_i/2V_p)$ where V_p and v_i are, respectively, the peak and instantaneous values of the input signal, then the collector current will vary as a sine function. Whereas the individual collector voltage waveforms resemble half-wave rectified sinusoids in phase opposition, the complete sinusoid is available as the differential collector output. To establish a cosine law of conductance in the common emitter connexion, it is necessary to provide for diode turn-off with increasing input voltage, and this implies that the diode polarity is reversed. The current sink is necessary to provide a standing bias current without which the circuit could not operate.

Apart from savings in circuit complexity, the use of one shaping network for both positive and negative half-cycles contributes substantially to the reduction of second harmonic distortion. A flat top to the output sinusoid is also available since this is associated with zero conductance, a condition very closely approximated when all the silicon diodes are reverse biased. Imperfect emitter follower action remains a source of distortion; this may be minimized using additional active devices connected in the super-alpha type of configuration. Precision in-phase and anti-phase triangular inputs are required,

and another significant limitation of the circuit shown in Fig. 2(b) is its sensitivity to crossover distortion where I_c , the sink current, is either too large or too small. This type of distortion can be particularly troublesome in many applications.

3 Summation of Trapezoids

The manner in which a sinusoid may be synthesized by the summation of suitably proportioned trapezoids is illustrated for a four-segment quarter cycle approximation in Fig. 3(d). This particular piecewise linear approximation may be reduced to three trapezoids having the proportions shown in Fig. 3(a, b, c). The top segment now has zero slope, and this affects the optimum breakpoint locations as calculated by the chordal approximation method. The necessary modifications to the theory are given in Appendix 1.

It is possible to derive the height or amplitude of each trapezoid a_k in addition to the slope α_k by first establishing a relation for the slope when only one trapezoid is contributing. The value of s represents the number of trapezoids in the approximation and k takes on integral values. In the case of Fig. 3, the slope on the side of the third trapezoid (c) fixes the slope of the total approximation between x_2 and x_3 such that

$$\alpha_3 = \frac{(y_3 - y_2)}{(x_3 - x_2)}$$

Similarly, the slope of the total approximation between first and second breakpoints is given by

$$\frac{(y_2 - y_1)}{(x_2 - x_1)}$$

when both (b) and (c) trapezoids are contributing to the total output. The slope of the second trapezoid alone is given by

$$\alpha_2 = \frac{(y_2 - y_1)}{(x_2 - x_1)} - \alpha_3$$

For the general case, the slope of the total approximation between the $(k-1)$ th and k th breakpoints in an approximation containing s trapezoids is given by

$$\frac{(y_k - y_{k-1})}{(x_k - x_{k-1})} = \alpha_k^s + \frac{(y_{k+1} - y_k)}{(x_{k+1} - x_k)}$$

where

$$y_0 = x_0 = 0$$

$$1 \leq k \leq s$$

$$a_k^s = x_k^s \cdot \alpha_k^s$$

3.1 The Trapezoid Generator

The basic circuit employed to generate a trapezoid of arbitrary dimensions is shown in Fig. 4. Transistors Tr1 and Tr2 form a differential pair with emitter degeneration resistors R_e . The combination of Tr3, R_e and the reference voltage source V_r provide a current sink to the differential pair with a restriction on the current I_c such that

$$I_c = \frac{V_r - V_{be}}{R_e}$$

and this leads to a symmetrical clipping action at the

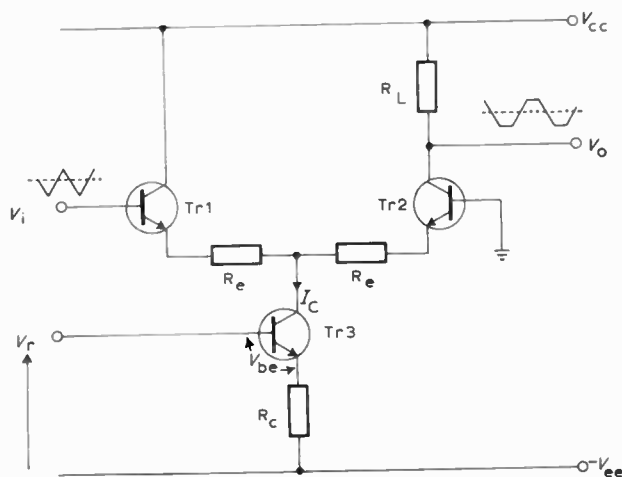


Fig. 4. Trapezoid generator.

output, so that for a triangular input, a well defined trapezoidal waveform may be generated.⁵ To define the breakpoints of this trapezoid the three ranges of v_i must be taken into account in defining the trapezoid:

(a) Tr2 cut off

$$\text{Input voltage } v_i > R_c I_c$$

$$\text{Output voltage } v_o = V_{cc} \quad (3)$$

(b) Tr1 and Tr2 conducting:

$$\text{Input voltage } -R_c I_c \leq v_i \leq R_c I_c$$

$$\text{Output voltage } v_o = V_{cc} - \frac{I_c R_L}{2} + \frac{v_i R_L}{2R_c} \quad (4)$$

(c) Tr1 cut off

$$\text{Input voltage } v_i < -R_c I_c$$

$$\text{Output voltage } v_o = V_{cc} - I_c R_L \quad (5)$$

In practice, some rounding of the corners of the trapezoid will occur, principally due to the reduction in V_{be} as the device current approaches zero; nevertheless, this is subjectively very slight for large-signal operation and may be considered advantageous since it tends to reduce rather than increase total harmonic distortion, when approximating a function with a continuous first derivative, e.g. sine, cosine.

To synthesize a complete sinusoid the number of these circuit elements utilized must correspond to the number of trapezoids s selected for the desired approximation. The bases of the input transistors are all driven in parallel from a low impedance source, whilst the collectors of the output transistors feed a single resistor R_L that develops an output voltage proportional to the sum of outgoing currents. Expressions for the resistor values R_c and R_e for each shaper unit may be established from a knowledge of the respective trapezoidal slopes α , amplitudes a and peak voltage excursions at the input V_i and output V_o respectively.

If the number of trapezoids selected as part of the design specification is s , the slope of the k th trapezoid is obtained by taking the differential of equation (4) and

normalizing:

$$\frac{V_i}{V_o} \cdot \frac{dv_{o(k)}^s}{dv_i} = \frac{V_i}{V_o} \cdot \frac{R_L}{2R_{c(k)}^s} = \alpha_k^s \cdot \frac{\pi}{2} \quad (6)$$

From equations (3) and (5) the relative trapezoidal amplitudes $V_{o(k)}^s$ are given by

$$\frac{V_{o(k)}^s}{V_o} = \frac{I_{c(k)}^s \cdot R_L}{2V_o} = a_k^s \quad (7)$$

where

$$\sum_{k=1}^s a_k^s = 1 \quad \text{and} \quad \sum_{k=1}^s I_{c(k)}^s = I_t$$

Using these equations, all the resistor values may be calculated for a given I_t .

$$R_L = \frac{2V_o}{I_t}; \quad R_{c(k)}^s = \frac{[V_r - V_{be}]}{a_k \cdot I_t}, \quad R_{e(k)}^s = \frac{2}{\pi} \frac{V_i}{\alpha_k^s \cdot I_t} \quad (8)$$

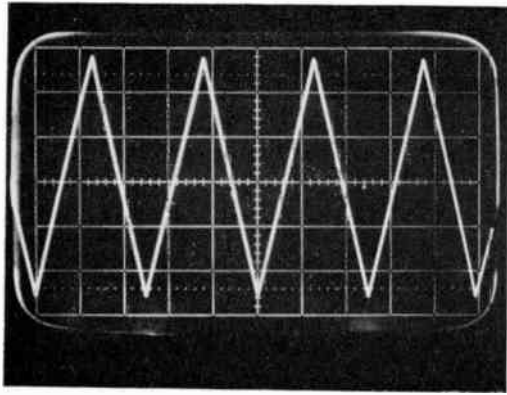
3.2 The Circuit Realization

The circuit diagram for a complete shaper unit is shown in Fig. 5. In this circuit overall temperature compensation of the current sources has been achieved by the addition of the complementary device Tr4. To a first approximation the base-emitter forward bias voltage V_{be} will also be eliminated from equation (8) thereby simplifying the calculations for $R_{c(k)}^s$. An exact analysis would have to take account of the variation in base-emitter voltage with collector current since

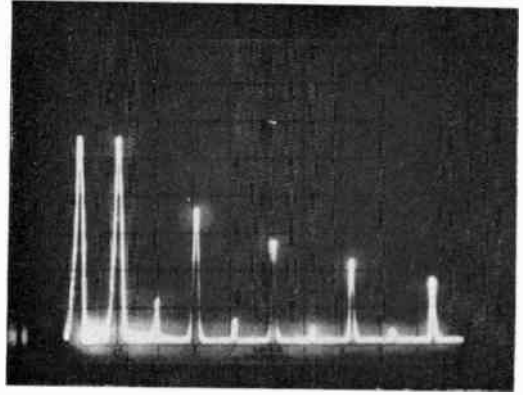
$$I_c \approx I_e = I_{es}^{-1} \exp(V_{be}q/KT)$$

I_{es} being the emitter reverse saturation current, q the electronic charge and K Boltzmann's constant. The range of I_c for an eight-segment approximation corresponds to a variation in V_{be} of about 45 mV, and this is small by comparison with a typical V_r of 5 V. Nevertheless, an increase in distortion is detectable ($\sim 0.15\%$) and this may be eliminated by a small adjustment ($\sim 0.5\%$) to the nominal values for $R_{c(k)}^s$. It has been found, in practice, that high stability resistors of $\sim 0.5\%$ tolerance provide a near optimum compromise between cost and performance for a majority of applications, and this should ensure that the measured distortion figures do not greatly exceed the theoretical values.

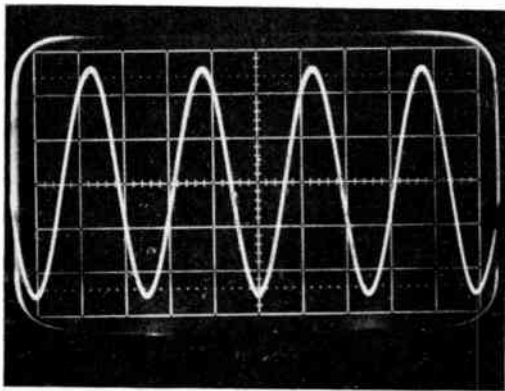
In the selection of a suitable transistor, the three most important parameters are the base-emitter voltage V_{be} spread, the large signal current gain h_{FE} , and the reverse breakdown voltage of the base-emitter junction V_{EBO} . For any two transistors in a differential pair, imperfect matching for V_{be} gives rise to the same effect as a d.c. offset present at the input, that is, the generation of even harmonics at the output. However, by using a 10 V peak-to-peak triangle wave input, it has been found that up to 30 mV mismatch can be tolerated without significantly affecting the purity of the resulting sinewave. Individual variations in h_{FE} produce errors in proportion to the change in base current as a fraction of the total emitter current. Using transistors with a high h_{FE} thus eliminates the need for selection, since the base current is then comparatively negligible. Finally, V_{EBO} must be large enough to prevent reverse breakdown of the base-emitter junction. Specifying V_{EBO} as greater than 4 V is



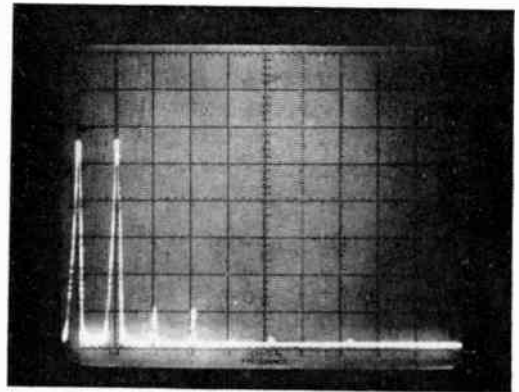
(a)



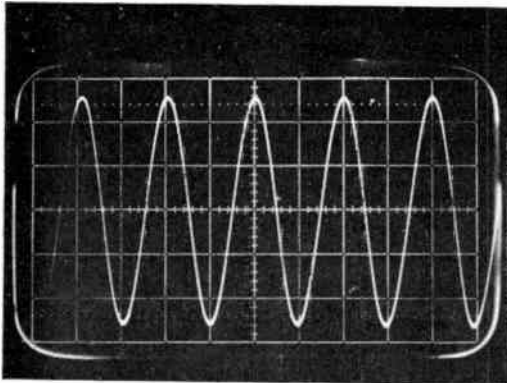
(b)



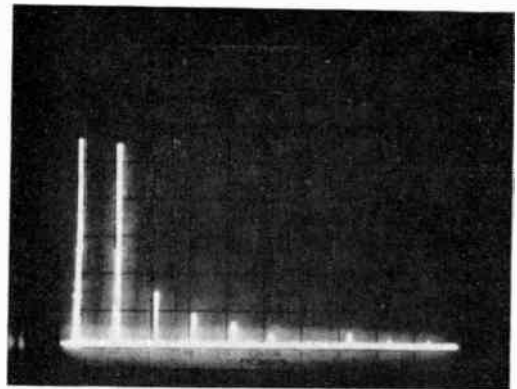
(c)



(d)



(e)



(f)

Fig. 6. Time and frequency domain analysis of prototype waveforms

Scales: (a, c) Vertical: 2 V/div
Horizontal: 20 μ s/div

(b, d) Vertical: 10 dBm/div
Horizontal: 20 kHz/div
Marker at 1 kHz
Bandwidth 0.1 kHz

(e) Vertical: 2 V/div
Horizontal: 100 ns/div

(f) Vertical: 10 dBm/div
Horizontal: 5 MHz/div
Marker at 1 MHz
Bandwidth 30 kHz

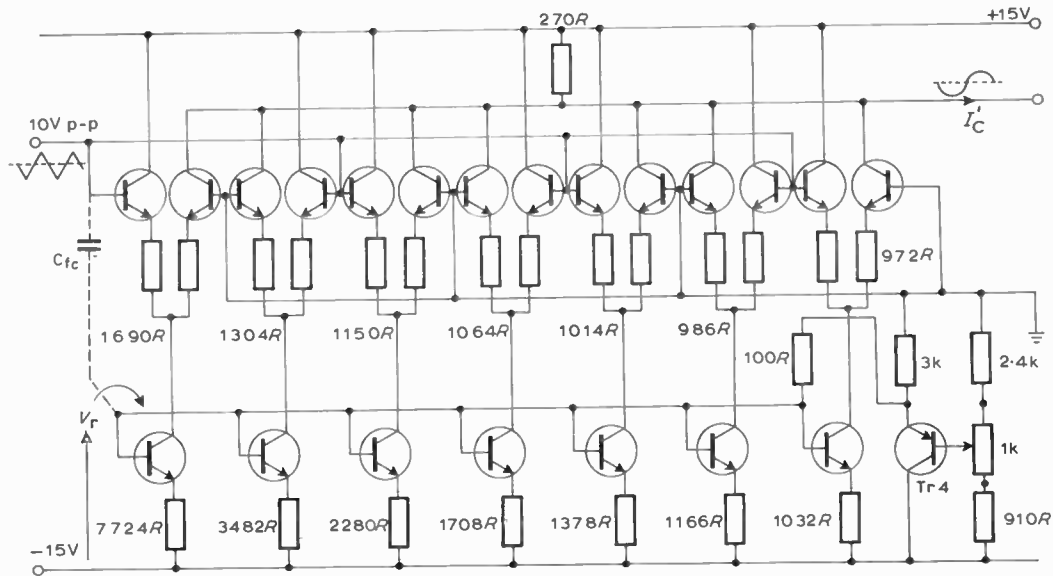


Fig. 5. Triangle to sine shaper unit.

(Note: all resistors $\frac{1}{2}\% \frac{1}{2}$ W metal film; all transistors MPS 6522 (p-n-p), MPS 6520 (n-p-n)

sufficient to provide protection against this breakdown mechanism in the circuit of Fig. 5. Under test, this circuit successfully synthesized a sinusoidal waveshape with a total distortion measured at 0.15% at audio frequencies compared with the theoretical value of 0.11% (see Table 2), using preselected resistors within the specified tolerance. Temperature stability was excellent and the layout reasonably non-critical. The distortion reaches 0.3% at 100 kHz and continues the upward trend as frequency is increased.

A complete picture of the practical performance is obtained from observations on the prototype waveforms in both time and frequency domains. Figure 6 (a, b, c and d) have been taken at 20 kHz and demonstrate the equivalent filter action of the shaper on the triangle wave input. Even to the discerning eye the time domain waveforms appear quite distortionless, yet a spectral analysis demonstrates even harmonic contamination of the basic triangle wave. In the case of the sinusoid output no harmonic is within 40 dBm of the fundamental though even and odd harmonics are present. These results serve to emphasize the need for spectral analysis of the waveforms at these distortion levels, particularly when specifying such circuits for signal sources.

The increase in distortion may, in part, be attributable to the base-emitter capacitance C_{be} of T_{r1} in Fig. 4. Where dv_i/dt is negative and the base-emitter junction is also reverse biased, the current flowing in R_1 is approximately $I_c + C_{be}(dv_i/dt)$. Alternatively for positive dv_i/dt the current becomes $I_c - C_{be} dv_i/dt$. To counteract this effect an additional capacitor, C_{fc} ($\sim 5pF$) may be inserted as shown in Fig. 5. A controlled disturbance affecting each current sink in this case tends to neutralize the unwanted capacitance feedthrough from input to output.

The useful frequency range may be considerably extended by simply scaling down the resistance values to

give higher current operation, whilst selecting a transistor having a geometry designed to minimize inter-electrode capacitances as well as maintaining the forward current gain at higher current levels. A prototype was constructed based on the above using scaled ($\times 0.5$) component values shown in Fig. 5 which operated satisfactorily up to the limit of the available triangle generator at 5 MHz using a layout specially designed to minimize series inductance in the base connexion, which can otherwise lead to parasitic oscillation in a high performance circuit of this nature. Figure 6(e, f) shows an example of operation at these frequencies. There is some suggestion of increase in harmonic distortion but still insufficient to be discernable in the time waveform.

Since the common collector resistor R_L is referenced to the positive supply, it is usually desirable to eliminate the resulting d.c. offset on the signal within the design of a power output amplifier which may typically provide a 10 V peak to peak maximum output when matched into a 50 Ω load. Alternatively, R_L may be replaced by a current summing operational amplifier with variable current biasing and a gain control potentiometer connected in the feedback loop. In this way the signal offset and signal amplitude can be adjusted independently of each other; an additional feature which can be useful in certain applications.

3.3 Advantages

The relative advantages of the trapezoidal approximation technique may be summarized as:

(i) Fully temperature compensated design showing no detectable increase in distortion when temperature cycled over an ambient temperature range of $0^\circ \leq T \leq 50^\circ C$.

(ii) The particularly good high-frequency performance of the circuit may be attributed to the use of current rather than voltage switching techniques. Each dif-

Table 2. Quarter cycle linear segment approximation (trapezoidal)

| Number of Segments | Maximum Departure | Harmonic Content % of fundamental | Segment Number | Abscissa of Breakpoint | Ordinate of Breakpoint |
|--------------------|-------------------|-----------------------------------|---|--|--|
| r | 0 | | k | x_k^r | y_k^r |
| 1 | - | - | - | - | - |
| 2 | 0.0525 | 4.44 | 1 2 | 1.1084 1.5708 | 0.9475 0.9475 |
| 3 | 0.0168 | 1.44 | 1 2 3 | 0.7481 1.3105 1.5708 | 0.6971 0.9831 0.9831 |
| 4 | 0.0082 | 0.70 | 1 2 3 4 | 0.5858 1.0140 1.3895 1.5708 | 0.5611 0.8572 0.9918 0.9918 |
| 5 | 0.0048 | 0.41 | 1 2 3 4 5 | 0.4901 0.8439 1.1477 1.4316 1.5708 | 0.4755 0.7520 0.9166 0.9951 0.9951 |
| 6 | 0.0032 | 0.27 | 1 2 3 4 5 6 | 0.4259 0.7312 0.9905 1.2291 1.4579 1.5708 | 0.4163 0.6710 0.8395 0.9454 0.9968 0.9968 |
| 7 | 0.0023 | 0.17 | 1 2 3 4 5 6 7 | 0.3794 0.6500 0.8784 1.0867 1.2841 1.4758 1.5708 | 0.3727 0.6075 0.7720 0.8874 0.9615 0.9978 0.9978 |
| 8 | 0.0017 | 0.11 | 1 2 3 4 5 6 7 8 | 0.3437 0.5883 0.7936 0.9799 1.1551 1.3237 1.4888 1.5708 | 0.3387 0.5566 0.7148 0.8321 0.9165 0.9713 0.9983 0.9983 |
| 9 | 0.0013 | 0.07 | 1 2 3 4 5 6 7 8 9 | 0.3155 0.5394 0.7269 0.8962 1.0547 1.2063 1.3537 1.4987 1.5708 | 0.3116 0.5149 0.6658 0.7822 0.8711 0.9356 0.9778 0.9987 0.9987 |

ferentially connected pair of transistors functions as a non-saturating current switch at the boundaries of the linear region.

(iii) A minimum of adjustment is required. One variable resistor sets the signal amplitude level for least distortion. Comparatively large variations in the amplitude of the triangle wave can be satisfactorily accommodated by adjusting this one component.

(iv) No crossover distortion. All sections of the circuit are operating in their linear regions when the input voltage passes through zero. Similarly, the peak of the sinusoid is not marked by an abrupt change of slope or 'spiking' at the output.

(v) Low sensitivity to even harmonic distortion. Even harmonic distortion can only result from V_{be} variations or mismatched emitter resistors.

(vi) Suitable for thin or thick film integration. The limited spread in resistor values combined with duplication of the individual sections makes the circuit ideal for integration where the production volume is sufficient to justify the initial tooling costs.

3.4 Results of Computer Studies

Tables 1 and 2 summarize the results obtained for a sinusoid having up to nine breakpoints in a quarter cycle approximation. The breakpoint analysis method is given in Appendix 1, and the harmonic analysis in Appendix 2 respectively.

The abscissae and ordinates given in Table 1 are generally in accord with the findings of Barnes³ who published results for up to eight segments. There are, however, small discrepancies between the figures for harmonic content with the larger numbers of segments.

For the case where $r = 7$, Barnes quotes a figure for harmonic content some 25% lower than is indicated by our calculations.

It is immediately apparent from the results of Tables 1 and 2 for an equal number of segments that harmonic content is consistently higher for the trapezoid approximation. However, for a comparison which neglects the 'flat top' given by the trapezoidal method, the position is reversed, as would be expected.

4 Conclusions

The results of this work have developed a further method for piecewise approximation of a sinusoid. The troublesome 'spiking' that is often associated with diode shapers at the peaks of the sinusoid has been removed with the 'flat top' approximation, whilst the circuit is insensitive to even harmonic distortion and cannot give rise to any form of crossover distortion at the output. In this paper, the generation of the primary sinusoidal waveform only has been considered, but it is anticipated that the method has wider application in the synthesis of arbitrary shaped waveforms.

5 Acknowledgments

The authors are particularly indebted to the Wayne Kerr Co. Ltd. for provision of financial and technical support in a continuing programme of research in electronic instrumentation at Swansea.

6 References

1. Burt, E. G. C. and Lange, O. H., 'Function generators based on linear interpolation with applications to analogue computing', *Proc. Instn. Elect. Engrs*, 103C, pp. 51-8, 1956.
2. Aird, R. J. and Court, J. T., 'An improved method for the design of electronic function generation networks', *Trans. Inst. Meas. and Control*, 5, pp. 271-5, 1972.
3. Barnes, L., 'Linear segment approximations to a sine wave', *Electronic Engng*, 40, pp. 502-8, 1968.
4. Klein, G. and Hagenbeuk, H., 'Accurate triangle-sine converter', *ibid.*, 39, pp. 700-4, 1967.
5. Paull, C. J. and Evans, W. A., 'New approach to triangle-sine-wave generation', *Electronics Letters*, 6, pp. 620-1, September 17th, 1970.

7 Appendix 1: Breakpoint Analysis

Figure 7 shows a section of a sinusoid combined with a straight line approximation to the curve. Where the breakpoints x_k are uniformly spaced, and the form of the approximation is known, e.g. tangential, chordal, etc., it is a relatively simple matter to calculate both the abscissae and ordinates defining the extremities of each linear segment. However, since the radius of curvature is not constant, the maximum departures d_k , d_{mk} will vary considerably between segments and this will, in turn, increase the total harmonic distortion content on the approximated waveform.

A computer analysis by Barnes³ of a selection of alternative forms of approximation has shown, using the Newton-Raphson method, that a substantially lower figure for total harmonic distortion can be achieved with a chordal approximation, where the absolute magnitudes of the maximum departures are made equal for all segments. To determine the co-ordinates of the break-

points for this case, a simple alternative method was found useful for computation purposes. In Fig. 7 the first segment is shown to originate from the origin, and this is clearly essential if a discontinuity between quadrants is to be avoided. As nothing more is known about this first segment, a trial value is assigned to the abscissa of the intermediate maximum departure point, x_{m1} . It can readily be shown that the slopes of the sinusoid and linear segment are equal at this point and a value for $d_{m1} = D$ is provided by the equation

$$D = \sin x_{m1} - x_{m1} \cdot \cos x_{m1}$$

To locate the first breakpoint, a second trial value is taken; this time for x_1 . The difference between the ordinates of the segment and the sinusoid is calculated as

$$d_1 = \sin x_{m1} - D + (x_1 - x_{m1}) \cos x_{m1} - \sin x_1$$

Since it is desired to make $d_1 = D$, a better approximation for x_1 can now be formed from the equation.

$$x_1 \text{ (new)} = x_{m1} + \frac{\{(A-1)D + d_1\} \{x_1 - x_{m1}\}}{AD}$$

where A is a constant chosen to give rapid convergence. Setting $A = 4$ was found to be quite satisfactory in practice.

When the first breakpoint has been found to a sufficient accuracy, the intermediate maximum departure point for the second segment x_{m2} can be located by a similar process, thus:

$$d_{m2} = \sin x_{m2} - (\sin x_1 + D + \cos x_{m2})(x_{m2} - x_1)$$

leading to a better estimate for x_{m2} given by:

$$x_{m2} \text{ (new)} = x_1 + \frac{\{(A-1)D + d_{m2}\} \{x_{m2} - x_1\}}{AD}$$

For the general case of the k th segment of a total of r segments in the approximation:

$$d_{mk}^r = \sin x_{mk}^r - (\sin x_{k-1}^r + D + \cos x_{mk}^r)(x_{mk}^r - x_{k-1}^r)$$

and

$$x_{mk}^r \text{ (new)} = x_{k-1}^r + \frac{\{(A-1)D + d_{mk}^r\} \{x_{mk}^r - x_{k-1}^r\}}{AD}$$

Using the above equations with k taking all integral

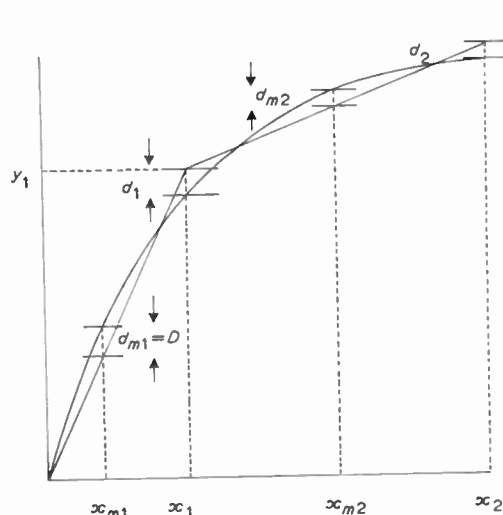


Fig. 7. Chordal approximation.

values up to a value r yields a value for the final breakpoint x_r^r . This is compared with $\pi/2$ and a new trial value of x_{m1} selected in a new computational run such that

$$x_{m1}(\text{new}) = \frac{x_{m1}\pi}{2x_r^r}$$

Values quite accurate enough are obtained for practical purposes when:

$$x_r^r - \pi/2 < 10^{-3}$$

The 'flat top' approximation is obtained with essentially the same procedure except that the abscissa of the midpoint of the final segment now has to equal $\pi/2$. The new values of x_{m1} must now be assigned as follows:

$$x_{m1}(\text{new}) = x_{m1} \frac{\pi}{2x_m^r(s+1)}$$

where the number of trapezoids $s = (r-1)$.

8 Appendix 2: Harmonic Analysis

The general expression for the Fourier series of a periodic waveform is given by

$$f(x) = \frac{a_0}{2} + \sum_{n=1}^{\infty} (a_n \cos nx + b_n \sin nx)$$

In Fig. 3(d) the linear segment approximation contains no d.c. level ($a_0 = 0$) and is an odd function of x . Furthermore, rotation symmetry exists with alternate half-cycles being identical but opposite in sign. Applying these constraints the general expression is given by

$$(x) = \sum_{n=1}^{\infty} b_n \sin nx$$

n odd.

where

$$b_n = \frac{-2}{\pi n^2} \int_0^{\pi} f''(x) \sin nx \, dx$$

n odd.

$f''(x)$ shown in Fig. 3(f) is the second differential of the linear segment approximation waveform and consists of a series of delta functions with the general term k for a total of r linear segments given by

$$\left[\frac{(y_{k+1}^r - y_k^r)}{(x_{k+1}^r - x_k^r)} - \frac{(y_k^r - y_{k-1}^r)}{(x_k^r - x_{k-1}^r)} \right] [\delta(x - x_k^r) + \delta(x + x_k^r - \pi)]$$

where

$$y_0^r = x_0^r = 0$$

Inserting the series in the equation for b_n yields the following expression:

$$b_n = \frac{4}{\pi n^2} \sum_{k=1}^r \frac{(y_k^r - y_{k-1}^r)}{(x_k^r - x_{k-1}^r)} [\sin nx_k^r - \sin nx_{k-1}^r]$$

n odd

i.e.

$$f(x) = \frac{8}{\pi} \sum_{m=0}^{\infty} \frac{\sin(2m+1)x}{(2m+1)^2} \sum_{k=1}^r \frac{(y_k^r - y_{k-1}^r)}{(x_k^r - x_{k-1}^r)} \times \cos[(m+\frac{1}{2})(x_k^r + x_{k-1}^r)] \sin[(m+\frac{1}{2})(x_k^r - x_{k-1}^r)]$$

For the trapezoidal approximation r is replaced by s in the above expression.

Manuscript first received by the Institution on 13th February 1974 and in final form on 10th June 1974. (Paper No. 1607/CC 211)

© The Institution of Electronic and Radio Engineers, 1974

The Authors



Dr. C. J. Paull graduated with a B.Sc.(Eng.) degree from the Department of Electrical Engineering, University College London in 1966. He then served on the staff of the London Electricity Board for a short time before embarking on research in signal synthesis and processing techniques at the University College of Wales, Swansea, where he subsequently obtained both M.Sc., and Ph.D., degrees. Dr. Paull held the Wayne

Kerr Industrial Fellowship at Swansea prior to taking up his present appointment as a Lecturer in the Department of Electrical and Electronic Engineering at Nottingham University.



Mr. W. A. Evans graduated with a B.Sc. in pure science with honours in physics at the University College of Swansea in 1957 and obtained an M.Sc. degree in information engineering at Birmingham University in 1958. His industrial experience has included computer design with Ferranti Packard Electric Limited, Toronto, and participating in the Canadian space program whilst a member of the Scientific Staff of

RCA Victor Company Montreal. In 1966 he re-entered academic life as a Lecturer at the University College of North Wales, returning to Swansea as a Lecturer in the Department of Electronic and Electrical Engineering in 1968. His interests lie in electronic instrumentation and at Swansea he directs a research group particularly concerned with system identification and waveform synthesis.

Dr. Paull and Mr. Evans received the J. Langham Thompson premium for 1973 for their paper on a frequency response analysis using a commutated filter.

Low-pass filters of even orders with equal ripple delay and Chebyshev stopband attenuation

Professor B. D. RAKOVICH, Dipl.Eng., Ph.D.*

and

V. S. STOJANOVICH, Dipl.Eng.†

SUMMARY

A class of low-pass filter functions of even degree is presented having equal ripple delay response and Chebyshev stopband attenuation. A special type of equal ripple delay approximation, referred to as the constrained Chebyshev approximation, that was previously employed to construct filter functions of odd degree, is modified so that it can also be used advantageously in the design of even-ordered low-pass filters. A comparison of results reveals that by this method a considerable amount of performance improvement of the resulting filter can be obtained. Tables are presented giving the zero and pole locations of these filters for $n = 4, 6, 8$ and 10 together with some other important parameters both in the frequency and in the time domain.

1 Introduction

It is well known that all-pole low-pass filters approximating to a linear phase exhibit almost negligible overshoot in the transient response to a unit step excitation. Nevertheless, they have limited use in many pulse applications since their magnitude characteristic is rather unsatisfactory both in the passband and in the stopband. The stopband performance of these filters can be improved by adding one or more pairs of real frequency transmission zeros that do not influence the phase but completely suppress the output at the corresponding frequency. This method, first introduced by Feistel and Unbehauen,^{1,2} consists of choosing the polynomial in the denominator of the rational transfer function which approximates the ideal phase characteristic in the maximally flat sense or in the Chebyshev sense and then adding an even or odd polynomial in the numerator so that the Chebyshev stopband magnitude response is obtained. If Chebyshev approximation to a linear phase or a constant group delay is used to construct the polynomial in the denominator of the transfer function, the approximation error must be small, otherwise a large long-lasting overshoot or undershoot is produced in the transient response to unit step excitation of the resulting filter.

It has been shown in two recent papers^{3,4} that this situation can be very much improved by using a special type of equal ripple approximation of a constant group delay, referred to as constrained Chebyshev delay approximation, to determine denominator polynomial of the transfer function. The constrained Chebyshev delay approximation is obtained by imposing a constraint on the error curve at the origin. As revealed by computer analysis, by decreasing the delay error at the origin $\varepsilon(0)$ from its upper limit $\varepsilon(0) = \varepsilon_{\max}$ towards its lower limit $\varepsilon(0) = -\varepsilon_{\max}$, considerable improvements both in the transient behaviour and the magnitude response of filters of odd degree are obtained. In the even-ordered case the standard error curve has a minimum at the origin so that this technique would require $|\varepsilon(0)| > \varepsilon$. On the other side, increasing $\varepsilon(0)$ towards its upper limit deteriorates the frequency and time domain characteristic of the filter, and, hence, the conclusion has been reached^{3,4} that the technique of constrained Chebyshev approximation is not useful in the design of filtering networks of even degree.

The main objective of this paper is to show that by suitable modification of the procedure used to obtain the denominator polynomial, the constrained Chebyshev delay approximation can also be applied to advantage for the design of rational transfer functions of even degree approximating a constant group delay and exhibiting Chebyshev type of stopband attenuation. Zero and pole locations and other relevant parameters of some selected approximants of 4, 6, 8 and 10 degrees are tabulated and the results are compared with those for the Chebyshev delay approximation with the standard error curve. This comparison reveals that the constrained Chebyshev delay approximation leads to a considerable amount of performance improvement of the resulting filter both in the frequency and time domain.

* Faculty of Electrical Engineering, University of Belgrade, Belgrade, Yugoslavia.

† Department of Electrical Engineering, University of Nish, Nish, Yugoslavia.

2 Approximation Technique

The design procedure used in this paper is very similar to that described for filters of odd degree.⁴ A different approach is adopted only to derive the denominator polynomial of the transfer function which forces a constrained equal ripple approximation of a constant group delay. Hence, as in the odd-ordered case, we start from the transfer function of the form

$$F_{2n}(s) = \frac{M_{2n-2}(s)}{P_{2n}(s)} = \frac{\prod_{v=1}^n \left(1 + \frac{s^2}{\omega_v^2}\right)}{\sum_{i=0}^{2n} A_i s^i} \quad A_0 = 1 \quad (1)$$

where $P_{2n}(s)$ is a strictly Hurwitz polynomial and $M_{2n-2}(s)$ is an even polynomial with all zeros on the imaginary axis. Let the transmission coefficient be defined as

$$S_{12}(s) = (4R/R_2)^{1/2} K F_{2n}(s) \quad (2)$$

where K is a constant which for equal resistance terminations must be chosen such that $|S_{12}(0)| = 1$. For such a realization it is also necessary that $|F_{2n}(j\omega)| \leq 1$ for all ω .

Since the numerator of (1) is an even polynomial the group delay response is completely determined by the denominator polynomial $P_{2n}(s)$

$$D(A, \omega) = -\frac{d\phi}{d\omega} = \frac{\text{Im}'(\omega) \text{Re}(\omega) - \text{Im}(\omega) \text{Re}'(\omega)}{\text{Re}^2(\omega) + \text{Im}^2(\omega)} \quad (3)$$

where $\text{Re}(\omega)$ and $\text{Im}(\omega)$ are the real and imaginary parts of $P_{2n}(A, j\omega)$ respectively and, for simplicity of notation, the set of the coefficients A_1, A_2, \dots, A_{2n} is denoted by A .

The well-known Abele solution⁵ having the standard error curve is obtained by solving the following set of non-linear equations

$$D(A, \omega_i) - 1 = (-1)^i \epsilon_{\max} \quad i = 1, 2, \dots, 2n+1 \quad (4)$$

where ω_i ($i = 1, 2, \dots, 2n+1$) are critical or extremal points including the end points of the approximation interval.

The constrained Chebyshev approximation is generated by varying the value of the first maximum of the delay error curve in the range from ϵ_{\max} to $-\epsilon_{\max}$. In the even-ordered case the critical point at the origin corresponds to a minimum so that the first maximum is obtained for $i = 2$ and hence

$$-\epsilon_{\max} < \epsilon(\omega_2) < \epsilon_{\max} \quad (5)$$

The polynomial in the denominator of (1) can be determined for any prescribed ϵ_{\max} and $\epsilon(\omega_2)$ by solving the system of non-linear equations (4) and then the method developed by Temes and Gui⁶ is used to find the transmission zeros that forces an equal ripple stopband attenuation. This procedure has been described in the previous paper,⁴ the only difference is that the following mapping function is used for n even :

$$s^2 = \sigma_0^2 \frac{z^2 - \omega_0^2}{z^2 + \omega_0^2} \quad (6)$$

where the positive parameters σ_0 and ω_0 can be found for any prescribed stopband attenuation (α_s) and the known denominator polynomial of (1). This has been discussed in detail by Unbehauen.²

3 Frequency and Time Domain Characteristics

The computer analysis has revealed that the results obtained by the foregoing method of constrained

Table 1

| $2n$ | $\epsilon_{\max}^{(*)}$ | α_s (dB) | $\sigma_{p1} \pm j\omega_{p1}$ | $\sigma_{p2} \pm j\omega_{p2}$ | $\sigma_{p3} \pm j\omega_{p3}$ | $\pm j\omega_{01}$ | $\pm j\omega_{02}$ | ω_{3dB} | t_r | P_1^{dB} | P_2^{dB} |
|------|-------------------------|--------------------|--------------------------------|--------------------------------|--------------------------------|--------------------|--------------------|----------------|-------|-------------------|-------------------|
| 4 | 0.05 | 40 | -0.45181 $\pm j0.23773$ | -0.30479 $\pm j0.72587$ | | 1.09383 | | 0.407 | 5.452 | 0.78 | 0.36 |
| 4 | 0.10 | 40 | -0.32242 $\pm j0.18831$ | -0.19929 $\pm j0.57212$ | | 1.08927 | | 0.359 | 6.179 | 1.50 | 0.79 |
| 4 | 0.15 | 40 | -0.30922 $\pm j0.19440$ | -0.17553 $\pm j0.58522$ | | 1.08694 | | 0.374 | 5.967 | 2.11 | 1.08 |
| 4 | 0.20 | 40 | -0.29892 $\pm j0.19969$ | -0.15600 $\pm j0.59425$ | | 1.08515 | | 0.390 | 5.785 | 2.83 | 1.39 |
| 4 | 0.30 | 40 | -0.28236 $\pm j0.20928$ | -0.12449 $\pm j0.60622$ | | 1.08251 | | 0.428 | 5.477 | 4.58 | 2.06 |
| 6 | 0.05 | 60 | -0.28256 $\pm j0.14719$ | -0.21257 $\pm j0.46391$ | -0.16921 $\pm j0.78343$ | 1.02933 | 1.37017 | 0.314 | 6.999 | 0.75 | 0.43 |
| 6 | 0.10 | 60 | -0.26148 $\pm j0.15212$ | -0.17548 $\pm j0.47676$ | -0.14503 $\pm j0.80433$ | 1.02758 | 1.35322 | 0.336 | 6.678 | 1.76 | 0.90 |
| 6 | 0.15 | 60 | -0.24902 $\pm j0.15635$ | -0.15078 $\pm j0.48447$ | -0.12794 $\pm j0.81367$ | 1.02648 | 1.34310 | 0.366 | 6.405 | 2.99 | 1.44 |
| 6 | 0.20 | 60 | -0.24011 $\pm j0.16041$ | -0.13189 $\pm j0.49022$ | -0.11424 $\pm j0.81806$ | 1.02569 | 1.33626 | 0.411 | 6.164 | 4.39 | 2.04 |
| 6 | 0.30 | 60 | -0.22705 $\pm j0.16856$ | -0.10340 $\pm j0.49933$ | -0.09248 $\pm j0.81953$ | 1.02467 | 1.32793 | 0.502 | 5.747 | 7.62 | 3.42 |

* $\epsilon(\omega_2) = -0.85 \epsilon_{\max}$ in all cases

Table 2

| $2n$ | $\epsilon_{\max}^{(*)}$ | α_s (dB) | $\sigma_{p1} \pm j\omega_{p1}$ | $\sigma_{p2} \pm j\omega_{p2}$ | $\sigma_{p3} \pm j\omega_{p3}$ | $\sigma_{p4} \pm j\omega_{p4}$ | $\sigma_{p5} \pm j\omega_{p5}$ | $\pm j\omega_{01}$ | $\pm j\omega_{02}$ | $\pm j\omega_{03}$ | $\pm j\omega_{04}$ | ω_{3dB} | τ_r | $p_1\%$ | $p_2\%$ |
|------|-------------------------|--------------------|--------------------------------|--------------------------------|--------------------------------|--------------------------------|--------------------------------|--------------------|--------------------|--------------------|--------------------|----------------|----------|---------|---------|
| 8 | 0.05 | 80 | -0.23077 $\pm j0.12030$ | -0.17623 $\pm j0.38258$ | -0.16075 $\pm j0.66037$ | -0.13250 $\pm j0.90860$ | | 1.01352 | 1.14163 | 1.62742 | | 0.287 | 7.758 | 0.97 | 0.51 |
| 8 | 0.10 | 80 | -0.21209 $\pm j0.12362$ | -0.14349 $\pm j0.39019$ | -0.13234 $\pm j0.67210$ | -0.11346 $\pm j0.92447$ | | 1.01258 | 1.13268 | 1.59966 | | 0.320 | 7.354 | 2.45 | 1.10 |
| 8 | 0.15 | 80 | -0.20162 $\pm j0.12687$ | -0.12258 $\pm j0.39544$ | -0.11400 $\pm j0.67697$ | -0.10026 $\pm j0.92996$ | | 1.01195 | 1.12726 | 1.58429 | | 0.364 | 7.006 | 4.24 | 1.78 |
| 8 | 0.20 | 80 | -0.19444 $\pm j0.13023$ | -0.10695 $\pm j0.39993$ | -0.10016 $\pm j0.67917$ | -0.08978 $\pm j0.93112$ | | 1.01146 | 1.12358 | 1.57470 | | 0.402 | 6.699 | 6.25 | 2.56 |
| 8 | 0.30 | 80 | -0.18452 $\pm j0.13735$ | -0.08386 $\pm j0.40839$ | -0.07947 $\pm j0.68016$ | -0.07323 $\pm j0.92720$ | | 1.01079 | 1.11933 | 1.56500 | | 0.447 | 6.174 | 10.92 | 4.43 |
| 10 | 0.05 | 100 | -0.19294 $\pm j0.10074$ | -0.14778 $\pm j0.32137$ | -0.13820 $\pm j0.55867$ | -0.13073 $\pm j0.78222$ | -0.10844 $\pm j0.98489$ | 1.00798 | 1.07452 | 1.26045 | 1.87313 | 0.266 | 8.491 | 1.28 | 0.59 |
| 10 | 0.10 | 100 | -0.17682 $\pm j0.10325$ | -0.11968 $\pm j0.32665$ | -0.11242 $\pm j0.56585$ | -0.10767 $\pm j0.79129$ | -0.09290 $\pm j0.99714$ | 1.00761 | 1.06975 | 1.24531 | 1.83869 | 0.305 | 7.997 | 3.21 | 1.27 |
| 10 | 0.15 | 100 | -0.16804 $\pm j0.10595$ | -0.10206 $\pm j0.33079$ | -0.09631 $\pm j0.56898$ | -0.09291 $\pm j0.79364$ | -0.08221 $\pm j1.00017$ | 1.00731 | 1.06645 | 1.23652 | 1.82039 | 0.339 | 7.575 | 5.53 | 2.06 |
| 10 | 0.20 | 100 | -0.16217 $\pm j0.10882$ | -0.08902 $\pm j0.33465$ | -0.08437 $\pm j0.57060$ | -0.08182 $\pm j0.79338$ | -0.07377 $\pm j0.99930$ | 1.00670 | 1.06375 | 1.23069 | 1.80935 | 0.364 | 7.208 | 8.11 | 2.96 |

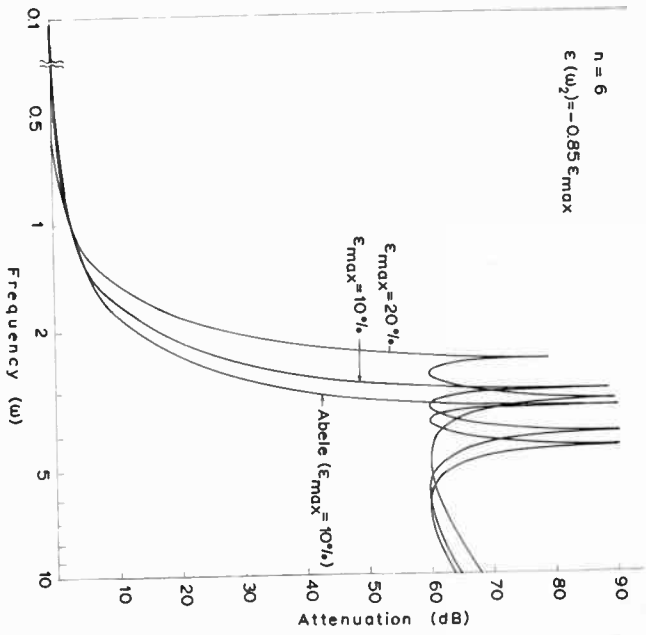


Fig. 1. Magnitude responses of the sixth-order filters for $\epsilon_{\max} = 0.1$ and $\epsilon_{\max} = 0.2$; $\delta(\omega_2) = -0.85\epsilon_{\max}$ and the Abele filter for $\epsilon_{\max} = 0.1$.

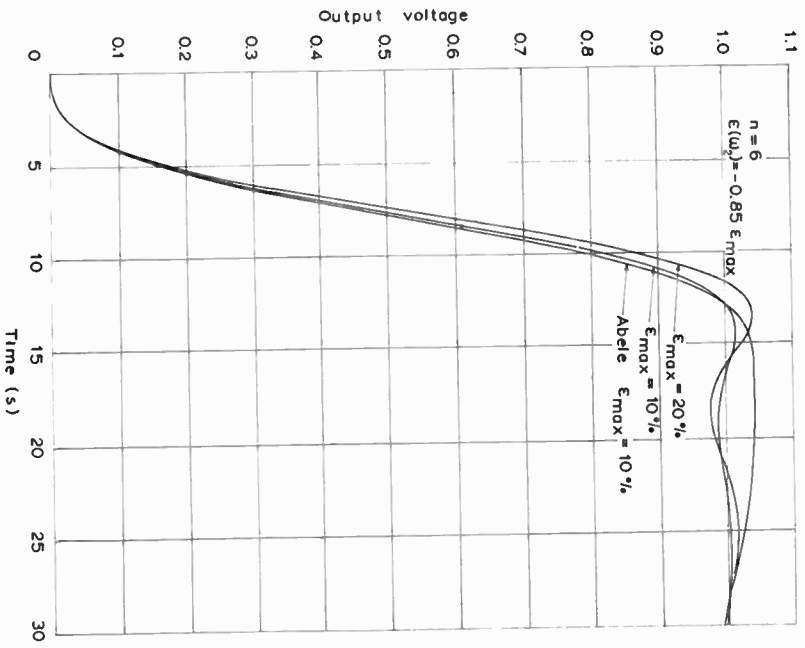


Fig. 2. Transient responses of the sixth-order filters with the minimum stopband attenuation $\alpha_s = 60$ dB for $\omega_s \geq 1$.

Chebyshev approximation for filter functions of even degree agree in all important respects with those for n odd.⁴ Hence, the main results will be only briefly summarized in the following.

(i) Decreasing the first maximum of the delay error curve from its upper limit $\varepsilon(\omega_2) = \varepsilon_{\max}$ towards its lower limit $\varepsilon(\omega_2) = -\varepsilon_{\max}$ first slightly increases and then decreases the delay approximation bandwidth. This indicates that the Abele solution with the standard error curve ($\varepsilon(\omega_2) = \varepsilon_{\max}$) is neither unique nor the best Chebyshev approximation of a constant delay. However, the increases of delay bandwidth obtained in this way are too small to be of any practical significance.

(ii) Increasing the maximum delay deviation ε_{\max} increases the overshoot and decreases the 10–90% rise-time. The overshoot increases more slowly than in the case when the equal-ripple delay polynomial with the standard error curve (Abele's solution) is used in the denominator of the transfer function. Hence, a large variety of filter specifications in the time domain can be obtained by varying ε_{\max} in the range $0 < \varepsilon_{\max} < 0.2$.

(iii) For a given minimum stopband attenuation α_s (dB), the optimum order of the polynomial in the denominator of (1) is equal to the nearest integer to $\alpha_s/10$. In the even ordered case the optimum value for $\varepsilon(\omega_2)$ is equal to $-0.85\varepsilon_{\max}$. These values lead to considerable improvement of the magnitude stopband characteristic and the transient response of the resulting filter.

As an illustration in Figs. 1 and 2 the magnitude and transient responses of the sixth-order constrained approximants for $\varepsilon_{\max} = 0.1$ and $\varepsilon_{\max} = 0.2$ and $\varepsilon(\omega_2) = -0.85\varepsilon_{\max}$ are compared with those for the Abele solution ($\varepsilon_{\max} = 0.1$). In Fig. 1 the $\omega_{3\text{dB}}$ bandwidth is normalized to unity and the minimum stopband attenuation is $\alpha_s = 60$ dB in all cases. The transient responses to a unit step excitation (Fig. 2) are compared on the basis of equal stopband attenuation, i.e. the frequency at which the attenuation of 60 dB is first reached is made equal to unity in all cases. The constrained approximant for $\varepsilon_{\max} = 0.1$, $\varepsilon(\omega_2) = -0.85\varepsilon_{\max}$ provides smaller transition bandwidth and almost three times smaller overshoot than the corresponding Abele solution. On the other side, the constrained approximant for $\varepsilon_{\max} = 0.2$, $\varepsilon(\omega_2) = -0.85\varepsilon_{\max}$ yields the overshoot (4.4%) which is almost equal to that of the Abele approximant for $\varepsilon_{\max} = 0.1$ (4.5%). But the former has smaller rise-time in the transient response and very much reduced transition bandwidth as can be seen from Figs. 1 and 2.

Finally in order to facilitate the practical design of these filters, Tables 1 and 2 are presented giving the locations of poles ($\sigma_{ip} \pm j\omega_{ip}$) and zeros ($\sigma_{io} \pm j\omega_{io}$) of the transfer functions of even degree that approximate a constant delay to within a given error ε_{\max} and provide Chebyshev stopband attenuation. The minimum stopband attenuation for all approximants is $\alpha_s = 10n$ where n is the order of the filter and $\varepsilon(\omega_2) = -0.85\varepsilon_{\max}$. Also included in these Tables are the normalized $\omega_{3\text{dB}}$ bandwidth, the 10–90% rise-time, the first overshoot ($p_1\%$)

and the first undershoot ($p_2\%$). The frequency is normalized so that the minimum stopband attenuation α_s is first reached at $\omega = 1$.

4 Conclusion

The constrained Chebyshev approximation technique, which was previously used to develop transfer functions of low-pass filters approximating a constant delay and exhibiting Chebyshev stopband attenuation, has been extended in this paper so as to include the filter functions of even degree. As in the odd-ordered case, the constrained Chebyshev approximants of even degree have been shown to provide considerable improvements in the magnitude characteristic and in the transient response to a unit step input when compared to the filter functions with Chebyshev delay approximation having the standard error curve. The latter are known to produce a large long-lasting overshoot in the transient response to a unit step input for n even unless the specified delay error is very small. Also for larger values of ε_{\max} the condition $|F_{2n}(0)| \geq |F_{2n}(j\omega)|$ is not fulfilled, meaning that the realization with equal resistance terminations is not possible without use of an ideal transformer or some other artifice. On the other hand, if the constrained Chebyshev approximant is used in the denominator of (1) the condition $|F_{2n}(0)| > |F_{2n}(j\omega)|$ can be fulfilled even for $\varepsilon_{\max} = 0.2$ and the realization with equal resistance terminations is always possible.

5 Acknowledgment

The authors wish to acknowledge the Research Council of S.R. Serbia for financial support of work of which that described forms a part.

6 References

1. Feistel, K. H. and Unbehauen, R., 'Tiefpässe mit Tschebyscheff-Character der Betriebsdämpfung im Sperrbereich und maximal geübener Laufzeit', *Frequenz*, **19**, pp. 265–82, August 1965.
2. Unbehauen, R., 'Low-pass filters with predetermined phase or delay and Chebyshev stopband attenuation', *IEEE Trans. on Circuit Theory*, **CT-15**, pp. 337–41, December 1968.
3. Rakovich, B. D. and Djurich, B. M., 'Chebyshev approximation of a constant group delay with constraints at the origin', *IEEE Trans. on Circuit Theory*, **CT-19**, pp. 467–75, September 1972.
4. Rakovich, B. D. and Stojanovich, V. S., 'On the design of equal ripple delay filters with Chebyshev stopband attenuation', *The Radio and Electronic Engineer*, **43**, pp. 257–65, April 1973.
5. Abele, T., 'Übertragungsfaktoren mit Tschebyscheffscher Approximation konstanter Gruppenlaufzeit', *Arch. Elek. Übertragung*, **16**, pp. 9–18, January 1962.
6. Temes, G. C. and Gyi, M., 'Design of filters with arbitrary passband and Chebyshev stopband attenuation', *IEEE Int. Conv. Digest*, pp. 184–5, 1967.

Manuscript received by the Institution on 12th December 1973.
(Paper No. 1608/CC212.)

© The Institution of Electronic and Radio Engineers, 1974

A novel radar situation display

A. HARRISON, B.Sc., M.R.I.N., C.Eng., F.I.E.R.E.*

Based on a paper presented at a meeting of the Aerospace, Maritime and Military Systems Group in London on 20th February 1974

SUMMARY

The difficulty of manual plotting in a multi-ship situation has led to the search for an automatic plotting method. Earlier schemes failed for various known reasons. A combination of the Kelvin Hughes 'Photoplot' display and the Thorn image retaining panel marked a new approach, which led to this successful television display. The characteristics of the image retaining panel and the way it is utilized in the equipment are described. Photographs of situations at sea as displayed by the equipment demonstrate most of the advantages of this presentation.

1 Introduction

In 1944, the Admiralty Signal Establishment (now ASWE) was asked by the Government to draw up a specification for Civil Marine Radar. This was drafted in 1945, issued in revised form at the IMRAMN¹ in November 1946 and is substantially unchanged today. It is interesting to read the comment in the IMRAMN report that 'Discussion with various shipping interests confirmed that there was in fact a requirement for a radar set for navigation and pilotage as distinct from a collision warning set, which would of course be a much simpler and cheaper device'. Doubts about the latter part of this statement must have arisen very early, and indeed there was some dissent expressed in the report (Hogben). Figure 1 shows a photograph of a radar display of the Thames Estuary at Southend. While a navigational 'fix' appears easy, it is difficult to distinguish between moving or anchored ships, or buoys, so a collision risk is not obvious. Plotting the successive positions of a target at equal times originated in the Royal Navy before the p.p.i. display came into use, and was recommended by Captain F. J. Wylie in 1949² for civil marine use, to resolve the doubts and disclose ships on a collision course. The Ministry of Transport introduced plotting techniques into the radar observer's training courses for this purpose, and plotting facilities will be required by the proposed UK Radar Rules now being formulated by the Department of Trade.

While this technique of manual plotting is delightfully simple when dealing with a single ship, it becomes impractical in a crowded traffic situation. It was realized that an automatic plotting system could be achieved by the electronic storage and recall of successive p.p.i. pictures. In 1947 Andrew Haeff of the Naval Research Laboratory in Washington used a memory c.r.t. to

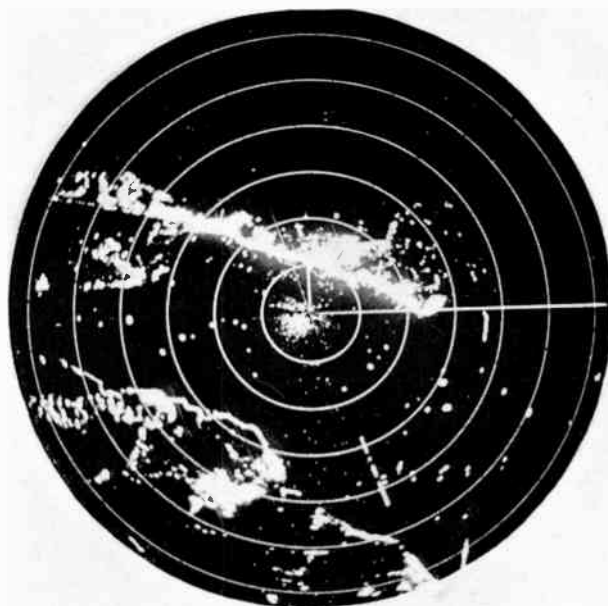


Fig. 1. Normal marine radar display. Ships, buoys, etc., in Thames Estuary.

* Kelvin Hughes Division, Smiths Industries Ltd., New North Road, Hainault, Ilford, Essex IG6 2UR.

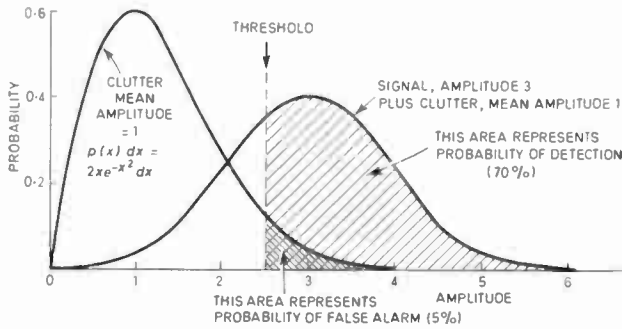


Fig. 2. Amplitude probability-density function for:
Clutter alone, mean amplitude unity.
Signal (+10 dB) plus clutter.

produce plots of the track of a moving target. This is mentioned in a review by R. F. Hansford,³ which also expresses dissatisfaction with the size and brightness of the radar display. In 1957 Thomas J. Kelly of Raytheon used a storage c.r.t. to produce a ship's-head-up display with own ship at the centre, showing true ships' tracks, i.e. aspect.⁴ In 1962 B. W. Manley of Mullard produced a display showing tracks, using a technique of transferring pictures between two tenicon memory c.r.t.s.⁵ Yet none of these devices has come into general use, and one is bound to wonder why. In the writer's view there are two key factors. The first is that the storage medium used was an integral part of a c.r.t., usually a complex double c.r.t. Stabilization against ship motion has to be applied, perhaps equally in both halves, and the system is generally inflexible, complicated and expensive.

The second is the clutter problem, which always arises in any integrating system. The random signals characteristic of hydrometeor clutter from rain, snow, hail, or the sea, and also receiver noise, have amplitudes which can be expressed statistically in terms of the probability-density function,

$$p(x) dx = 2x \exp(-x^2) dx$$

which has been normalized to a mean amplitude of 1. This is the Rayleigh distribution expressed graphically in Fig. 2. A steady signal of amplitude 3 would appear on the same graph as a vertical line of unit length, at 3 on the horizontal axis. If this signal is in the middle of a clutter field, however, a combined signal is produced, whose mathematical expression is quite intractable and of little importance. This combined signal may be readily visualized by thinking of a clock face. The minute hand pointing straight up represents the steady signal of amplitude 3. The hour hand pointing to any figure, and of any length from 0 to 3, represents the clutter. The combined signal is represented by the vector joining the points of the two hands. Its probability density function has been included in Fig. 2.

In any practical radar system, a threshold must be set, above which the receiver output is considered to be a signal, e.g. amplitude 2.5 in Fig. 2. The area under the curve to the right of the threshold represents the probability of detection of this signal in clutter. If the signal is absent, some of the area under the clutter curve falls to the right of the threshold. The system accepts this as

a signal, but it is false, and the shaded area represents the probability of a 'false alarm'.

Obviously one can reduce the probability of a false alarm by resetting the threshold to a higher amplitude, but only at the expense of reducing the probability of detection of real signals. A visually observed c.r.t. can be operated easily with 1000 false alarms per second (noise background), but an integrating system can tolerate only a very low false alarm rate—e.g. ten false alarms per second, integrated for ten minutes, puts 6000 false alarms on the screen, to form a grey background and degrade the signal contrast. It is not merely a question of raising the threshold—sea clutter suppression requires a critical setting of swept gain (i.e. a time varying threshold) wide dynamic range, perhaps even a logarithmic receiver, techniques which were not sufficiently advanced at the time of these earlier systems.

In 1963 Dr. P. W. Ranby of Thorn Electrical Industries announced the invention⁶ of an electroluminescent panel,⁷ which, when polarized by a steady (d.c.) voltage, could be stimulated to fluorescence where light fell on it, would continue to fluoresce after the light was extinguished, and could be erased by removal of the voltage. It was not immediately recognized that this device presented the possibility of a new approach to the problem of automatic radar plotting.

2 Photographic Storage Displays

As we saw in Fig. 1 the radar picture makes no distinction between fixed and moving targets, presenting a virtually instantaneous 'snapshot' of the situation, with no indication of the collision risk. In the 'Photoplot' display, simplified from a military equipment, the signals for one revolution of the radar aerial are photographed on cine film, processed to a dry state in two and a half seconds, and projected as a big bright picture, observable by several people together. The storage capabilities of the photographic film are still outstanding in definition, and capacity (2000 television lines on 16 mm film), and its permanence is described as 'archival'. We had used this equipment at sea to make automatic plots of tracks of ships, as in Fig. 3, but certain defects became obvious. Although moving targets were immediately evident, there was no direct indication of the direction of movement. While one stored picture was being displayed the storage of the subsequent data entailed a delay before it could be projected—quite intolerable in a possible collision situation. Finally, there was an understandable user dislike of a wet chemical process, no matter how well engineered. Nevertheless, at the time we could see no alternative to this approach.

It was some time later that we became aware of the Thorn Image Retaining Panel, recognized its qualities as a radar data storage medium, and carried out operational experiments and sea trials, still using the photoplot as a light amplifier.¹² These trials made the maximum use of current equipment, displaying a conventional North-stabilized true motion picture, 600 mm (24 in) diameter. The 82 mm (3½ in) radar c.r.t. had a fibre optic face plate, with B phosphor, against which the image retaining panel was registered to record the radar

c.r.t. data. The panel was then moved aside, a mirror was swung into position, and coincident images of the panel 'history' and the c.r.t. 'present moment' were exposed on the cinefilm. After 20 seconds the film was rapidly processed, moved to the projection gate, and the cycle repeated. Thus the displayed data was the up-to-date position data on the radar c.r.t. combined with the stored data (history) forming tracks on the image retaining panel.

At this stage it was noted that the panel was exposed to the radar c.r.t. for only 4 seconds in 20, i.e. for 1/5th of the time, and the c.r.t. was not being driven hard. If it could produce higher light output, an $F/1.4$ lens known to be available could project an image of the c.r.t. on the panel, at unity magnification, and this would expose the panel to the same total light (Appendix, Sect. 8.1). Further, with such an optical system, the panel can be moved by the gyro compass and log to correspond to ship movement, and at the same time observed via a television system to give a bright image with own ship at the centre, on a television monitor. Experiments quickly verified these conclusions, and it only remained to engineer the design to a form which satisfied the users requirement and the conditions of use on board ship.

3 Plotting 'History' versus Auto-track and Prediction

It is possible to select a target vessel and plot it automatically, the selection being manual or automatic—e.g. nearest. Plot data stored in a computer can be used in a calculation to predict the future track of the vessel, on the usual assumption that the speed and course are maintained unchanged. This is a very attractive idea which has been enthusiastically taken up in some quarters. There are however errors in the data, particularly bearing errors arising in the radar and the gyro (Appendix, Sect. 8.2); these are small when considering

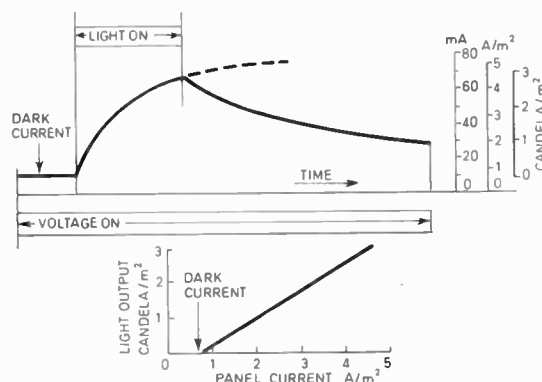


Fig. 4. Characteristics of image retaining panel.

the accuracy of the indicated present or past position (i.e. plotting), but they can have a serious effect on the accuracy of the predicted future position.

ASWE have conducted sea trials,⁸ using digital bearing transmission systems and a computer program planned to minimize these errors. The results were disappointing, indicating that the standard deviation of the predicted c.p.a. was about 10% of the range to the target. An averaging system to reduce the errors of bearing proved ineffective, because some bearing errors are cyclic with periods of ½ min and more (Appendix, Sect. 8.2.2). This is longer than the permissible averaging time,⁹ which cannot be extended unduly, since it introduces a lag,¹⁰ which delays not only the prediction, but also the vitally important observation of a change in the target's course or speed. These long period errors can be reduced, but only at some expense (Appendix, Sect. 8.2.2). The cost-effectiveness of all such systems is still in question.

Maintaining a plot of 'history', for sufficient time (6 or 12 min perhaps) to obtain tracks a mile or two long, ensures that the errors are effectively smoothed out by eye on the plotted track, and a mental extrapolation to indicate the future position of a target does not strain the accuracy of the data. A similar 'smoothing by eye' effect takes place in the standard procedure of manual plotting. At the same time, any significant change in the track, e.g. a sudden bend caused by the vessel changing course, is clearly indicated as soon as it is justified by the data accuracy. This is not easily visible when plotting manually. The advent of the image retaining panel, making this technique possible in an economic system, led us to adopt the 'history' only approach in the situation display.

4 Characteristics of Image Retaining Panel

Figure 4 shows how an energized panel takes a small current in darkness; when exposed to light, it starts to consume an increased current, and fluoresces with an intensity proportional to the current increase. The build-up and decay appear somewhat similar to the voltage across a resistance-capacitance integrator when a voltage pulse is applied to its input. In the build-up time, the voltage across the capacitor after a time t is given by

$$v = E(1 - e^{-t/\tau})$$

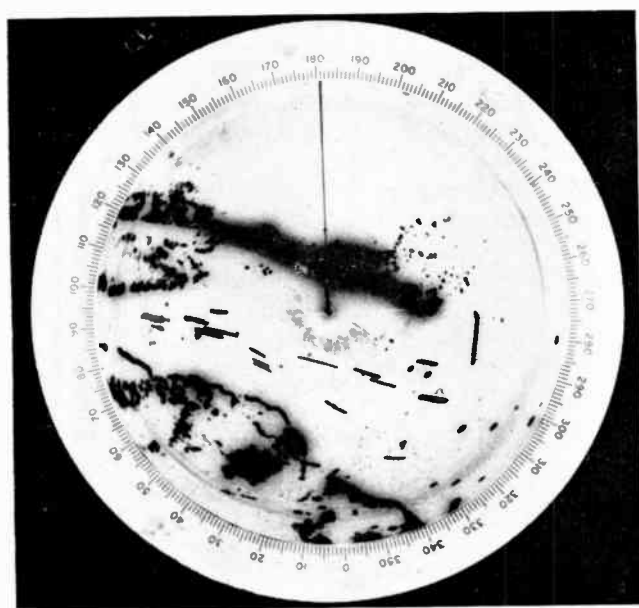


Fig. 3. Photoplot marine radar display with 6 minute exposure. Ship tracks, buoys, etc., in Thames Estuary.

while in the decay period

$$v = E e^{-\gamma t}$$

where $\gamma = 1/RC$, which is constant. RC is the time-constant of integration.

The image retaining panel can be considered as an integrator in this way, only if γ , instead of being constant, is proportional to the current in the panel—as though the decay time-constant increased as the decay progresses, giving a 'stretched exponential' form to the curve. The behaviour of the panel leads to the idea of an equivalent circuit consisting of:

- (a) A small capacitor—which has nothing to do with the storage properties, but is merely a consequence of the physical construction—a dielectric between two conducting plates. Erasure will not be completed when the polarizing voltage is removed, if the voltage is restored before this capacitor has time to discharge through the internal resistance of the panel—a few milliseconds (about $0.005 \mu\text{F}/\text{cm}^2$).
- (b) A fixed resistor which carries the dark current (about $0.5 \text{ M}\Omega/\text{cm}^2$).
- (c) A variable resistor, which decreases in value when excited by light, recovering slowly in the dark at a rate depending on its difference from the initial dark condition; or immediately if the current is interrupted, subject to (a) above (about infinity to $0.1 \text{ M}\Omega/\text{cm}^2$).

These three items, in parallel, appear to be in series with—

- (d) A potential barrier somewhat like a two-way Zener diode (about 40 V).

This equivalent circuit may be considered to apply to a complete panel—e.g. when floodlit—or any element of it when irradiated by part of a bright image, by suitable choice of component values.

The spectral characteristics of the panel show that it is excited by any visible light except a band in the yellow, which is the region of the emitted light. It is also excited by infra-red, X-rays, and electron bombardment.

The panel has an indefinitely long life, i.e. it does not 'wear out'. It can be damaged beyond recovery by overheating if the current rises above about $5 \text{ A}/\text{m}^2$. This limits its light output to about $3 \text{ candela}/\text{m}^2$.

5 The Equipment

The final design uses an optical projection system by which the radar data on the c.r.t. is transferred to the image retaining panel by a projection lens, and the stored image is viewed via a 45° dichroic mirror in a closed circuit television system. The television camera can also view, through the dichroic mirror, an illuminated data panel, which displays a compass repeater round the radar picture, superimposed calibration rings, ship's head marker, and a cursor, compass stabilized and divided into intervals which allow range measurement to about 2% accuracy. This is illustrated diagrammatically in Fig. 5, while the final engineered display is pictured in Fig. 6.

Without entering into a detailed discussion of the two-colour light projection geometry, it will help the reader to understand how the display works if, for the moment, he regards the television system as retransmitting a bright and enlarged picture of the c.r.t. directly, with own ship's present position *always at the centre of the picture* and ship's head up, as it is in a normal p.p.i. The electroluminescent panel when entirely stationary may be regarded as firstly reinforcing this direct picture and secondly providing memory 'tracks' of any targets which move relative to own ship, in the same way as does the afterglow (much more limited) of an unstabilized normal p.p.i. display. However, if the electroluminescent panel is rotated by the ship's gyro-compass, round an axis normal to its surface at own ship's position, and in synchronism with own ship's course changes, these tracks become geographic relative tracks, own ship being still shown as a stationary spot at the display centre. If as a further facility the electroluminescent panel, as well as being rotated, is moved 'backwards' at a rate fed in by the ship's speed log (reduced by the scale factor which the display has to the dimensions of the real world) all the tracks become true tracks. Although own ship's echo is still *always at the display centre* it now has a tail behind it which records its past history. A ship's-head-up presentation is permanently preserved, but a compass bearing ring rotates (with the panel) around the perimeter of the display to show true bearings. This facility to give own ship's present position always at the display centre is in sharp distinction to most true motion displays.

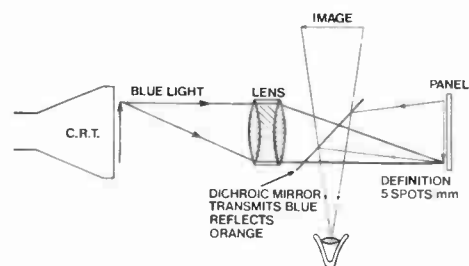


Fig. 5. Diagram of optical system for situation display, showing how a radar picture is stored on the panel and viewed.

The cycle of 'history' plotting is terminated at 3 or 6 minute intervals (according to the display range scale), after which the panel is erased, repositioned at a fixed starting point, and a new cycle commences. The observer can initiate this re-start at any time, or he can inhibit it if he wishes to retain that history for a longer period. Eventually, however, the full extent of the panel surface will have been explored, and the cycle must be re-started.

Some important operational features follow from the integrating characteristics of the panel. Receiver noise and clutter must be set to a level much lower than is usual if they are not to build up to a background which will hide tracks. In other words, the false alarm rate must be much lower than for a normal raw radar display. This does not lead to the loss of small targets however, since the same integration characteristic ensures the retention of every trace of a small target on the

display. Thus, three men hunting for bait on the muddy Southend foreshore at a mile range left clearly visible trails.

Similarly, sixty-odd ocean-going sailing yachts in a Channel race, extending from 0 to 6 miles from the ship, were clearly tracked, when a standard c.r.t. display of the same radar data failed to show every target on every aerial revolution—the number appeared less than half. High-speed craft *may* move too fast to build up a track, but in practice aircraft at landing speed—say 100 knots—have been observed as a line of separated dots, while hovercraft, hydrofoils and high-speed launches (40–60 knots) leave clear trails, even on the shortest display range.

It is thought that the technical advantages of this design arise from the very good receiver design (control of threshold) and the separation of display functions, so that each part needs to be efficient in one way only, for example,

- | | |
|------------------------|---|
| C.R.T.: | displays raw radar, with no storage and no stabilization. |
| Image Retaining Panel: | stores radar data, and is a convenient vehicle for the injection of ship movement (course and speed). |
| Data Panel: | displays the gyro (course) repeater, range rings, compass stabilized cursor, range in use, etc. |
| C.C.T.V. | provides light amplification for bright picture. |

Since the final display is on a television monitor, this allows us to use some television techniques. The first of these is optional picture reversal—black targets on a white background, or white targets on a black background; some users prefer the latter at night. Second, the picture may be repeated elsewhere (e.g. in the chartroom) by the use of a second monitor display, with individual control of contrast and brilliance to suit the

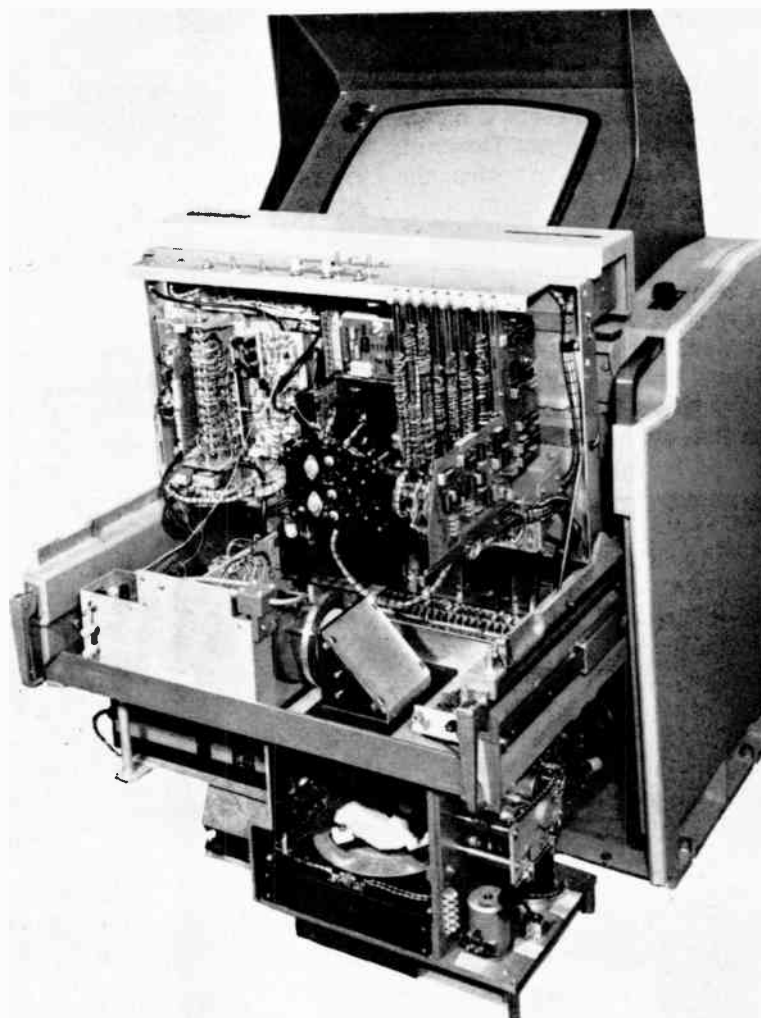


Fig. 6. Situation display equipment open for servicing. Television display c.r.t. at top. Electronic units on hinged shelf. Optical units on sliding shelf—radar c.r.t. on top left, television camera below it, panel transport mechanism lower right.

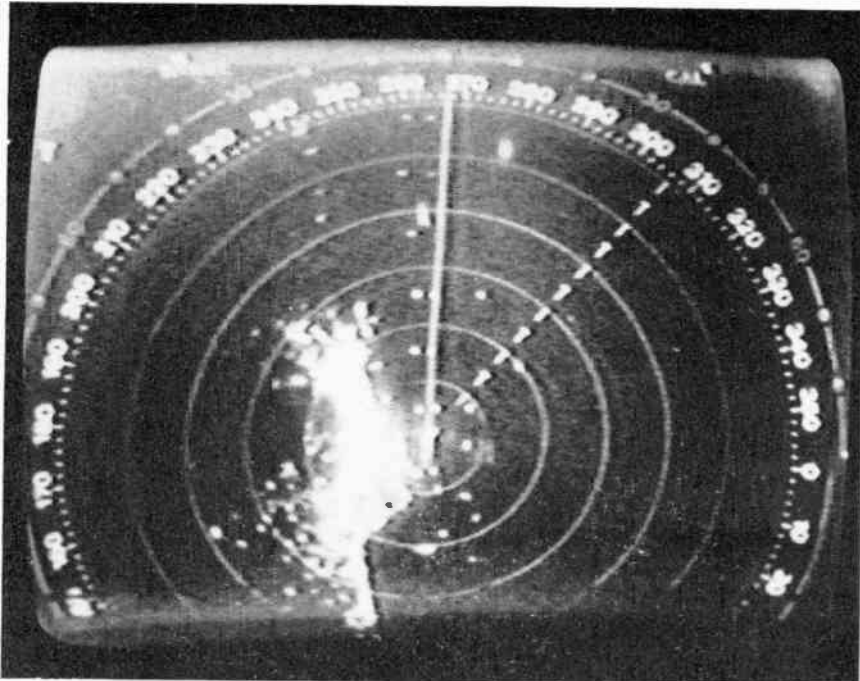


Fig. 7. Situation display.
Leaving Dunkerque.

been discarded to make the best use of the television format. This is quite acceptable since the range to a collision is less important than the time available, and an approaching ship must be travelling at more than three times our speed before the 'time to go' from astern is less than the 'time to go' from ahead. This is unlikely; but in any case, such an overtaking ship should keep clear. The bearing of a target in this arc where the bearing scale is not displayed can be obtained by reading the arrowhead on the cursor reciprocal.

Figure 7 shows the picture presented on the 6 mile range shortly after leaving Dunkerque. The harbour astern, the coastline, and the buoyed channel are evident, with a clearly distinguished ship (note the track) approaching in the channel at 3.8 miles range. Two miles astern, a small vessel is moving away from the coast; a tender is waiting to take off the pilot at about 1/10 mile ahead and slightly to the right. The 'T' on the left of the screen indicates that the ship's speed is being fed to the display, and the tracks of other ships are True. The inner scale of degrees is the compass (gyro) repeater scale, and the ship's head marker shows us on this scale that we are heading 267 degrees—almost due West. The outer scale facilitates reading bearings with respect to ship's head, where accuracy is not so essential.

ambient lighting. Third, a video tape recording may be made at sea, and replayed later. (Parts of such a record of a Channel crossing between Dunkerque and Dover on board the *Anderida* car ferry were replayed when the paper was presented at the Institution.)

6 Results Obtained

Photographs of this replay of the recording on a television monitor naturally show some loss of quality (definition, distortion of shape, linearity and steadiness) as compared with the original, but they indicate the type of picture presented to the ship's Master (Figs. 7, 8 and 9). It will be noted that half the view astern has

after leaving Dunkerque. The harbour astern, the coastline, and the buoyed channel are evident, with a clearly distinguished ship (note the track) approaching in the channel at 3.8 miles range. Two miles astern, a small vessel is moving away from the coast; a tender is waiting to take off the pilot at about 1/10 mile ahead and slightly to the right. The 'T' on the left of the screen indicates that the ship's speed is being fed to the display, and the tracks of other ships are True. The inner scale of degrees is the compass (gyro) repeater scale, and the ship's head marker shows us on this scale that we are heading 267 degrees—almost due West. The outer scale facilitates reading bearings with respect to ship's head, where accuracy is not so essential.

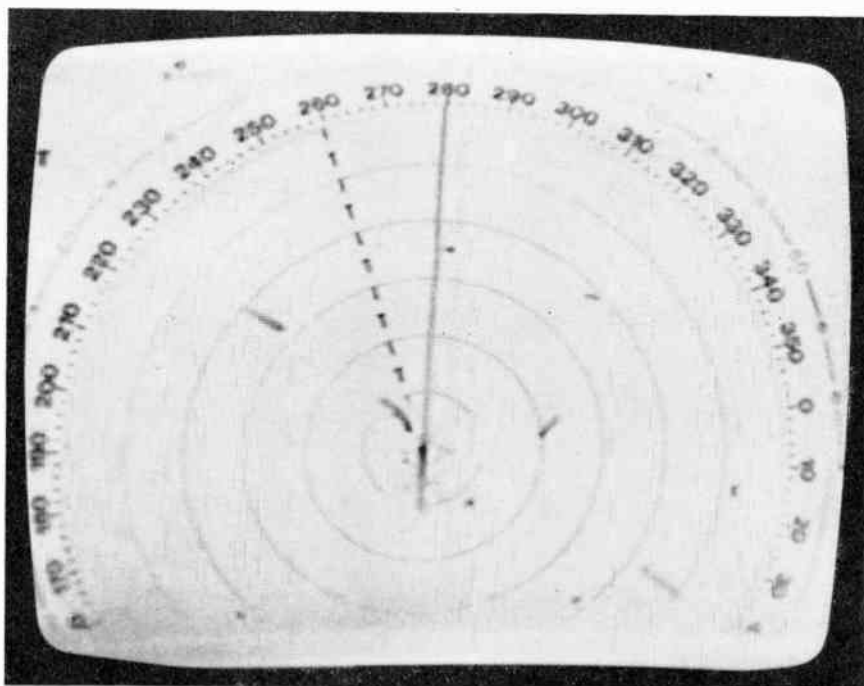


Figure 8 shows an interesting situation. We have—in strict accordance with the rule of the road at sea—held our course and speed, despite the collision risk. Ship X, very near to us to the left, has delayed her correct collision avoiding action to the last minute (literally), perhaps to pass the buoy just visible to the right of her track, $\frac{3}{4}$ mile from us. She has turned, is still turning, and will pass clear down our left side, perhaps 0.2 mile away. On any other display there would appear to be the risk of imminent collision,

Fig. 8. Situation display.
A close but safe situation.

Fig. 9. Situation display.

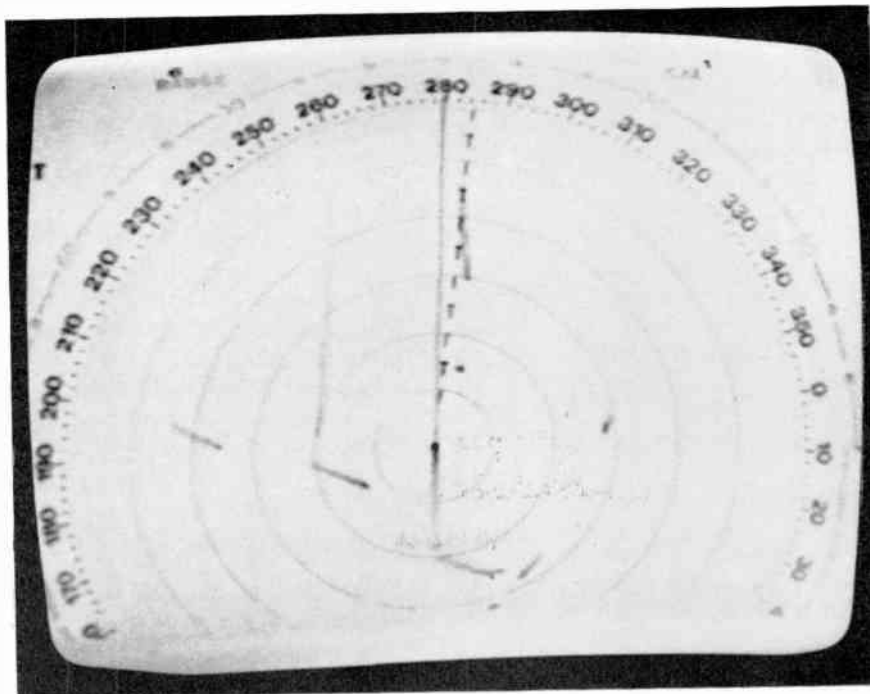
Ship ahead will pass clear to right; hovercraft clear to left; two ships astern in a dangerous situation.

now less than half a minute ahead. Emergency avoiding action, permitted to us by the rules in the case of imminent collision, would appear to be advisable—but this display has shown clearly that the collision risk has passed.

Figure 9 brings out three points. First, having just missed us, Ship X, now $2\frac{1}{2}$ miles away on a bearing of 070 degrees (5 o'clock) has taken very rash action. She should not be turning at all (unless the risk of collision is now imminent), but in any case not to her left. In fact, the other ship she is trying to avoid *should* have turned to *her* right, and if she had . . . well, that's how collisions occur at sea. Second, the long trail which has extended down the screen with its head now 2 miles away on 200 degrees (9 o'clock) is produced by a hovercraft travelling at 45 to 50 knots. Third, look carefully at the track of the ship approaching ahead, now at 3 miles range next to the dotted cursor. The track shows wriggles, greater than yawing of that ship could produce. This is photographic evidence of radar bearing errors such as those discussed in the Appendix (Sect. 8.2). Measured from the photograph, and using our own track as a scale representing 15 knots, the period of one complete cycle of this apparent wriggle is about $1\frac{1}{2}$ minutes. These errors are *not* present on ships' tracks on some other bearings, which is implicit in the formula in Section 8.2.2.

Predictions made from data acquired during part of one of these cycles would seem to indicate that the vessel ahead will pass 2 miles to the right . . . or $\frac{1}{2}$ mile to the left . . . or various distances between these limits, including zero, i.e. a collision. On *this* display it is quite clear that the other vessel is on a nearly reciprocal course, and is likely to pass about one mile clear on our right.

What these photographs cannot show is that in operation, as the ship manoeuvres, the display moves, duplicating the apparent movement of the real world outside the ship, in a way which makes it easy to understand. The trails indicate the aspect of other vessels, as well as their position and speed, facilitating the recognition of a collision risk and the evaluation of possible avoiding action. Thus, a number of well-known and proved techniques have been combined with one new device in a novel and extremely cost-effective manner, to produce a desired result so far not achieved in any other way. The reaction from ship's officers and pilots to the displays now at sea shows that this display is quickly understood and immediately used, often with



appreciative comment on its clarity and ease of interpretation.

7 References

1. IMRAMN, Ministry of Transport International Meeting on Radio Aids to Marine Navigation, May 1946, H.M.S.O.
2. Wylie, F. J., 'The operational value of shipborne radar' (Institute of Navigation Symposium, February 1949), *J. Inst. Navigation*, 2, No. 2, p. 130, April 1949.
3. Hansford, R. F., 'Development of shipborne navigational radar', *J. Inst. Navigation*, 1, p. 118, 1947.
4. Kelly, T. J., 'Improvement in radar presentation'. International meeting on The Use of Radar at Sea, Genoa, Italy, May 1957.
5. Manley, B. W., 'True motion in relative displays', *J. Inst. Navigation*, 15, p. 172, 1962.
6. U.K. Patent No. 966730, etc., 1963.
7. Ranby, P. W., 'An electroluminescent image retaining panel', *Electrical Review*, 174, No. 13, p. 474, 27th March 1964.
8. Shuffleton, W. N. and Evans, N. G., 'A critical evaluation of an experimental collision avoidance system', International Conference on Advances in Marine Navigational Aids, July 1972, p. 177. (IEE Conference Publication No. 87.)
9. Harrison, A., 'The risk of error in predicted c.p.a.', *ibid.*, p. 75.
10. Gasparini, O., Grasso, G., and Pardini, S., 'A smoothing logic with high precision in velocity for naval collision avoidance', *ibid.*, p. 81.
11. Gustafson, B. G. and Ås, B-O., 'System Properties of Jumping-Frequency Radars'. (Svenska AB Philips, Stockholm, 1965).
12. Embling, C. A. and Stewart, J. P., 'A history recording radar display with prediction', *J. Inst. Navigation*, 21, No. 4, p. 471, 1968.
13. Whipps, S. L., 'The Advantages to be Gained by Positioning the Master Gyro Compass Unit at the Roll Centre of a V.L.C.C.' Unpublished internal memorandum, Kelvin Hughes, February 1971.

8 Appendices

8.1 Feasibility of Illuminating the Panel by a Lens

In changing the 'history' display from the photoplot to television the radar data have to be projected on to the image retaining panel in a different way. In the photoplot system direct contact is made with the fibre optic faceplate of the radar c.r.t., and all the light from the screen is conveyed to the panel, during four seconds in each twenty. In the television system an image of the radar display on a small c.r.t. is projected continuously on to the panel by a lens. The question is, will this provide sufficient light to give full exposure of the panel?

Let luminous intensity at screen of c.r.t. = L (lumens/m²)

(a) Using Photoplot

Exposure is 4 s in each 20 s

Illuminance at panel = L (lux)

Panel exposure in 20 s = $4L$ (lux-seconds) (1)

(b) Using lens and television system

Exposure is continuous, i.e. 20 s in each 20 s

Lens: Dallmeyer OCTAC $F/1.4$;

Focal length $f = 0.08$ m

Diameter of lens aperture = $f/1.4 = 0.7f$ (m)

Area of lens aperture = $\pi(0.35f)^2 = 0.386f^2$ (m²) (2)

It is known that the c.r.t. current can be increased by higher drive, and the B phosphor can be replaced by the photographically more efficient P phosphor. This will increase the luminous intensity at the screen of the c.r.t. to at least $7L$ (lumens/m²). For unit magnification of the projected image, lens-to-c.r.t. distance will be $2f$ (m).

Illuminance at lens (Lambertian distribution)
 = $7L/\pi(2f)^2 = 0.56L/f^2$ (lux) (3)

Hence from (2) and (3):

$$\begin{aligned} \text{light entering lens} &= 0.386f^2 \times 0.56L/f^2 \\ &= 0.215L \text{ (lumens)} \end{aligned}$$

$$\begin{aligned} \text{panel exposure in 20 s} &= 20 \times 0.215L \\ &= 4.3L \text{ (lux-seconds)} \end{aligned}$$

which is approximately the same as (1) and is therefore sufficient to make the system feasible.

8.2 Errors in Radar Bearing Data

8.2.1 Glint

Glint is the variation in the shape and position of the echo from a ship. Reference 11 quotes recordings of the apparent position of a stationary ship at 10 km range, using a 16 mm cine camera on an auto-follow radar. The centre of the apparent radar position moved from point to point within and even just beyond the full length of the ship, which subtended 10 milliradians (0.57°). The standard deviation of the error was nearly 3 milliradians (0.17°), or about one-third the apparent angular size of the vessel. This error is random.

8.2.2 Tilt error

This is due to tilt of the axis of rotation of the radar aerial. Reference 9 calculates that a tilt of T radians

produces a bearing error E equal to

$$-\frac{T^2}{4} \sin 2A \text{ radians} = -\frac{T^2}{4} \text{ at maximum}$$

where A is the target's bearing with respect to the direction of tilt. If $T = 10^\circ$, $E = \frac{1}{2}^\circ$ approx. Note that T is squared, which indicates that the error E is *not* reversed by the reverse tilt, i.e. opposite roll.

By converting T into roll and pitch, and A into target's bearing with respect to ship's head, it is shown in Reference 9 that the error has two cyclic components, their frequencies being the beat frequencies between roll and pitch.

Typically these can be roll 12 seconds, pitch 10 seconds, with beats which are:

$$\text{sum} = \frac{12 \times 10}{12 + 10} = 5\frac{1}{2} \text{ s}$$

$$\text{difference} = \frac{12 \times 10}{12 - 10} = 60 \text{ s} = 1 \text{ min}$$

To be successful in minimizing cyclic errors, averaging must extend over an interval of several cycles, i.e. several minutes in this case. If it is essential to obtain accurate predictions in a shorter time than this, the error must be eliminated, e.g. by stabilization, or correction via a vertical reference gyro also linked to the computer-radar system.

8.2.3 Gyro errors

These are caused by transverse acceleration of the directional gyro.¹³ If the gyro is fitted at a height h above the roll centre, in a ship rolling to a maximum angle R at a frequency $\omega/2\pi$ it suffers a maximum transverse acceleration $\omega^2 Rh$ when $\omega t/\pi = 1/2, 3/2, \dots$, etc. The gyro will therefore experience a false vertical at each end of the roll, the apparent angle from the true vertical being B , where

$$\tan B = \omega^2 Rh/g$$

If $R = 10^\circ$

$h = 20$ m

$\omega = 0.7$ (period of roll, 9 s).

Then maximum $B = 9\frac{1}{2}^\circ$ approx.

If the ship is also pitching by an angle a (say 3°) a gymbal error θ is generated where

$$\tan \theta = \sin B \tan a$$

For the values quoted $\theta_{\max} = 35$ min—over half a degree. Because of the required combination of roll and pitch, this error can be resolved into sum and difference components, the latter being of long period, e.g. 1 minute or more as in 8.2.2. This error can be reduced by fitting the gyro near the roll centre. If h is 4 m, the error does not exceed 0.1° for a $\pm 10^\circ$ roll and $\pm 3^\circ$ pitch.

Manuscript first received by the Institution on 11th March 1974 and in final form on 24th April 1974. (Paper No. 1606/AMMS 58.)

© The Institution of Electronic and Radio Engineers, 1974

Application of the normal spectrum technique to the calculation of distortion noise in delta modulators

M. PASSOT, M.Sc., Ingenieur E.C.L.*

and

R. STEELE, B.Sc., C.Eng., M.I.E.E.†

SUMMARY

The paper establishes the theoretical behaviour of the linear delta modulator with the aid of the normal spectrum technique.

The spectral density functions of the signal at the output of the decoder and of the distortion due to quantization effects are calculated for band-limited white noise input signals. The expressions of these spectral density functions derived with the normal spectrum technique enable the results of computer simulation to be easily explained.

Graphical results are presented of the spectral density function of the distortion signal for the coder having different step-sizes and clock rates, and of the decoded signal to noise ratio against input signal power. The computer simulation verifies the authenticity of the theory.

* *Compagnie Electro-Mecanique, Paris; formerly at Loughborough University of Technology.*

† *Electronic and Electrical Engineering Department, University of Technology, Loughborough, Leicestershire LE11 3TU.*

List of Symbols

| | |
|----------------------|---|
| b_n | n th order coefficient associated with $H_n(x)$ |
| $C_{1,n}; C_{2,n}$ | centred and off-centred coefficients respectively |
| C_p^n | binomial coefficients |
| $e(t)$ | error signal in delta modulator |
| $f(x)$ | probability density function of input signal |
| f | frequency |
| f_{c2}, f_{c1} | highest and lowest frequencies in input signal respectively |
| F_p | clock rate of delta modulator |
| $F[], F^{-1}[]$ | Fourier transform and inverse Fourier transform of $[]$ respectively |
| $h(t)$ | impulse function of hold circuit |
| $H_n(x)$ | Hermite polynomial of order n |
| K | gain factor of delta modulator |
| $L(t)$ | binary waveform at the output of the delta modulator |
| N_d^2 | distortion power |
| $N_n =$ | $n! \sigma^{2n}; 0 \leq n < \infty; n$ integer valued |
| $R(), \rho()$ | autocorrelation functions |
| $S(f)$ | spectral density function |
| $S_{nn}^*(f)$ | sampled distortion spectral density function |
| $S_c^*(f), S_o^*(f)$ | sampled centred and off-centred spectral density functions respectively |
| s.q.n.r. | signal/quantization-noise ratio |
| $x(t)$ | band-limited white noise input signal |
| $y(t)$ | signal at the output of the integrator |
| $y_1(t), y_2(t)$ | signals at the output of staircase functions 1 and 2 respectively |
| γ | step-size in $y(t)$ waveform |
| $\delta()$ | delta function |
| $\lambda_x(f)$ | normalized input spectral density function of $x(t)$ when $x(t)$ is low-pass white noise |
| σ^2 | variance of $x(t)$ |
| $\phi_x(f)$ | normalized input spectral density function of $x(t)$ when $x(t)$ is band-pass white noise |

1 Introduction

The motivation for this work came from the British Post Office Research Department at Dollis Hill. Arising out of calculations of the spectral density function of the distortion in p.c.m. systems using the relatively unknown method of 'normal spectrum technique', a contract was placed with the writers to investigate the application of this technique to delta modulation, as the results might be of interest in the context of other Post Office work.

A spin-off from the Loughborough work was a paper on the subject of the application of the normal spectrum technique to the estimation of the distortion spectral density function in delta modulation systems when the latter is frequently overloaded. The paper was published at the Joint Conference on Digital Processing of Signals in Communications held at Loughborough University in April 1972.⁵

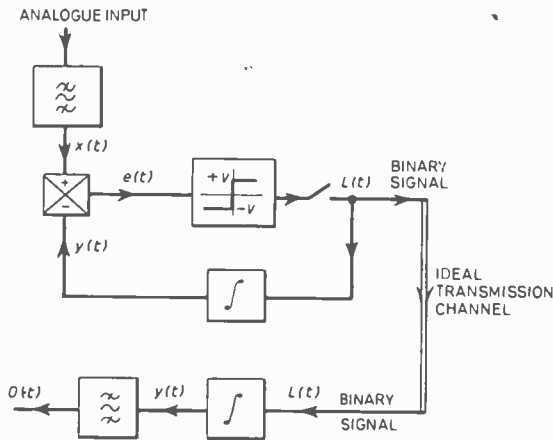


Fig. 1. Block diagram of delta modulation system.

The present paper relates to the essential part of the project and considers the application of band-limited white noise to the delta modulation system, where the latter is *not* overloaded. This problem was considered by van de Weg⁴ but he did not use the normal spectrum technique and he considered a slightly different problem. This paper demonstrates how to apply the normal spectrum technique and shows (unlike van de Weg) that the mathematical results relate in a relatively obvious way to the computer simulated ones. This paper gives results which are relatively easy to understand, and presents graphs of distortion spectral density function and signal/noise ratio as a function of coder parameters, enabling the reader to gain an insight into the way the coder behaves.

Delta modulation and pulse code modulation codecs employed for the purpose of transmitting speech signals in a binary form are frequently tested by using the well-defined band-limited white noise signal. This signal has a Gaussian amplitude probability density function which has orthogonal properties with the Hermite polynomial. When such a Gaussian signal is applied to a memoryless non-linearity the autocorrelation and spectral density functions of the output signal can be expressed in terms of the Hermite polynomial. There are advantages in making use of the Hermite polynomial to calculate these functions as mentioned in Appendix 1, and the method is known as the normal spectrum technique.

Because the delta modulator is shown in Section 2 to be composed of the type of non-linearities which can be suitably handled by this technique, the main objectives of the paper are to apply this technique to calculate the spectral density functions of the signal at the output of the decoder, the quantization noise and decoded signal/noise ratio. A bonus obtained by using the analytical method is that the computer simulation results are easily interpreted in terms of the mathematical conclusions.

Before using the normal spectrum technique the close-loop non-linear sampled data control system, known as a delta modulator, must be rearranged as an open loop system. This is discussed in Section 2.

2 Open-loop Model of the Delta Modulator

The linear delta modulation system is shown in Fig. 1. Its behaviour has been described in many papers¹⁻⁵ and consequently will not be repeated here, except to say that in Fig. 1 $x(t)$ is a band-limited input signal which is encoded into a binary waveform $L(t)$ by the encoder. The decoding is achieved by integrating $L(t)$ to form $y(t)$ which is a step-like approximation to $x(t)$ as illustrated in Fig. 2. The final decoded output $o(t)$ is obtained from $y(t)$ by passing the latter through a filter which removes its unwanted high frequencies.

In spite of the apparent simplicity of the delta modulation system there is surprisingly great difficulty in calculating its performance. The analysis is profoundly reduced by replacing the delta modulator by an open loop model whose output voltage is identical to the voltage $y(t)$ at the output of the integrator in Fig. 1. Such a model was proposed by van de Weg in his classic paper.⁴

The justification of this model will briefly be recalled before embarking on the analysis of the behaviour of this model when it is probed with Gaussian input signals.

An essential pre-requisite to the establishment of this model is that the delta modulator does not experience slope overload. Given this condition, at any particular sampling instant, the value of the voltage $y(t)$ after two successive sampling instants will be either the same or it will have increased or decreased by 2γ , where γ is the step size in the $y(t)$ waveform. This statement is easily verified by inspection of Fig. 2 which shows $y(t)$ tracking the baseband input signal $x(t)$.

This characteristic of the delta modulator means that an open loop model can be postulated as shown in Fig. 3. The staircase functions employed in this model are shown in Fig. 4. At $t = 0$ let $y(t) = 0$, hence the output $y(t)$ at even clock times corresponds to sampling the output of the staircase 1, namely $y_1(t)$, at even clock times and holding this sample for one clock period, i.e. half the sampling time of $y_1(t)$. The output $y(t)$ at odd clock times involves sampling $y_2(t)$ at these times and holding these samples for one clock period. Observe that the necessity for having two staircase functions is due to the certainty of the magnitude of $y(t)$ every other clock instant, and the changes if they occur will not be γ but 2γ . It is this 2γ which determines the 'tread' of the staircase. The relative displacement of the two staircases

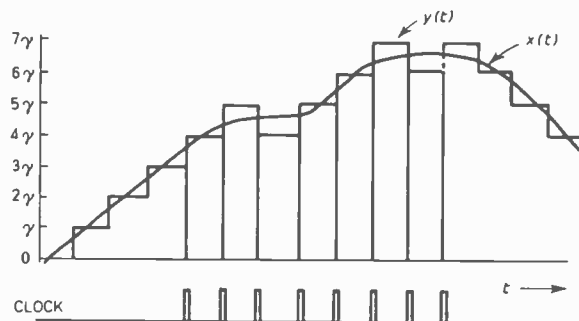


Fig. 2. $y(t)$ tracking $x(t)$.

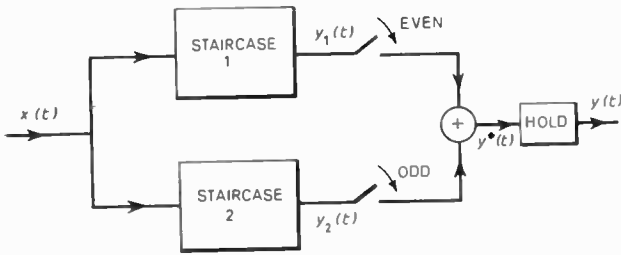


Fig. 3. Infinite staircase model of delta modulator.

enables $y(t)$ in Figs. 1 and 3 to be identical.

Thus $y(t)$ in the model is formed by sampling $y_1(t)$ at even clock times, sampling $y_2(t)$ at odd clock times, combining these samples in an adder, and finally holding these samples for one clock period.

It should be noted that if slope overload occurs, a condition which commences when the slope of the input signal exceeds the maximum slope of $y(t)$, then the value which $x(t)$ can acquire between two adjacent clock intervals may be greatly in excess of 2γ , and therefore the staircase functions are invalidated. In slope overload approximate models can be used.^{3,5}

3 Derivation of the Sampled Spectral Density Function of the Signal at the Output of the Integrator

The autocorrelation of the signal at the output of the adder in Fig. 3 at even clock times is

$$R_{yy}^*(2mT) = R_{y_1y_1}^*(2mT) + R_{y_2y_2}^*(2mT) \quad (1)$$

and at odd clock times is

$$R_{yy}^*\{(2m-1)T\} = R_{y_1y_2}^*\{(2m-1)T\} + R_{y_2y_1}^*\{(2m-1)T\} = 2R_{y_1y_2}^*\{(2m-1)T\} \quad (2)$$

Equations (1) and (2) are obvious if an arbitrary waveform is sketched and its autocorrelation function examined at odd and even sampling intervals.

The complete expression of the autocorrelation function of $y^*(t)$ at clock times is

$$R_{yy}^*(nT) = R_{yy}^*(2mT) + R_{yy}^*\{(2m-1)T\}$$

Let

$$\begin{aligned} \rho_1(\theta) &= R_{y_1y_1}(\theta) + R_{y_2y_2}(\theta) \\ \rho_2(\theta) &= 2R_{y_1y_2}(\theta) \end{aligned}$$

Using the result given in Appendix 9.3, and noting that the effect of alternating sampling is that the sampling rate of the staircase functions is $F_p/2$,

$$\begin{aligned} \rho_1^*(2mT) &= \rho_1(\theta) \cdot \frac{F_p}{2} \sum_{m=-\infty}^{\infty} \delta(\theta - 2mT) \\ \rho_2^*\{(2m-1)T\} &= \rho_2(\theta) \cdot \frac{F_p}{2} \sum_{m=-\infty}^{\infty} \delta(\theta - (2m-1)T) \end{aligned}$$

Hence

$$R_{yy}^*(nT) = \rho_1^*(2mT) + \rho_2^*\{(2m-1)T\} \quad (3)$$

The next step is to take the Fourier transform of equation (3). Now the Fourier transform of an impulse train, where each impulse is separated by $2T$ seconds

and an impulse exists at $t = 0$, is a frequency impulse train whose impulses are spaced by $(1/2T)H_z$ and every impulse has a positive magnitude of $(1/2T)$. This is the situation of the 'even' impulse train. The Fourier transform of the 'odd' sampled impulse train is a frequency impulse train whose impulses are again spaced by $(1/2T)H_z$ but whose polarity alternates between adjacent impulses, although their magnitudes are $(1/2T)$.

Thus if

$$F[\rho_1^*(2mT)] = S_1^*(f)$$

where $F[]$ means Fourier transform then

$$F[\rho_2^*\{(2m-1)T\}] = (-1)^m S_2^*(f)$$

Using the result of equation (35), the Fourier transform of equation (3) is

$$S_{yy}^*(f) = \left(\frac{F_p}{2}\right)^2 \sum_{m=-\infty}^{\infty} \left\{ S_1 \left(f + m \frac{F_p}{2} \right) + (-1)^m \cdot S_2 \left(f + m \frac{F_p}{2} \right) \right\} \quad (4)$$

In order to express $S_{yy}(f)$ in terms of the normal spectrum the arguments in Appendix 9.4 are invoked where it is noticed that a sampled spectrum having an equation of the form shown in equations (35) or (4) can be represented in the normal spectrum form of equation (37).

Now

$$\frac{F_p^2}{4} \sum_{m=-\infty}^{\infty} S_1 \left(f + m \frac{F_p}{2} \right)$$

forms a Fourier transform pair with

$$R_{y_1y_1}^*(2nT) + R_{y_2y_2}^*(2nT)$$

hence

$$S_1^*(f) = \sum_{n=0}^{\infty} b_{1,n}^2 N_n \{ \phi_x^n(f) \}^* + \sum_{n=0}^{\infty} b_{2,n}^2 N_n \{ \phi_x^n(f) \}^* \quad (5)$$

where $b_{1,n}$ and $b_{2,n}$ are related to the staircase functions 1 and 2 respectively (see Fig. 3) and are defined by equation (28) for $y_1(x)$ and $y_2(x)$ respectively.

By a similar argument and the application of equation (38) in Appendix 9.6 the spectral density component of $S_{yy}^*(f)$ at odd sampling times is

$$S_2^*(f) = \sum_{n=0}^{\infty} 2b_{1,n} \cdot b_{2,n} \cdot N_n \{ \phi_x^n(f) \}^* \quad (6)$$

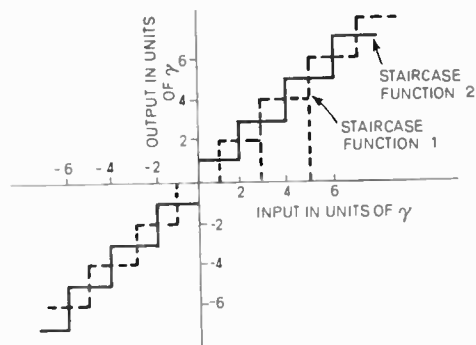


Fig. 4. Staircase functions.

where

$$\{\phi_x^n(f)\}^* = \frac{F_p^2}{4} \sum_{m=-\infty}^{\infty} \phi_x^n\left(f + m \frac{F_p}{2}\right)$$

at even sampling times, and is amended by the inclusion of $(-1)^m$ to give $\{\phi_x^n(f)\}^*$ at odd sampling times.

Summing equations (5) and (6) enables equation (4) to be expressed as:

$$S_{yy}^*(f) = \frac{F_p^2}{4} \sum_{n=0}^{\infty} \sum_{m=-\infty}^{\infty} \left\{ b_{1,n}^2 N_n \cdot \phi_x^n\left(f + m \frac{F_p}{2}\right) + b_{2,n}^2 N_n \cdot \phi_x^n\left(f + m \frac{F_p}{2}\right) + 2b_{1,n} \cdot b_{2,n} N_n \cdot \phi_x^n\left(f + m \frac{F_p}{2}\right) \cdot (-1)^m \right\} \quad (7)$$

This equation can be simplified by splitting the sum into m odd, where $m = 2p - 1$; and m even, where $m = 2p$. This means that the double summation in equation (7) now contains 6 additive terms instead of three. The $(-1)^m$ becomes $(-1)^{2p} = 1$ and $(-1)^{2p-1} = -1$ and hence equation (7) is:

$$S_{yy}^*(f) = \frac{F_p^2}{4} \left\{ \sum_{n=0}^{\infty} \sum_{p=-\infty}^{\infty} N_n (b_{1,n} + b_{2,n})^2 \cdot \phi_x^n(f + pF_p) + \sum_{n=0}^{\infty} \sum_{p=-\infty}^{\infty} N_n (b_{1,n} - b_{2,n})^2 \cdot \phi_x^n\left(f + (2p-1) \frac{F_p}{2}\right) \right\} \quad (8)$$

and using equation (36),

$$S_{yy}^*(f) = \sum_{n=0}^{\infty} N_n \cdot \frac{1}{4} (b_{1,n} + b_{2,n})^2 \{\phi_x^n(f)\}^* + \sum_{n=0}^{\infty} N_n \cdot \frac{1}{4} (b_{1,n} - b_{2,n})^2 \left\{ \phi_x^n\left(f - \frac{F_p}{2}\right) \right\}^* \quad (9)$$

In equation (7) the sampling rate was $F_p/2$, but in equation (9) the first term is sampled at F_p while the second term involves sampling at $F_p/2$. $\phi_x^n(f + pF_p)$ is identical to $\phi_x^n(f + (2p-1)F_p/2)$ by frequency shifting, and $(b_{1,n} \pm b_{2,n})^2$ is relatively easy to compute. Thus equation (9) is easier to compute than equation (7).

Summarizing, the sampled autocorrelation functions and the cross-correlation function for the signals $y_1(t)$ and $y_2(t)$ which appear at the output of the staircase functions were used to establish the sampled autocorrelation function $R_{yy}^*(\cdot)$ at the output of the adder in Fig. 3. The corresponding spectral density function $S_{yy}^*(f)$ was established for sampling at half the delta modulator clock rate at odd and even clock instants. A subsequent manipulation resulted in two sets of sampled spectral densities, one set corresponding to sampling at the delta modulator clock rate of F_p , and the other shifted by a frequency $F_p/2$. These spectra are referred to here as centred and off-centred sampled normal spectral density functions.

4 Calculation of the Distortion Spectrum

The distortion in the decoded signal is due to $x(t)$ being quantized in amplitude and time. The difference between the signals at the output and input of the staircase functions causes amplitude quantizations.

Let $\Delta y_1(t)$ and $\Delta y_2(t)$ be the differences between the output and input signals of staircase functions 1 and 2 respectively shown in Fig. 4:

$$y_1(t) = x(t) + \Delta y_1(t) \quad (10)$$

$$y_2(t) = x(t) + \Delta y_2(t) \quad (11)$$

Let $b'_{1,n}$ and $b'_{2,n}$ be related to signals $\Delta y_1(t)$ and $\Delta y_2(t)$ respectively.

Before proceeding to establish the distortion spectral density, the relationship between the b coefficients associated with the $y_1(t)$, $y_2(t)$ signals and the $\Delta y_1(t)$, $\Delta y_2(t)$ signals must be established.

From equation (28)

$$b'_n = \frac{1}{N_n} \int_{-\infty}^{\infty} H_n(x) \cdot (z(x) - x) \cdot f(x) dx$$

$$= b_n - \frac{1}{N_n} \int_{-\infty}^{\infty} H_n(x) \cdot x \cdot f(x) dx$$

$$b'_n = b_n - b_{x,n} \quad (12)$$

Now

$$b_{x,1} = \frac{1}{\sigma^2} \int_{-\infty}^{\infty} x^2 f(x) dx$$

$$b_{x,2} = \frac{1}{2\sigma^4} \int_{-\infty}^{\infty} x^3 f(x) dx - \frac{1}{2\sigma^2} \int_{-\infty}^{\infty} x f(x) dx$$

$$b_{x,3} = \frac{1}{6\sigma^6} \int_{-\infty}^{\infty} x^4 f(x) dx - \frac{1}{2\sigma^4} \int_{-\infty}^{\infty} x^2 f(x) dx$$

Now

$$\int_{-\infty}^{\infty} x^n f(x) dx = \begin{cases} 1, 3, \dots (n-1)\sigma^n, & \text{for } n \text{ even} \\ 0 \dots & \text{for } n \text{ odd} \end{cases}$$

Hence,

$$b_{x,1} = 1 \text{ and } b_{x,n} = 0 \text{ for } n \geq 2 \quad (13)$$

and equation (12) becomes

$$b'_1 = b_1 - 1, \quad n = 1 \\ b'_n = b_n, \quad n \geq 2 \quad (14)$$

Because of the asymmetrical property of the characteristic, the b coefficients for n even are zero, and using the result of equation (14), the sampled spectral density of the $y(t)$ signal is from equation (9).

$$S_{yy}^*(f) = \frac{\sigma^2}{4} (b'_{1,1} + b'_{2,1} + 2)^2 \{\phi_x(f)\}^* + \frac{1}{4} \sum_{n=2}^{\infty} N_n (b'_{1,n} + b'_{2,n})^2 \{\phi_x^n(f)\}^* + \frac{1}{4} \sum_{n=0}^{\infty} N_n (b'_{1,n} - b'_{2,n})^2 \left\{ \phi_x^n\left(f - \frac{F_p}{2}\right) \right\}^*$$

and

$$(b'_{1,1} + b'_{2,1} + 2)^2 = 4(1 + b'_{1,1} + b'_{2,1}) + (b'_{1,1} + b'_{2,1})^2$$

so that:

$$S_{yy}^*(f) = \sigma^2(1 + b'_{1,1} + b'_{2,1}) \{\phi_x(f)\}^* + \frac{1}{4} \sum_{n=0}^{\infty} N_n (b'_{1,n} + b'_{2,n})^2 \{\phi_x^n(f)\}^* + \frac{1}{4} \sum_{n=0}^{\infty} N_n (b'_{1,n} - b'_{2,n})^2 \left\{ \phi_x^n\left(f - \frac{F_p}{2}\right) \right\}^* \quad (15)$$

or

$$S_{yy}^*(f) = \sigma^2(1 + b'_{1,1} + b'_{2,1})\{\phi_x(f)\}^* + S_{nn}^*(f) \quad (16)$$

$S_{nn}^*(f)$ is the sampled distortion spectral density of the delta modulator and given by:

$$S_{nn}^*(f) = \sum_{n=0}^{\infty} \left(\frac{b'_{1,n} + b'_{2,n}}{2}\right)^2 N_n \{\phi_x^n(f)\}^* + \sum_{n=0}^{\infty} \left(\frac{b'_{1,n} - b'_{2,n}}{2}\right)^2 N_n \left\{\phi_x^n\left(f - \frac{F_p}{2}\right)\right\}^* \quad (17)$$

Equations (9) and (16) both represent the sampled density of the delta modulator output signal $y(t)$. However, equation (16) separates this $S_{yy}^*(f)$ into two terms; one $S_{nn}^*(f)$ is due to time and amplitude quantization and therefore is a distortion term, while the first term in this equation indicates a 'gain' factor K for the coder.

$$K = (1 + b'_{1,1} + b'_{2,1}) \quad (18)$$

K in most cases is not significantly different from 1.

4.1 Centred and Off-centred Spectral Densities

A more convenient way of writing equation (17) is to put

$$C_{1,n} = N_n \left(\frac{b'_{1,n} + b'_{2,n}}{2}\right)^2 \quad (19)$$

$$C_{2,n} = N_n \left(\frac{b'_{1,n} - b'_{2,n}}{2}\right)^2 \quad (20)$$

such that

$$S_{nn}^*(f) = \sum_{n=0}^{\infty} C_{1,n} \{\phi_x^n(f)\}^* + \sum_{n=0}^{\infty} C_{2,n} \left\{\phi_x^n\left(f - \frac{F_p}{2}\right)\right\}^* = S_c^*(f) + S_o^*(f) \quad (21)$$

$S_c^*(f)$ and $S_o^*(f)$ are the centred and off-centred sampled spectral densities respectively. This terminology has been used as $S_o^*(f)$ consists of $\phi_x^n(f)$ shifted in frequency by $F_p/2$.

The introduction of these spectral densities gives understanding to the variation of $S_{nn}(f)$ with frequency as will be demonstrated in subsequent sections.

Some useful observations concerning the variation of $C_{1,n}$ and $C_{2,n}$ as a function of n for constant input power of unity and two values of step-sizes equal to 1.0 and 2.0 are as follows:

- (i) As n is increased from zero, $C_{2,n}$ has a maximum before $C_{1,n}$ irrespective of step-size (γ).
- (ii) For a given n , there are more maxima and minima in the $C_{1,n}$ and $C_{2,n}$ coefficients if the step size is increased.
- (iii) For small step-size $C_{2,n}$ is more important than $C_{1,n}$ for a large range of n from zero upwards. Hence $S_{nn}(f)$ will be largely controlled by $S_o(f)$, indicating large values of $S_{nn}(f)$ in the vicinity of $F_p/2$.
- (iv) The average magnitude of $C_{1,n}$ and $C_{2,n}$ decrease with increasing n .
- (v) The average magnitude of $C_{1,n}$ and $C_{2,n}$ is higher when the step-size is increased.

4.2 Distortion Noise

If the input signal is band-limited between frequencies f_{c2} and f_{c1} , then the distortion power is

$$N_d^2 = 2 \int_{f_{c1}}^{f_{c2}} S_{nn}(f) df \quad (22)$$

A useful representation of N_d^2 is obtained with the aid of equation (21),

$$N_d^2 = 2 \int_{f_{c1}}^{f_{c2}} \{S_c^*(f) + S_o^*(f)\} \cdot |H(j2\pi f)|^2 df \quad (23)$$

where $H(j2\pi f)$ is the transfer function of the sample and hold circuit:

$$H(j2\pi f) = \frac{1}{F_p} \cdot \frac{\sin(\pi f/F_p)}{(\pi f/F_p)} \quad (24)$$

4.3 Signal/Quantization-noise Ratio (s.q.n.r.)

Provided the coder is symmetrical and there are no channel errors, then there is no noise at the output of the decoder in the absence of a signal due to the bandpass filter in the decoder.

From equations (16), (18) and (23)

$$\text{s.q.n.r.} = \frac{\sigma^2 K \int_{f_{c1}}^{f_{c2}} \{\phi_x(f)\}^* \cdot |H(j2\pi f)|^2 df}{\int_{f_{c1}}^{f_{c2}} (S_c^*(f) + S_o^*(f)) \cdot |H(j2\pi f)|^2 df} \quad (25)$$

5 Presentation of Results

The sampled distortion spectral density function $S_{nn}^*(f)$ has been calculated, and then normalized by dividing by F_p^2 to give the ordinates in Figs. 5, 6 and 7.

The actual $S_{nn}(f)$ which occurs in a delta modulator is equal to $(S_{nn}^*(f)/F_p^2)$ multiplied by

$$[\{\sin(\pi f/F_p)\}/(\pi f/F_p)]^2$$

The theoretical results are compared with those obtained by computer simulation of the delta modulator. In all cases the highest frequency in the input signal has been normalized to unity, although the lowest frequency in this signal has been varied in some experiments.

In order to calculate $S_{nn}^*(f)$ for step sizes γ other than unity, σ in all the equations is replaced by (σ/γ) .

As the theory presupposes that slope overload is avoided then it is necessary for the slope of the input signal to be less than or equal to γF_p . A Gaussian signal having a mean square value of σ^2 and band-limited to $f_{c2} Hz$ has a mean square derivative of σ_d^2 where

$$\sigma_d^2 = \frac{\sigma^2}{3} \cdot (2\pi f_{c2})^2$$

If $\sigma_d < (\gamma F_p/4)$ the probability of the coder experiencing slope overload is less than 4×10^{-5} .

Hence

$$\frac{F_p}{f_{c2}} \geq \frac{\sigma}{\gamma} \cdot \frac{8\pi}{\sqrt{3}}$$

for low-pass white noise input, and f_{c2} is replaced in

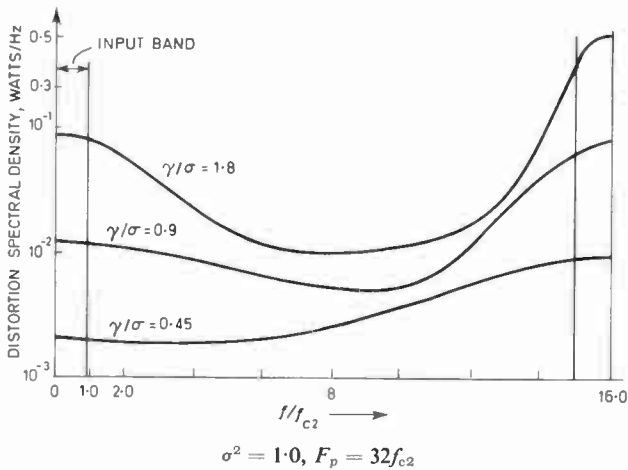


Fig. 5. Effect of step-size on distortion spectral density.

the above inequality by

$$f_{c2} \cdot \left\{ \frac{1 - \left(\frac{f_{c2}}{f_{c1}}\right)^3}{1 - \left(\frac{f_{c2}}{f_{c1}}\right)} \right\}^{1/2}$$

for band-pass white noise input.

6 Discussion of Results

From the theoretical results established in this paper and in particular equations (21), (35) and (23) the sampled distortion spectral density function $S_{nn}^*(f)$ at the output of the integrator in the delta modulator is composed of two periodic spectral density functions. The centred spectral density function $S_c(f)$ is located at d.c., $\pm f_p$, $\pm 2f_p$, $\pm 3f_p$, etc., while the off-centred spectral density functions $S_o(f)$ is centred at $\pm f_p/2$, $\pm 3f_p/2$, $\pm 5f_p/2$, etc. The part of $S_{nn}(f)$ which gives rise to the quantization noise in the final decoded signal $0(t)$ is located in the frequency band occupied by $x(t)$. Thus the most important constituents of $S_{nn}(f)$ are the spectra located at d.c. and at $\pm f_p/2$.

When the input signal is low-pass white noise, and the delta modulator has a large step-size γ , both the centred and off-centred spectra are significant resulting in an

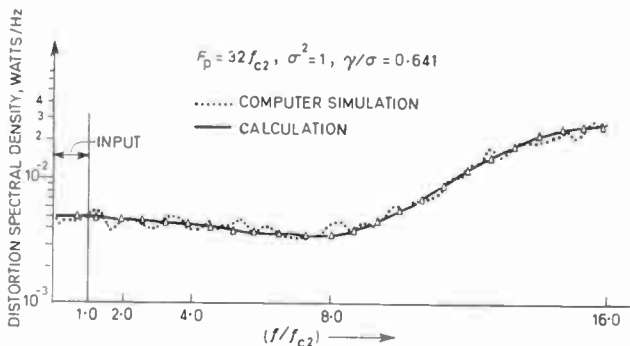


Fig. 6. Distortion spectral density function. Comparison between the theoretical curve and the one obtained by computer simulation. Clock rate = $32f_{c2}$, input power = 1.0, step size = 0.641.

$S_{nn}^*(f)$ function which is peaked at d.c. and $\pm f_p/2$, with a minimum close to $\pm f_p/4$. By choosing a low value of γ , which represents a good coding condition, the coefficients $C_{2,n}$ defined by equation (20) are negligible for low values of n with the result that only the off-centred spectra $S_o(f)$ make significant contributions to $S_{nn}(f)$. The situation is illustrated in Fig. 5 where it is seen that the quantization noise in the message band is greatly reduced for lower values of γ .

Application of a narrow-band input signal, such as one whose spectral density function $S_{xx}(f)$ is defined from $0.8f_{c2}$ to f_{c2} , causes $S_{nn}^*(f)$ to oscillate about the curves displayed in Fig. 5. This oscillatory nature originates from the repeated autoconvolution of $S_{xx}(f)$. The curves in Fig. 5 are smooth because $S_{xx}(f)$ is a wideband signal, and its repeated autoconvolution causes overlapping of the spectra.

Figure 6 shows the distortion spectral density function obtained by using the theoretical results established in the paper, and the curve produced by computer simulation of the delta modulation system. The slight discrepancy between the two curves is due to imperfect Gaussian input signal used in the simulation.

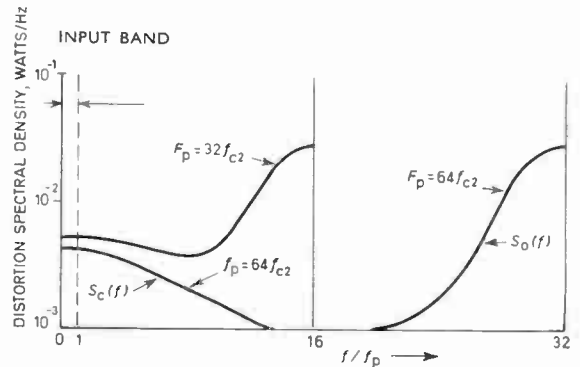


Fig. 7. Effect of clock rate on distortion spectral density.

$$\gamma/\sigma = 0.65, \sigma^2 = 1$$

Variation of the clock rate f_p does not influence the shape of the centred and off-centred distortion spectra, but it does affect their location. If f_p is increased to the point where the off-centred spectra at $\pm f_p/2$ do not contribute to the in-band noise then no further increase in f_p will reduce the effects of quantization noise. This is demonstrated in Fig. 7, where it is apparent that increasing f_p to $64f_{c2}$ is unnecessary as the spectra at $\pm f_p/2$ has already ceased to contribute to the quantization noise in the message band for lower values of f_p .

The decoded s.q.n.r. is only marginally affected by the shape of the input spectral density function provided that these functions occupy the same bandwidth. However, the s.q.n.r. is greater for a signal whose input spectral density occupies a narrower frequency band than another signal, although the power in both signals is identical.

The s.q.n.r. as a function of input level is shown in

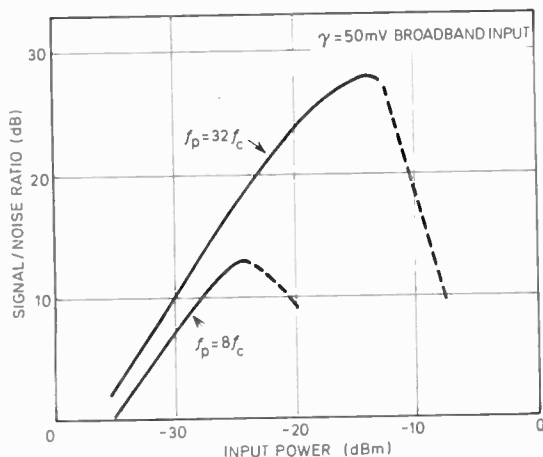


Fig. 8. Signal to noise ratio as a function of input power.

Fig. 8 for two different f_p/f_c ratios. The solid lines represent s.q.n.r., while the dotted lines indicate the presence of a slope overload condition. These curves highlight that for a given set of coding conditions there is only one optimum input level, and that because the s.q.n.r. increases nearly linearly with input level, the quantization noise is nearly independent of the level of the input signal.

Considerable attention has been given to the distortion spectral density function $S_{nn}(f)$ prior to the final filtering in the decoder. It has been shown that a knowledge of $S_{nn}(f)$ enables the noise in the message band, i.e. the noise which will be passed by the final low pass filter, to be ascertained as a function of the input signal and the parameters of the delta modulation codec.

7 Acknowledgments

The authors wish to express their gratitude to the Post Office for sponsoring this work and specifying that the Normal Spectrum technique should be used. They are also grateful to R. W. Berry of the Post Office for his advice and to Professor J. W. R. Griffiths of Loughborough University for his encouragement.

8 References

1. Steele, R., 'Delta Modulation Systems' (Pentech Press, London, 1974).
2. Passot, M. and Steele, R., 'Application of the Normal Spectrum Technique to the Calculation of Distortion Noise in Delta Modulators', Departmental Memorandum No. 76, Electronic and Electrical Engineering Dept., University of Technology, Loughborough. (Obtainable on request from the University Library.)
3. Aaron, M. R., Fleischman, J. S., McDonald, R. A. and Protonotarios, E. N., 'Response of delta modulation to Gaussian signals', *Bell Syst. Tech. J.*, **48**, pp. 1167-95, May-June 1969.
4. van de Weg, H., 'Quantizing noise of a single integration delta modulation system with N-digit code', *Philips Res. Repts*, **8**, pp. 367-85, 1953.
5. Steele, R. and Passot, M., 'Slope-limiter model of a delta modulator in slope overload with Gaussian input signal', Joint Conference on 'Digital Processing of Signals in Communications', University of Loughborough, 1972, pp. 285-304. (IERE Conference Proceedings No. 23.)

6. Thomson, W. E., 'The response of a linear system to random noise', *J. Instn Elect. Engrs*, **102**, Part C, pp. 46-48, September 1954. (IEE Monograph No. 106R.)
7. Barrett, J. R. and Lampard, D. G., 'An expansion for some second-order probability distributions and its application to noise problems', *IRE Trans. on Information Theory*, IT-1, No. 1, pp. 10-15, March 1955.
8. Kettel, E., 'The non-linear distortion of a noise signal with normal distribution', *Archiv Elektrischen Ubertrag.*, **22**, No. 4, pp. 165-70, April 1968.

9 Appendices

These appendices which state some important results used in this paper have been derived in references 1 and 2.

9.1 Normal Spectrum Technique

Details of this relatively little known technique are given in references 6, 7 and 8. Because this paper is concerned with the application of this technique only the essential assumptions and formulae will be stated.

The input signal $x(t)$ having a Gaussian amplitude probability density function $f(x)$, variance σ^2 , zero mean, autocorrelation coefficient $\rho_x(\tau)$, normalized spectral density $\phi_x(f)$ and stationary statistical properties, is applied to an isolated memoryless non-linear element having a non-linear characteristic. If this characteristic has an output and an input designated v and u respectively, then v is a non-linear function of u , i.e. $v = z(u)$ say. When $x(t)$ is applied to the non-linear element, the resulting $y(t)$ signal is equal to $z(x(t))$.

Then the normal spectrum techniques expresses the autocorrelation function $R_y(\tau)$ of the signal $y(t)$ at the output of the non-linear element as:

$$R_y(\tau) = \sum_{n=0}^{\infty} b_n^2 N_n \rho_x^n(\tau) \tag{26}$$

where

$$N_n = n! \sigma^{2n} \tag{27}$$

$$b_n = \frac{1}{N_n} \int_{-\infty}^{\infty} H_n(x) z(x) f(x) dx \tag{28}$$

$$f(x) = \frac{1}{\sigma\sqrt{2\pi}} \cdot \exp\left(-\frac{x^2}{2\sigma^2}\right) \tag{29}$$

and $H_n(x)$ is the Hermite polynomial of order n expressed by

$$H_n(x) = (-1)^n \sigma^{2n} \exp\left(\frac{x^2}{2\sigma^2}\right) \frac{d^n}{dx^n} \left\{ \exp\left(-\frac{x^2}{2\sigma^2}\right) \right\} \tag{30}$$

In equations (28), (29) and (30), $x(t)$ has been written as x . The corresponding spectral density $S_y(f)$ is

$$S_y(f) = \sum_{n=0}^{\infty} b_n^2 N_n \phi_x^n(f) \tag{31}$$

where

$$\phi_x^n(f) = \int_{-\infty}^{\infty} \rho_x^n(\tau) \exp(-j2\pi f\tau) \cdot d\tau \tag{32}$$

For convenience $\phi_x(f)$ will be considered to be band-pass white noise, although the technique is independent of the shape of $\phi_x(f)$.

An advantage of this technique is that the autocorrelation and spectral density functions are represented by simple power series, rather than the joint

probability density function required in the integral form of these functions.

9.2 Autoconvolution of the Spectral Density of Band-pass White Noise

Equation (31) shows that the input spectral density has to be convolved with itself n times. For large values of n , $\phi_x^n(f)$ has a Gaussian shape. The method of calculating $\phi_x^n(f)$ when $\phi_x(f)$ is band-limited white noise is:

$$\phi_x^n(f) = \frac{1}{2^n} \sum_{p=0}^n C_p^n \cdot \lambda_x^n(f - (n-2p)f_{ab}) \quad (33)$$

where the $\lambda_x(f)$ function is the spectral density from $f = -1$ to $f = +1$, having a magnitude of 0.5 volts²/Hz, f_{ab} is the mid-band frequency of the band-limited signal and C_p^n are the binomial coefficients.

This calculation means that $\phi_x^n(f)$ is achieved by convolving the simple low-pass spectral density $\lambda_x(f)$ with itself n times and then weighted by binomial coefficients and shifted in frequency to various positions in the spectrum. This is simpler than convolving the band-pass spectral density $\phi_x(f)$ with itself n times.

As n is made large, the computation of $\phi_x^n(f)$ by equation (33) becomes arduous. However, as $\phi_x^n(f)$ tends to a Gaussian curve as n becomes large the necessity of using equation (33) is removed as the shape of the Gaussian curve is defined by a simple mathematical relationship.

9.3 Autocorrelation of Sampled Waveforms

The sampled autocorrelation function is equal at multiples of the sampling period to the autocorrelation function multiplied by the clock rate F_p . The value of F_p can be above or below the Nyquist rate. Stated mathematically

$$R^*(nT) = F_p R(nT) \quad (34)$$

9.4 Sampled Normal Spectra

A signal having a spectral density $S(f)$ when sampled at a rate of F_p will have a sampled spectral density $S^*(f)$:

$$S^*(f) = F_p^2 \sum_{m=-\infty}^{\infty} S(f+mF_p) \quad (35)$$

i.e. $S^*(f)$ consists of multiple spectra $S(f)$ spaced F_p apart. $S(f+mF_p)$ is immediately available in terms of normal spectra by invoking equation (31), and hence

$$S^*(f) = F_p^2 \sum_{m=-\infty}^{\infty} \sum_{n=0}^{\infty} b_n^2 N_n \phi_x^n(f+mF_p)$$

Writing

$$\{\phi_x^n(f)\}^* = F_p^2 \sum_{n=-\infty}^{\infty} \phi_x^n(f+mF_p) \quad (36)$$

gives

$$S^*(f) = \sum_{n=0}^{\infty} b_n^2 N_n \{\phi_x^n(f)\}^* \quad (37)$$

Above a given value of n , the value of $\phi_x^n(f)$ is independent of n and frequency.

9.5 Sample and Zero-order Hold Circuit

It is shown² that the input and output autocorrelation functions of a sample and hold circuit are identical at multiples of the sampling period.

The output autocorrelation function is composed of straight line segments between the sampling instants.

9.6 Cross-spectral Density Function in Terms of Normal Spectra

Let $y(t)$ and $z(t)$ be two non-linear functions of $x(t)$ such that

$$y(t) = \sum_{n=0}^{\infty} b_{1,n} \cdot H_n[x(t)]$$

$$z(t) = \sum_{m=0}^{\infty} b_{2,m} \cdot H_m[x(t)]$$

then the cross-spectral density function is

$$S_{y,z}(f) = \sum_{n=0}^{\infty} b_{1,n} \cdot b_{2,n} \cdot N_n \phi_x^n(f) \quad (38)$$

Manuscript first received by the Institution on 5th January 1973, in revised form on 22nd January 1974 and in final form on 3rd May 1974. (Paper No. 1609/CC213.)

© The Institution of Electronic and Radio Engineers, 1974

Low-noise microwave amplification using transferred-electron and baritt devices

Professor P. N. ROBSON,
Ph.D., C.Eng., F.I.E.E.*

SUMMARY

The small signal amplifying properties of both GaAs and InP transferred electron devices and of Si baritt devices are considered using simple physical models. InP is predicted theoretically to be capable of providing devices having the lowest noise measure. The paper shows that, for transferred-electron amplifiers, an optimum value of n/μ product exists for lowest noise measure.

* Department of Electronic and Electrical Engineering, University of Sheffield, Mappin Street, Sheffield S1 3JD.

1 Introduction

In the last two-and-a-half years, two new microwave amplifiers, which have fairly low noise properties, have been demonstrated. They are the transferred electron amplifier (t.e.a.)¹⁻⁷ and the barrier injection transit-time diode (or baritt).^{8,9} The principal source of noise in both devices comes from the random motion of the free charge carriers. Because the electric fields in both devices are relatively high (more than several kV/cm), the free charge carriers are heated above the lattice temperature and are said to be 'hot'. The fluctuations generated by these hot carriers is a form of Johnson noise. Because, however, the carriers are not in thermal equilibrium with the lattice, the normal Nyquist treatment of noise is not valid.¹⁰

The purpose of the present paper, which is largely tutorial in content, is to show firstly how the noise figure of these amplifiers can be calculated, then to compare the theory with experiment where possible, and finally to show that the presently obtainable noise figures of 10dB at X band^{3,5} (~ 10 GHz) which are typical, are in some cases not a lower bound, particularly for t.e. amplifiers.

Both types of amplifier are reflexion amplifiers. The situation is shown schematically in Fig. 1 where the device is represented as a single-port network terminating

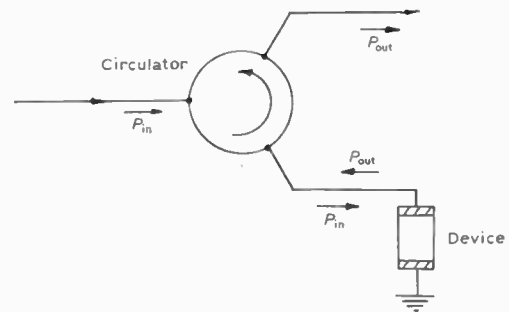


Fig. 1. Schematic of circulator coupled reflexion amplifier.

a length of transmission line. A circulator is used to separate input and reflected signals. If the amplifier has an input impedance with a negative real part at the frequency of operation, then the reflected signal will be greater than the incident signal and gain will ensue.

We start by calculating the input impedance of the t.e.a. as a function of frequency before going on to evaluate its noise figure. Instead of using the more conventional a.c. small signal analysis, we will concentrate throughout on calculating the impulse response since the physical operation appears so much more clearly by thinking in the time domain rather than the frequency domain.

2 Input Impedance of the T.E.A.

Transferred electron amplifiers have been made using the III-V compound semiconductors GaAs and InP to date. The important aspect of both materials is that above a certain threshold field, the electron drift velocity decreases with increasing electric field due to the transfer

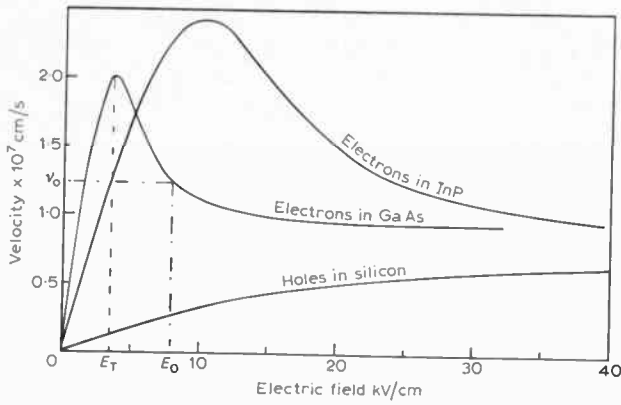


Fig. 2. Velocity-field characteristics.

of electrons to higher energy satellite conduction bands where the mobilities are low.¹¹ Figure 2 shows the room temperature velocity-field characteristics for both GaAs and InP.¹² The devices are usually made by growing an epitaxial n⁺nn⁺ sandwich. The carrier concentration in the two n⁺ end contacts is high (> 10¹⁷ cm⁻³) and in the central n region is normally in the range 10¹⁴–10¹⁵ cm⁻³. For a device designed to operate at 10 GHz the width of the n layer would be in the range 6–12 μm, depending somewhat on the material used. A typical cross-sectional area of the diode would be approximately 10⁻⁴ cm².

Consider now a device of the type just described embedded in the circuit shown in Fig. 3. The bias voltage V_B is applied through a blocking inductor L_B which prevents r.f. currents flowing in the bias supply. We will assume that, as a result of V_B, the d.c. electric field established across the sample is uniform and equal to E₀ say, where

$$E_0 = \frac{V_B}{l} \tag{1}$$

l being the length of the n region. The field in the highly doped contact regions is negligibly small. The assumption of a uniform electric field is not strictly valid; however, it only alters the final result in a small quantitative way but greatly simplifies the analysis. The free electron concentration is n₀. To obtain negative resistance E₀ must be greater than the threshold field E_T; reference to Fig. 2 shows that the corresponding drift velocity of electrons is v₀ say.

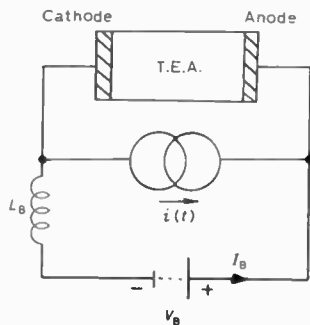


Fig. 3. Circuit used to calculate the impulse response of a t.e.a.

Suppose now the current generator shown in Fig. 3 injects an impulse of current into the sample at time t = 0. If the total charge contained within the current impulse is Q̃₀ then i(t) can be written

$$i(t) = \tilde{Q}_0 \delta(t) \tag{2}$$

where δ(t) is the unit delta function; the superscript tilde ~ denotes that the charge is a small perturbation. We will also assume that the direction of the impulse of current is such that electrons are injected into the cathode contact, and extracted from the anode. A charge -Q̃₀/A per unit cross-sectional area, where A is the diode area, thus appears at the cathode end of the diode and a corresponding positive charge +Q̃₀/A appears at the anode end. Subsequently neither charge can leak away around the external circuit since both the current generator and the bias circuit have infinite impedance. However, the electronic charge -Q̃₀ injected at the cathode rapidly detaches itself from the cathode and starts to drift across towards the anode with an average drift velocity of v₀. After some time t following the application of the delta function, the field distribution is as depicted in Fig. 4. The sheet of charge injected from the cathode will have moved a distance

$$x = v_0 t \tag{3}$$

in time t. The amount of charge per unit area in this sheet changes as it drifts across; suppose at time t it

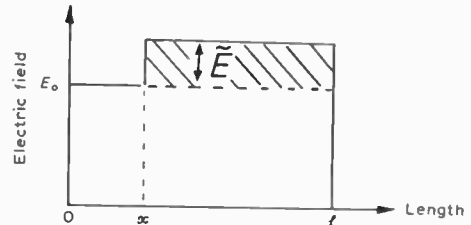


Fig. 4. Field distribution along a t.e.a. device after the injected charge layer has moved distance x; E₀ is the bias field.

is -Q̃/A. Application of Gauss' theorem shows that the field ahead of the sheet has increased by an amount Ẽ, (see Fig. 4) where

$$\tilde{E} = \frac{-\tilde{Q}}{A\epsilon} \tag{4}$$

ε being the permittivity of the semiconductor. As a consequence of the increase in field, the drift velocity ahead of the sheet of charge has changed by a small amount ṽ where, from Fig. 2, we note

$$\tilde{v} = \left[\frac{dv}{dE} \right]_{E=E_0} \tilde{E} \tag{5a}$$

dv/dE is the slope of the v/E curve at the bias field point, and is referred to as the differential mobility μ. It is seen to be negative for values of bias field greater than the threshold field E_T. We can write (5a) as

$$\tilde{v} = -|\mu| \tilde{E} \tag{5b}$$

for E₀ > E_T.

Since the velocity ahead of the charge sheet has decreased compared to that behind it, electrons must pile

up in the sheet and at the same time cause the region at the anode contact to become depleted of mobile charge. In a small interval of time dt , the number of electrons that pile up on unit area of the drifting charge sheet is just the difference between the number flowing in from the left and those flowing out to the right, namely $n_0 \tilde{v} dt$. Thus the electronic charge on the sheet per unit area increases from $-\tilde{Q}/A$ to $-(\tilde{Q} + d\tilde{Q})/A$ where

$$\frac{-d\tilde{Q}}{A} = (-e)n_0 \tilde{v} dt \tag{6}$$

$-e$ being the electronic charge. Using equations (5b) and (4), equation (6) may be written

$$\frac{d\tilde{Q}}{dt} = \frac{n_0 |\mu| e \tilde{Q}}{\epsilon} \tag{7}$$

The solution to (7), noting that at $t = 0$, $\tilde{Q} = -\tilde{Q}_0$ is

$$\tilde{Q} = -\tilde{Q}_0 \exp\left(\frac{t}{\tau}\right) \tag{8}$$

where

$$\tau = \frac{\epsilon}{n_0 |\mu| e} \tag{9}$$

Thus the injected charge $-\tilde{Q}_0$ increases exponentially with time as it drifts across the sample as a result of the material having a negative differential mobility. It is instructive to obtain an idea of a typical value of the dielectric relaxation time τ . In many practical devices $n_0 \approx 10^{15} \text{ cm}^{-3}$, ϵ for GaAs and InP is $\sim 12.5 \times 10^{-11}/36\pi \text{ F/cm}$; and devices are normally biased to a value of E_0 so that $|\mu| \approx 250 \text{ cm}^2/\text{Vs}$. The corresponding value of τ is then approximately 30 ps. This is a short time but not greatly different from the time taken for the injected charge to transit from cathode to anode, the so-called transit time T . The transit time is given by

$$T = \frac{l}{v_0} \approx 60 \text{ ps} \tag{10}$$

for a device $6 \mu\text{m}$ long and a value of $v_0 \approx 10^7 \text{ cm/s}$. In this particular example the injected charge would have grown by a factor $\exp 2 = 7.4$ times in transit from cathode to anode. This is a rather optimistic evaluation of the total growth since the natural self-diffusion of the thin sheet of charge will tend to counteract the growth due to the negative mobility. We will return to this aspect later.

We need now to calculate the open circuit voltage response \tilde{V} to the impulse of current. Reference to Fig. 4 shows that the extra voltage due to the injected charge is the area shaded, thus

$$\tilde{V} = -\tilde{E}(l-x) \tag{11}$$

From equations (3), (4) and (8), equation (11) can be written

$$\tilde{V} = \frac{\tilde{Q}_0}{A\epsilon} (l-v_0 t) \exp\left(\frac{t}{\tau}\right) \tag{12}$$

and exists for the transit time T only. Equation (12) thus gives the diode open-circuit response to the initial delta function of current $\tilde{Q}_0 \delta(t)$. It is convenient at this stage to consider the voltage response to a unit

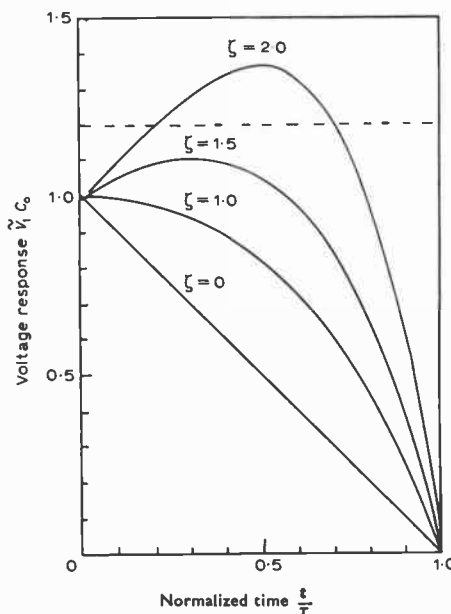


Fig. 5. Voltage impulse response of t.e.a. for varying growth factors ζ . Rectangular pulse approximation shown dotted.

delta function of current ($\tilde{Q}_0 \equiv 1$) which we define as \tilde{V}_1 . In this case (12) becomes, with slight rearrangement,

$$\tilde{V}_1 = \frac{(1-t/T) \exp\left[\frac{t}{T} \cdot \frac{T}{\tau}\right]}{C_0} \tag{13}$$

where C_0 is the geometrical capacitance of the device $\epsilon A/l$.

Reference to equation (8) shows that the injected charge grows $\exp(T/\tau)$ times in transit; we will define the exponent T/τ as the growth factor ζ whose value of course depends on the sample length, the carrier concentration n_0 , and the particular value of bias field E_0 .

In Fig. 5, the impulse response $\tilde{V}_1 C_0$ is plotted as a function of normalized time t/T for several values of ζ , using equation (13). The curve for $\zeta = 0$ represents the situation where the differential negative mobility $|\mu|$ is vanishingly small so that no growth of injected space charge takes place. For many practical t.e.a.s, ζ lies in the range 1 to 2.

So far we have only obtained the small signal impulse response. The small signal frequency response can be readily obtained by using the Fourier transform. The resistive component of the impedance $R(\omega)$ is given by the Fourier cosine transform of the impulse response, namely

$$R(\omega) = \int_{-\infty}^{\infty} \tilde{V}_1 \cos \omega t \cdot dt \tag{14a}$$

and the reactive component of impedance $X(\omega)$ by the Fourier sine transform

$$X(\omega) = - \int_{-\infty}^{\infty} \tilde{V}_1 \sin \omega t \cdot dt \tag{14b}$$

where ω is the angular frequency.

Before evaluating $R(\omega)$ for the general case, let us consider two simple cases:

(a) Impedance when $\zeta = 0$

In this case the impulse response is just

$$\tilde{V}_1 = \frac{(1-t/T)}{C_0}$$

i.e. a linearly decreasing voltage with time.

Equation (14a) then gives

$$R(\omega) = \frac{T}{C_0} \left[\frac{1 - \cos \theta}{\theta^2} \right] \tag{15a}$$

and (14b) gives

$$X(\omega) = \frac{T}{C_0} \left[\frac{\sin \theta - \theta}{\theta^2} \right] \tag{15b}$$

where θ is the transit angle ωT .

The value of $R(\omega)$ is plotted in Fig. 6 as a function of transit angle θ . We note that the resistance is always positive although it does drop to zero for $\theta = 2\pi, 4\pi$ etc. No reflexion amplification could be observed from such a sample.

(b) Rectangular pulse approximation

From Fig. 5, for $\zeta = 2$, a rough approximation to the shape is the rectangular pulse shown dotted. For this approximation we may write

$$\tilde{V}_1 \approx \frac{1.2}{C_0}$$

for $T \geq t \geq 0$.

In this case, using equations (14),

$$R(\omega) = \frac{1.2T}{C_0} \left[\frac{\sin \theta}{\theta} \right] \tag{16a}$$

$$X(\omega) = \frac{1.2T}{C_0} \left[\frac{\cos \theta - 1}{\theta} \right] \tag{16b}$$

Both $R(\omega)$ and $X(\omega)$ are plotted in Fig. 6. We see immediately that a region of negative resistance exists from $\theta = \pi$ to 2π . The reactance which is negative (capacitive) also varies strongly with transit angle. For $\theta = 2\pi$ the reactance is zero which means that we have established at this frequency a situation very similar to series resonance. Had the device series resistance been negative at this frequency, oscillations would have built up in an r.f. short-circuited device. Fortunately, as Fig. 6 shows, the resistance is just zero at this point and the device is marginally short-circuit stable. It takes little imagination to believe that for a growth rate $\zeta \geq 2$ the device will be short-circuit unstable. More exact calculations using equation (13) in conjunction with equation (14) shows that this is so and the exact limit for stability is¹³

$$\zeta \leq 2.09 \tag{17}$$

It can be argued that a device which is short circuit unstable can always be stabilized by operating it in series with a sufficiently large resistance say. The construction of suitable stabilizing networks however becomes increasingly difficult at microwave frequencies because of the distributed nature of circuit elements. Since the growth of injected space charge varies rapidly as $\exp(\zeta)$,

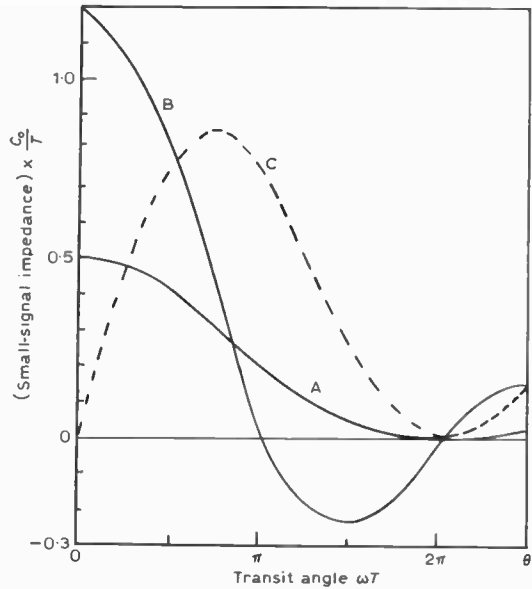


Fig. 6. Small signal impedance of t.e.a. versus transit angle; A resistance $R(\omega)$ for $\zeta = 0$; B resistance $R(\omega)$ and ; C reactance $-X(\omega)$ for rectangular pulse approximation respectively.

to all intents and purposes, a stable reflexion amplifier must satisfy inequality (17). Using equations (9) and (10), inequality (17) may be written

$$\frac{n_0 l |\mu| e}{\epsilon v_0} \leq 2.09 \tag{18}$$

There is not much latitude for varying the drift velocity v_0 (see Fig. 2), and for a given frequency of operation, l is fixed approximately by the condition $\pi < \theta \leq 2\pi$ (see Fig. 6) if negative resistance and consequently amplification is required. To satisfy (18) then, either n_0 or $|\mu|$ have to be sufficiently low. The first solution in the early days of transferred electron devices was to reduce n_0 and to work therefore with low doped devices ($n_0 < 10^{14} \text{ cm}^{-3}$). Such devices were referred to as *subcritically* doped. Perlmann⁶ later realized that by operating a device with a sufficiently high bias voltage and correspondingly high bias field (usually $E_0 \geq 3E_T$) the magnitude of the slope mobility $|\mu|$ could be reduced (see Fig. 2 again) sufficiently so that *super-critically* doped devices ($n_0 > 10^{15} \text{ cm}^{-3}$) could be stabilized. It is of course not necessary to satisfy (17) for an oscillating device; many of the early supercritical amplifiers were made using diodes designed as oscillators, but operated with a bias voltage at least three times that needed for oscillations to start.

(c) General solution for impedance

The general solution of equations (13) and (14a) gives, after some labour, the device resistance

$$R(\omega) = \frac{T}{C_0} \left\{ \frac{-\zeta}{\zeta^2 + \theta^2} + \frac{(\zeta^2 - \theta^2)(\exp \zeta \cos \theta - 1)}{(\zeta^2 + \theta^2)^2} + \frac{2\zeta \theta \exp \zeta \sin \theta}{(\zeta^2 + \theta^2)^2} \right\} = \frac{T}{C_0} U(\zeta, \theta) \tag{19}$$

It is readily seen in the limit $\zeta \rightarrow 0$, that (19) gives, as it should, the result noted in equation (15a).

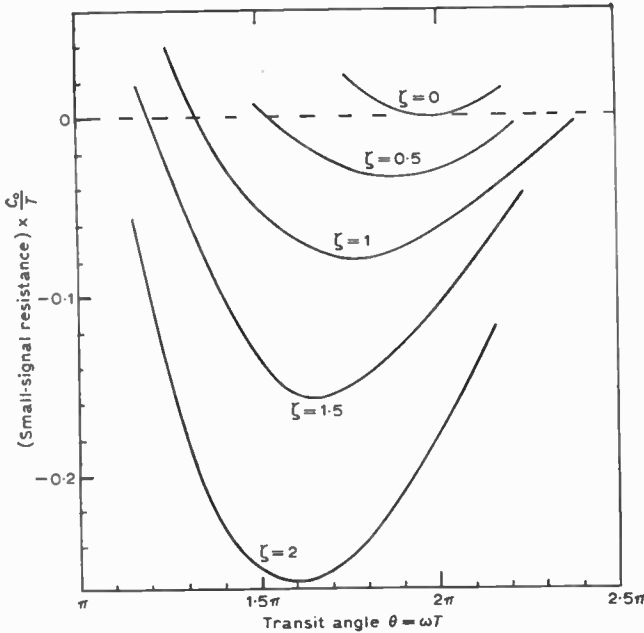


Fig. 7. Small signal resistance $R(\omega)$ versus transit angle θ for various growth factors ζ .

In Fig. 7 equation (19) is plotted as a function of transit angle θ for several values of ζ . The graph is limited to the interesting range of transit angles, from $\theta \approx \pi$ to $\theta \approx 2.5\pi$, where negative resistance is observed.

As expected, the maximum negative resistance is observed to increase as the growth factor ζ increases; the transit angle for maximum negative resistance also moves to lower values as ζ increases. The reader may find it helpful to sketch out the integrand in equation (14a) for various shapes of $\vec{V}_1(t)$ and then mentally perform the required integration. He should then be able to convince himself that, if the open circuit voltage response curves convex upwards, negative resistance is possible, whilst if it curves concave downwards no negative resistance is present at any frequency. Figure 8 depicts the situation schematically.

We shall later need to know $R(\omega)$ for small values of ζ since such small values pertain when the noise figure

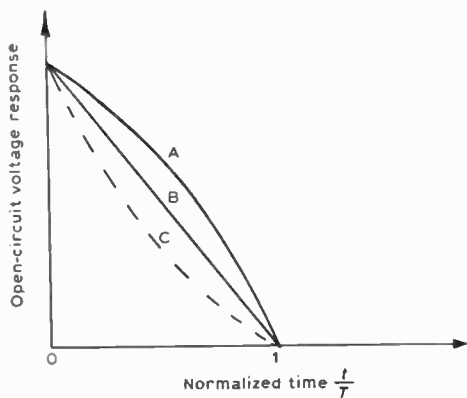


Fig. 8. Shape of impulse response (schematic) in order to give: A negative resistance; B minimum resistance zero; C positive resistance only.

is close to its minimum value. Inspection of Fig. 7 shows that for small values of ζ , the maximum negative resistance occurs very close to $\theta = 2\pi$. Its magnitude can readily be found by putting $\exp \zeta \approx 1 + \zeta$, $\theta = 2\pi$, and neglecting ζ^2 compared to θ^2 , in equation (19). Then, to first order in ζ ,

$$R_{\max} = \frac{-T\zeta}{2\pi^2 C_0} \quad (20)$$

The negative resistance is directly proportional to the growth factor ζ in this approximation. We shall see in Section 2.2 however that a correction has to be added to equation (20) to allow for the diffusion of the charge sheet as it moves across the sample from cathode to anode.

3 The Effect of Diffusion on the Input Resistance

An implicit assumption made so far has been that the injected charge sheet, even as it grew in transit, remained infinitely thin. Random fluctuations in the motion of the electrons causes them to diffuse with time so that the width of charge sheet increases. The total amount of charge in the sheet given by equation (8), namely $-\tilde{Q}_0 \exp t/\tau$, does not change however, so that the height of the step in field \vec{E} remains the same as before. The situation is shown in Fig. 9. If this is compared to Fig. 4 it will be noted that the effect of diffusion is to

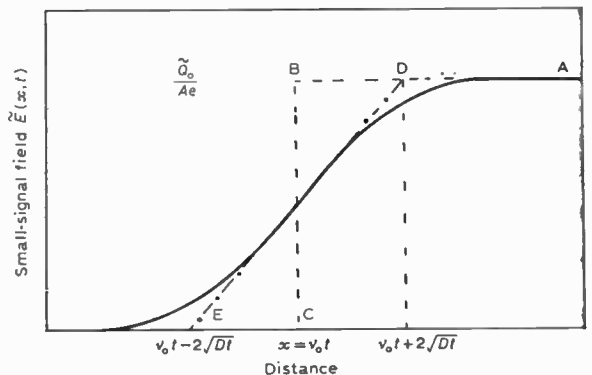


Fig. 9. The effect of diffusion on the small signal field. The solid line is the correct complementary error function; the chain dotted line is the linear approximation used here.

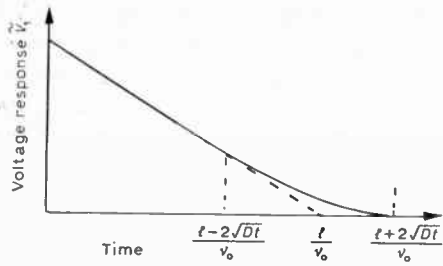
smear out the transition in field \vec{E} . The variation of field $\vec{E}(x, t)$ shown in Fig. 9, is derived in Appendix 1 and is given by

$$\vec{E}(x, t) = \frac{-\tilde{Q}_0}{2\epsilon A} \left[1 + \operatorname{erf} \left\{ \frac{(x - v_0 t)}{2\sqrt{(Dt)}} \right\} \right] \exp \left(\frac{t}{\tau} \right) \quad (21)$$

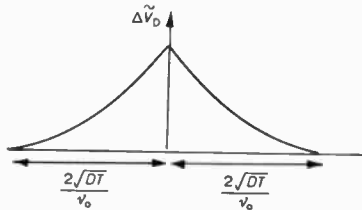
where the term in square brackets is unity plus an error function of argument $\{(x - v_0 t)/2\sqrt{(Dt)}\}$.

Also shown dotted in Fig. 9 is a good straight line approximation to (21) which for simplicity will be assumed to hold in what follows. The transition from low field to high field takes place over a distance of $\sim 4\sqrt{(Dt)}$ about the 'centre of gravity' x of the injected pulse, which moves with velocity v_0 so that, as before,

$$x = v_0 t \quad (3)$$



(a) Voltage response for velocity saturation $\zeta = 0$, with diffusion present.



(b) The difference caused by diffusion is shown enlarged in Fig. 10(b).

Fig. 10.

The variation of diffusion coefficient with electric field is shown in Fig. 12 for both GaAs and InP. A typical value for D at a bias field used might be $\sim 50 \text{ cm}^2/\text{s}$ for GaAs.¹⁵ The transit time we noted to be about 60 ps for a $6 \mu\text{m}$ long device. Thus the pulse would have spread to a total width $w \simeq 4\sqrt{(Dt)}$ by the time it reaches the anode, where

$$4\sqrt{(Dt)} \simeq 2.2 \mu\text{m}$$

This is some 37% of the total sample width and is thus quite significant.

We now have to ascertain the effect of this spreading on the impulse response. It is easiest to see initially for the case of no growth, namely $\zeta = 0$. In Fig. 5 we noted that the voltage response without diffusion was a linear decay. The effect of diffusion will not alter this voltage response until the charge sheet approaches the anode for, as seen from Fig. 9, the area under the curve with diffusion present, ADE, is just the same as that under the diffusionless curve ABC.

As the diffusing charge layer moves into the anode, the voltage response will fall less rapidly than in Fig. 5. The situation is shown in Fig. 10(a). The response is now not linear but concave downwards; such a response, as we have seen before, is not capable of producing negative or even zero resistance at any frequency.

The solid curve in Fig. 10(a) can be represented as the sum of the voltage response without diffusion together with a 'diffusion correction' $\Delta \tilde{V}_D$. The diffusion correction voltage is shown in Fig. 10(b). Simple geometrical integration, using the shape of the field distribution shown in Fig. 9, gives

$$C_0 \Delta \tilde{V}_D \simeq \frac{\sqrt{(DT)}}{2l} \left[1 - \frac{v_0 |\Delta t|}{2\sqrt{(DT)}} \right]^2 \quad (22)$$

where $|\Delta t|$ is time measured with respect to the transit

time $T = l/v_0$ as origin (see Fig. 10(b)). Equation (22) can be modified to take account of a finite value of space charge growth factor ζ by multiplying it simply by $\exp \zeta$. This follows from equation (21).

We are now in a position to calculate the change in the device resistance $\Delta R(\omega)$ caused by diffusion. Using equations (14a) and (22),

$$\Delta R(\omega) = \frac{\sqrt{(DT)} \exp \zeta}{C_0 l} \times \int_{[t-2\sqrt{(DT)}/v_0]}^{[t+2\sqrt{(DT)}/v_0]} \left[1 - \frac{v_0 |\Delta t|}{2\sqrt{(DT)}} \right]^2 \cos \omega t \, dt \quad (23)$$

We will only concern ourselves here with the correction for small growth factors. In this case, for maximum negative resistance $\omega T = 2\pi$, and assuming $2\sqrt{(Dt)} \ll l$, $\cos \omega t$ in the integrand in (23) may be replaced by unity. Performing the integration gives

$$\Delta R(\omega) = \frac{2T}{3C_0} \left[\frac{D}{v_0^2 T} \right] \exp \zeta \quad (24)$$

This quantity is positive which gives further confirmation of our view that diffusion reduces the negative resistance effect. By replacing $\exp \zeta$ by $(1 + \zeta)$, the total resistance, which is the sum of (20) and (24), is

$$R = -\frac{T}{C_0} \left\{ \frac{\zeta}{2\pi^2} - \frac{2}{3} \left[\frac{D}{v_0^2 T} \right] (1 + \zeta) \right\} \quad (25)$$

Negative resistance exists only so long as

$$\zeta \geq \frac{1}{(3v_0^2 T)/(4\pi^2 D) - 1} \quad (26a)$$

or to a good approximation

$$\zeta \geq \frac{4\pi^2 D}{3v_0^2 T} \quad (26b)$$

Taking the values used in previous examples, $v_0 = 10^7 \text{ cm/s}$, $D = 50 \text{ cm}^2/\text{s}$, $T = 60 \text{ ps}$, (26) gives

$$\zeta \geq \frac{1}{9.12 - 1} = 0.12 \quad (27)$$

4 Noise Figure of T.E.A.s

Consider a small sample of n-type semiconductor, length Δx , and cross-sectional area A . Under low field conditions, when the electrons are in thermal equilibrium with the lattice temperature T_0 , we can characterize the Johnson noise produced by this resistor using the equivalent circuit shown in Fig. 11. The value of the resistor R is

$$R = \frac{\Delta x}{n_0 e \mu A} \quad (28)$$

where n_0 is the free electron concentration as before, μ is the low field mobility. The mean square noise current per unit bandwidth is given by the usual Nyquist formula:

$$I_n^2 = \frac{4kT_0}{R} = \frac{4kT_0 \cdot n_0 e \mu A}{\Delta x} \quad (29)$$

where (28) has been used for R , and k is Boltzmann's constant. Under equilibrium conditions the Einstein

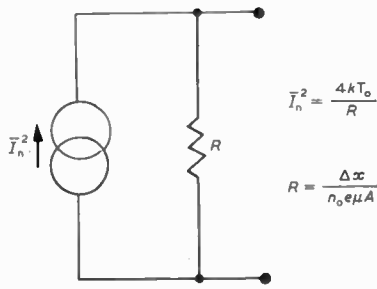


Fig. 11. Noise equivalent circuit for a resistor.

relationship holds, which is normally written

$$\frac{D}{\mu} = \frac{kT_0}{e} \tag{30}$$

Eliminating μkT_0 from (29) and (30)

$$I_n^2 = \frac{4n_0 e^2 D A}{\Delta x} \tag{31}$$

Although (31) was derived under the assumption of thermal equilibrium, its validity is far wider. In Appendix 2 a more rigorous derivation is given which shows (31) to be valid even under hot electron conditions if the correct value for D is used. This value, the so-called longitudinal diffusion coefficient, is a function of the local electric field and in Fig. 12 theoretically computed curves for GaAs¹⁵ and InP¹⁶ are shown. It is outside the scope of the present paper to go into details of the method of calculation; some insight is given in Appendix 2 but the references given above should be consulted for further details.

Now consider Fig. 13 where the noise current fluctuations developed by a small portion Δx of the t.e.a. are shown explicitly by the noise current generator I_n^2 . We have initially to evaluate the open-circuit mean square noise voltage $\Delta \bar{V}_n^2(x)$ developed between cathode and anode as a result of the fluctuations in current between x

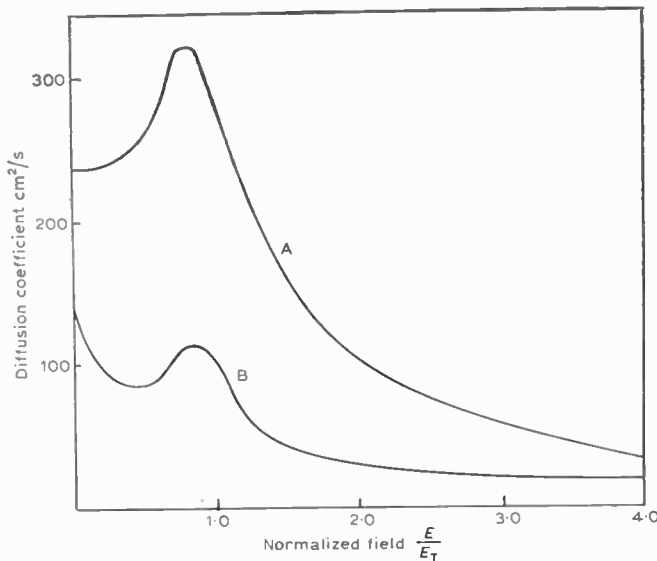


Fig. 12. Longitudinal diffusion coefficient as a function of field E normalized to the threshold field E_T for: A GaAs; B InP.

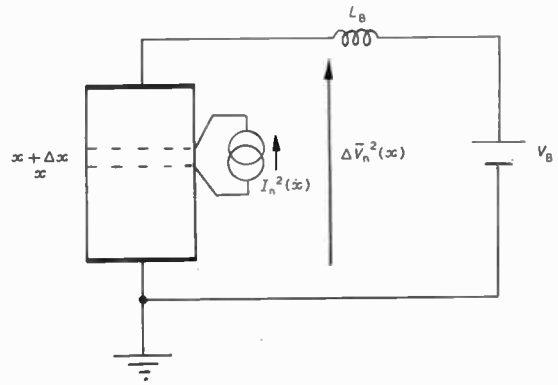


Fig. 13. Open-circuit mean square noise voltage $\Delta \bar{V}_n^2(x)$ and due to diffusion noise generated between x and $x + \Delta x$.

and $x + \Delta x$. Once again we use the impulse technique by imagining initially I_n to be an impulse of current $\tilde{Q}\delta(t)$. As before, a charge $-\tilde{Q}$ will appear at plane x whilst $+\tilde{Q}$ appears at plane $x + dx$. The corresponding field distribution is shown in Fig. 14; the field between x and $x + dx$ is

$$\Delta \tilde{E}_0 = \frac{\tilde{Q}}{\epsilon A} \tag{32}$$

and the voltage between x and $x + dx$ is

$$\Delta \tilde{E}_0 \Delta x = \Delta \tilde{V} = \frac{\tilde{Q} \Delta x}{\epsilon A} \tag{33}$$

As time progresses these two charge sheets will drift across to the anode, growing exponentially as they move, in accordance with equation (8). The distance between the plane x and the anode is $l - x$ and the transit time from x to l is thus $(l - x)/v_0$. The open-circuit impulse voltage response is therefore

$$\Delta \tilde{V}(t) = \frac{\tilde{Q} \Delta x}{\epsilon A} \exp\left(\frac{t}{\tau}\right) \tag{34}$$

from $t = 0$ to $t = (l - x)/v_0$, and zero thereafter. Using equations (14a) and (14b), the transfer impedance $\Delta R(\omega) + j\Delta X(\omega)$ relating the open circuit voltage at the anode to the current injected at x and extracted at $x + dx$ can be evaluated. Denoting $l - x$ by s , and the normalized distance $(l - x)/l$ as s' , we obtain, after some slight manipulation,

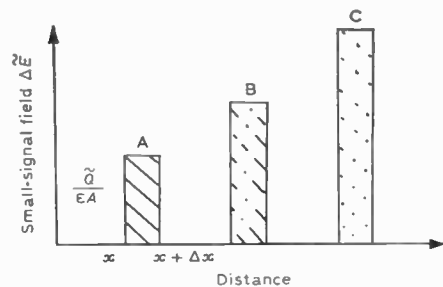


Fig. 14. Field $\tilde{Q}/\epsilon A$ induced between x and $x + \Delta x$; A due to impulse of current $\tilde{Q}\delta(t)$; B some time later; C later still, as charge layers have drifted and grown.

$$(\Delta R(\omega))^2 + (\Delta X(\omega))^2 = |\Delta Z(\omega)|^2 = \left[\frac{\Delta x T}{\epsilon A} \right]^2 \left[\frac{1 + \exp(2s'\zeta) - 2 \exp(s'\zeta) \cos s'\theta}{\zeta^2 + \theta^2} \right] \quad (35)$$

where the other symbols have previously been defined. This transfer impedance gradient $\Delta Z(\omega)/\Delta x$ has been called by Shockley the impedance field.¹⁰

Now the mean square open circuit noise voltage per unit frequency range $\Delta \bar{V}_n^2(x)$ due to noise injected between x and $x+dx$ is

$$\Delta \bar{V}_n^2(x) = I_n^2 |\Delta Z(\omega)|^2 \quad (36)$$

Using equations (35) and (31) and denoting the term in square brackets in equation (35) as $F(\zeta, \theta, s')$, we have

$$\Delta \bar{V}_n^2(x) = \frac{4n_0 e^2 D T^2 \Delta x}{\epsilon^2 A} F(\zeta, \theta, s') \quad (37)$$

The total mean square output noise voltage is found by summing the contributions of the mean square voltages from all incremental elements, of which that given in equation (37) is just one. Direct addition is in order since the noise voltages from all the elements are uncorrelated. Thus the total open circuit mean square noise voltage \bar{V}_n^2 developed across the device is, from equation (37),

$$\bar{V}_n^2 = \frac{4n_0 e^2 D T^2 l}{\epsilon^2 A} \int_0^l F(\zeta, \theta, s') dx \quad (38)$$

Performing the integration gives, after some manipulation,

$$\bar{V}_n^2 = \frac{4n_0 e^2 D T^2 l}{\epsilon^2 A} S(\zeta, \theta) \quad (39)$$

where

$$S(\zeta, \theta) = (\zeta^2 + \theta^2)^{-1} \times \left[\frac{\exp 2\zeta + 2\zeta - 1}{2\zeta} - \frac{2(\zeta \exp \zeta \cos \theta + \theta \exp \zeta \sin \theta - \zeta)}{\zeta^2 + \theta^2} \right] \quad (40)$$

The function $S(\zeta, \theta)$ is plotted in Fig. 15 over the useful range $2\pi > \theta > \pi$ for several values of ζ . Two points are worthy of note. $S(\zeta, \theta)$ and therefore the open-circuit mean square noise voltage falls monotonically with increasing transit angle and the noise voltage decreases as

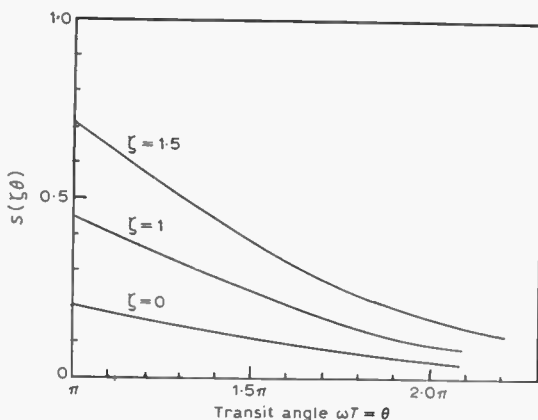


Fig. 15. The open-circuit mean square noise voltage factor $S(\zeta, \theta)$ as a function of transit angle θ for various growth factors ζ .

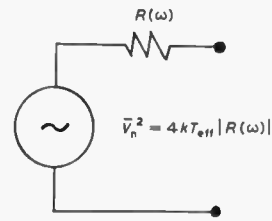


Fig. 16. Equivalent circuit representation of noise generated by t.e.a.

the growth factor ζ decreases to zero. For small values of ζ , it is easily seen from equation (40) that the function tends to $S(0, \theta)$ given by

$$S(0, \theta) = 2\theta^{-2} \left(1 - \frac{\sin \theta}{\theta} \right) \quad (41)$$

4.1 The Device Effective Noise Temperature T_{eff} and Noise Measure M

We now have the device open-circuit mean square noise voltage per unit bandwidth, at frequency ω (equation (39)), and the device series resistance $R(\omega)$ given by (19). Let us now represent the device as a Nyquist noise source with the equivalent circuit given in Fig. 16. It is convenient to define a fictitious effective noise temperature T_{eff} so that the open-circuit noise voltage is given by:

$$\bar{V}_n^2 = 4kT_{eff} |R(\omega)| \quad (42)$$

Using equations (39) and (42)

$$\frac{T_{eff}}{T_0} = \frac{n_0 e^2 D T^2 S(\zeta, \theta)}{\epsilon C_0 k T_0 |R(\omega)|} \quad (43)$$

where T_0 is the reference temperature, normally 290 K. The effective noise temperature ratio T_{eff}/T_0 is also called the noise measure M .¹⁷ The more commonly used method of specifying noise is the noise figure F and this is related to M through

$$F = 1 + M[1 - (1/G)] \quad (44)$$

where G is the power gain. If both G and M are much greater than unity, which is normally the case in many practical situations, then both F and M are essentially equal. It must be stressed however that T_{eff} is a convenient and compact way of specifying the noise performance only; in the case of transferred-electron and baritt amplifiers it has no obvious direct physical interpretation and certainly is not a measure of the electron temperature.

Using equations (43) and (19), the noise measure is

$$M = \frac{n_0 e^2 D l S(\zeta, \theta)}{v_0 \epsilon k T_0 U(\zeta, \theta)} \quad (45)$$

For a given device with a specified bias field and carrier concentration, the frequency dependence of the noise measure is proportional to the ratio S/U in equation (45). This ratio is plotted as a function of transit angle (θ) (or frequency) in Fig. 17, for various values of the growth factor ζ .

A number of interesting observations follow from Fig. 17. The noise measure shows a minimum value which occurs very close to $\theta = 2\pi$ for all practical values

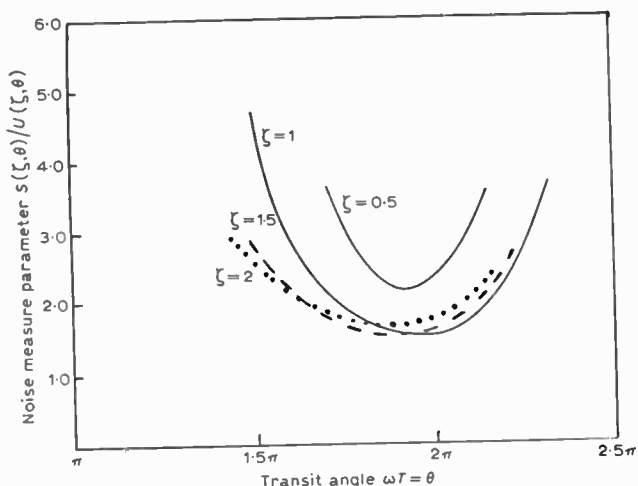


Fig. 17. Noise measure parameter $S(\zeta, \theta)/U(\zeta, \theta)$ as a function of transit angle θ , for various values of the growth parameter ζ .

of the growth factor ζ . Comparison of Fig. 7 and Fig. 17 shows that the minimum noise measure occurs at a slightly higher frequency than the maximum negative resistance, although this difference becomes less as ζ tends to zero. Of considerable importance is the fact that the minimum value of the S/U ratio varies very slowly with ζ in the range $0.5 \leq \zeta \leq 2$. For lower values of ζ than 0.5, the minimum starts to rise quite rapidly. Using equations (20) and (41), for small values of ζ , the minimum value of S/U is equal to $1/\zeta$ and occurs when $\theta \approx 2\pi$ if diffusion is neglected.

Thus, from the results of Fig. 17 and equation (45),

$$M_{\min} \approx \frac{1.5n_0e^2DI}{v_0\epsilon kT_0} \quad (46a)$$

for $1 \leq \zeta \leq 2$ and

$$M_{\min} \rightarrow \frac{n_0e^2DI}{v_0\epsilon kT_0} \left[\frac{1}{\zeta} \right] \quad (46b)$$

as ζ tends to zero. Remembering that

$$\zeta = \frac{T}{\tau} = \frac{Tn_0|\mu|e}{\epsilon} \quad (47)$$

equation (46b) can be written in a convenient form, by eliminating ζ ,

$$M_{\min} \rightarrow \frac{De}{|\mu|kT_0} \quad (48)$$

This simple relationship was first noted by Thim.¹⁸

4.2 The Effect of Varying the Doping Density on the Noise Measure

We noted in Section 2.1 that for a device having $l = 6 \mu\text{m}$, $n_0 \approx 10^{15} \text{ cm}^{-3}$, biased so that $|\mu| \approx 250 \text{ cm}^2/\text{Vs}$, $\tau \approx 30\text{ps}$ and $\zeta = T/\tau \approx 2$. For GaAs under such conditions $D \approx 50 \text{ cm}^2/\text{s}$. Thus equation (46a) is a valid expression for the minimum noise figure. Inserting the above values in equation (46a) gives

$$M_{\min} \approx 30 \approx 14.8 \text{ dB.}$$

Values such as this are frequently observed in devices

having doping densities in the 10^{15} cm^{-3} range.^{1,6} However, if we were to use a lightly-doped device, with $n_0 \approx 10^{14} \text{ cm}^{-3}$ say, biased again at the same field, then because n_0 is reduced by a factor of 10, ζ would be similarly reduced (eqn. (47)). Equation (48) is now valid. This gives

$$M_{\min} \approx 8 \approx 9 \text{ dB,}$$

some 6 dB less than with the higher doping.

This sample has a small growth factor of $\zeta = 0.2$. We noted in Section 2.2 that for small values of ζ , diffusion had an important damping effect on the magnitude of the negative resistance. Reference to equation (25) shows that in the present case, the negative resistance is $\{1 - (4\pi^2/3\zeta)(D/v_0^2T)\}$ times the value obtained neglecting diffusion. Putting in appropriate values gives this factor as 0.45. As equation (43) shows, the noise measure is inversely proportional to the negative resistance. Thus, taking account of diffusion, the minimum noise figure is $M_{\min} = 8/0.45 = 17.8 = 12.5 \text{ dB}$.

The improvement is therefore rather less than would be expected if diffusion were neglected. It is possible in the above manner to calculate the minimum noise figure as a function of carrier concentration for a range of bias field values. Figure 18 shows such a family of curves for GaAs. Since equation (45) shows that for a given bias field (and hence given v_0 , D and $|\mu|$) the noise measure is a function of the product n_0l , rather than n_0 alone, the abscissa chosen in Fig. 18 is n_0l . The noise figure is observed to decrease initially as the n_0l product is decreased, to pass through a minimum and then to start to increase again as diffusion reduces the magnitude of the negative resistance. This is contrary to the conclusions of Maloberti and Svelto,¹⁹ who predict a monotonic decrease in M as n_0l decreases, asymptotic to $De/(|\mu|kT_0)$ because they neglect diffusion.

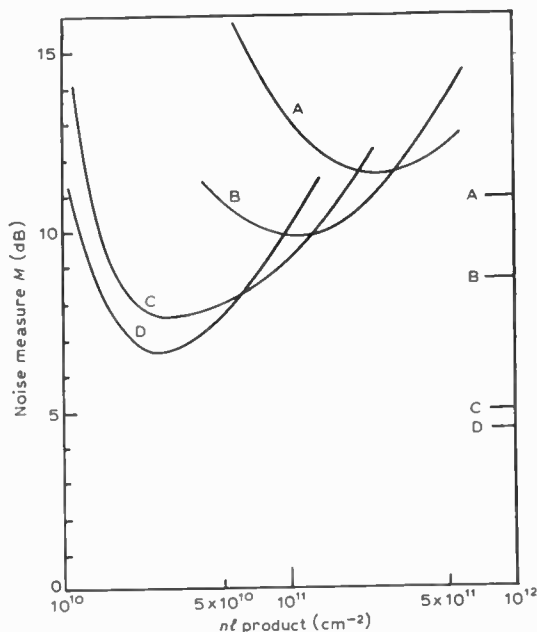


Fig. 18. Noise measure of GaAs t.e.a.s as a function of nl product for various bias fields: A 15 kV/cm, B 11.5 kV/cm, C 7.5 kV/cm, D 5 kV/cm. The corresponding values of $De/(|\mu|kT_0)$ are shown on the right-hand ordinate.

The appropriate values of $De/(|\mu|kT_0)$ are shown in Fig. 18 and it is clear that the minimum noise measures predicted are several decibels higher than this limit because of diffusion.

Figure 18 shows the optimum bias field for the lowest possible noise measure which, for GaAs, is ~ 5 kV/cm. This field is essentially the one corresponding to the minimum value of $D/|\mu|$. For lower fields than this the curves start to rise again. We conclude that the lowest noise measure for gallium arsenide is approximately 7 dB and occurs for a uniform field of ≈ 5 kV/cm and an n_0l product of $\sim 2.4 \times 10^{10}$ cm⁻². Special precautions would have to be taken however to prevent space charge injection from the cathode with such low doped material and a blocking contact of some sort would be mandatory.¹⁸

Figure 19 shows a similar set of results for InP for three different values of bias field. The $De/(|\mu|kT_0)$ values appropriate to each field are also shown in this Figure. The predicted noise measures are seen to be lower in InP than for GaAs and they approach quite closely the $De/(|\mu|kT_0)$ limit before starting to increase again. Both phenomena are a direct consequence of the lower diffusion coefficient in InP.

4.3 Experimental Observations

The variation of noise measure with frequency (or transit angle) shown in Fig. 17 has been observed experimentally by several authors. The effect is clearly seen, for example, in Fig. 2 of reference 5 or Fig. 5 of reference 3. The dependence of noise measure on n_0l product is less well documented however. Table 1 shows some values taken from the literature. Comparison of these results with those in Figs. 18 and 19 show that there is quite good agreement. However, little investigation has been undertaken with lower n_0l product devices.

Table 1

| n_0 cm ⁻³ | l μm | n_0l cm ⁻² | f GHz | $F = M+1$ dB | E_{bias} kV/cm | Reference |
|---------------------------|-----------|----------------------------|------------|-----------------|---------------------|-----------|
| GALLIUM ARSENIDE | | | | | | |
| 7×10^{14} | 8.5 | 6×10^{11} | 13 | 10.5 | 12 | (3) |
| 1.1×10^{15} | 9.0 | 10^{12} | 10 | 14.0 | 18 | (7) |
| 4×10^{15} | 2.0 | 8×10^{11} | 34 | 16.0 | 20 | (1) |
| INDIUM PHOSPHIDE | | | | | | |
| 4×10^{14} | 16.8 | 6.8×10^{11} | 9.2 | 11.5 | 36.0 | (5) |
| " | " | " | 10.5 | 9.8 | 30.0 | (5) |
| " | " | " | 11.0 | 9.4 | 24.0 | (5) |
| 5×10^{14} | 4.3 | 2×10^{11} | 34 | 7.5 | 21.0 | (2) |

5 Baritt Diode

Figure 15 shows that the open-circuit mean square noise voltage \bar{V}_n^2 is least when the growth rate ζ is zero. However, under these conditions the device does not present a negative resistance at any frequency, (see Fig. 7) and even for small values of ζ close to zero, the

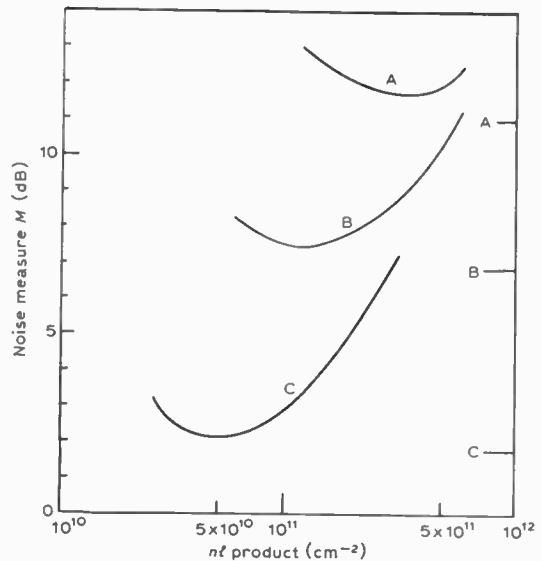


Fig. 19. Noise measure of InP t.e.a.s. as a function of nl product for various bias fields: A 40 kV/cm, B 30 kV/cm, C 20 kV/cm. The corresponding values of $De/(|\mu|kT_0)$ are shown on the right-hand ordinate.

negative resistance is so small that the resulting noise figure is high. One possible means of obtaining low noise amplification would be to work with $\zeta = 0$ and a low value of free carrier concentration n_0 , thus keeping \bar{V}_n^2 small, if means could be found at the same time for obtaining useful negative resistance under these conditions. This is achieved in the baritt diode.

The baritt diode is in essence a p^+np^+ or alternatively an n^+pn^+ transistor structure with the base floating. The base-collector junction is reverse biased so that the base-collector depletion region extends right to the emitter junction, which is necessarily forward biased. Alternative structures can be realized using Schottky barriers rather than p-n junctions. To date, all experimental devices have used silicon as the semiconductor material rather than GaAs or other III-V compounds and the preferred structure has been p^+np^+ with the n layer doping $N_D \sim 10^{15}$ electrons/cm⁻³ and the base width in the range 5–10 μm.

Figure 20 shows the electric field distribution in such a punched-through structure. Since majority carriers (electrons in the device shown in Fig. 20) are completely swept out of the active region, we can neglect them and concern ourselves solely with the holes injected from the p^+ region over the forward biased emitter-base (or cathode) junction.

Figure 20(b) shows the corresponding potential distribution for two applied bias voltages V_{B1} and V_{B2} , $V_{B2} > V_{B1}$. A potential maximum appears just in front of the cathode p^+n junction and the resulting barrier restricts the amount of hole current flowing. The barrier height is lower for V_{B2} than V_{B1} and hence the bias current J_{B2} is greater than J_{B1} .

The field gradient in Fig. 20 is given by

$$\frac{dE}{dx} = \frac{eN_D}{\epsilon} \approx 16 \text{ kV/cm}/\mu\text{m}$$

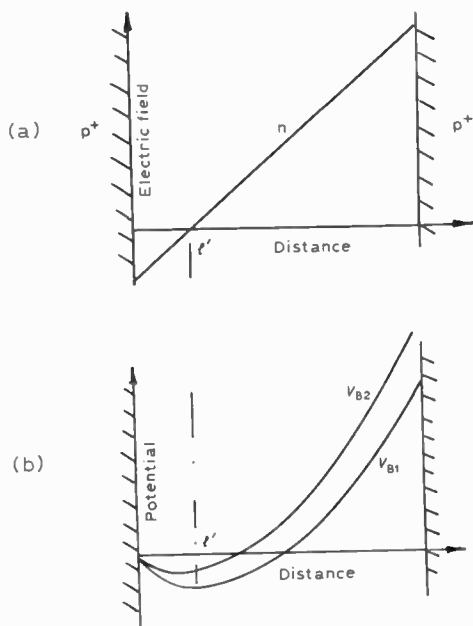


Fig. 20. (a) Electric field distribution in a baritt diode. (b) Potential distribution for two bias voltages V_{B1} and V_{B2} , $B_{B2} > V_{B1}$.

for $N_D \approx 10^{15} \text{ cm}^{-3}$. If the n layer length l were $5 \mu\text{m}$, then the field at the base-collector metallurgical junction (anode) would be 80 kV/cm . Over most of the device, as reference to Fig. 2 shows, the drift velocity of the injected holes is constant at the saturated velocity $v_0 \approx 10^7 \text{ cm/s}$. It follows that the differential mobility dv/dE is zero, and hence, from equation (9), $\tau = \infty$. Thus $\zeta = T/\tau = 0$ over all the base length is a good approximation.

The impedance of the baritt can now be calculated in the same manner as for the t.e. amplifier, using the impulse response method. A delta function of current $\tilde{Q}_0\delta(t)$ results in a surface charge density $+\tilde{Q}_0/A$ appearing at the cathode and $-\tilde{Q}_0/A$ at the anode. However, all the charge at the cathode is not immediately injected into the depleted n region as in the case of the t.e. amplifier. The barrier restricts the rate at which it can leak into the n region and it consequently decays as $(\tilde{Q}_0/A) \exp(-t/\tau_b)$ where τ_b is the barrier time constant.

5.1 Barrier Time-constant τ_b

The barrier height V_b is seen from Fig. 20(a) and (b) to be given by

$$V_b = \frac{eN_D l'^2}{2\epsilon} \tag{49}$$

where l' is the distance of the potential maximum from the p^+ cathode junction. The bias hole current density is

$$J_B = J_{ho} \exp\left[\frac{-eV_b}{kT_0}\right] \tag{50}$$

where J_{ho} is the thermal flux of holes incident on the barrier from the p^+ contact. An increase in the voltage ΔV_b applied across the barrier results in the barrier height being lowered from V_b to $V_b - \Delta V_b$. The increase in bias current ΔJ_B is given, from equation (50) by

$$\Delta J_B = \frac{J_B e \Delta V_b}{kT_0} \tag{51}$$

The barrier differential resistance per unit area R_b is therefore

$$R_b = \frac{\Delta V_b}{\Delta J_B} = \frac{kT_0}{eJ_B} \tag{52}$$

The capacitance of the barrier depletion region, per unit area, is

$$C_b = \epsilon/l' \tag{53}$$

Thus the R-C time constant τ_b of the barrier is given by

$$\tau_b = R_b C_b = \frac{kT_0 \epsilon}{eJ_B l'} \tag{54}$$

Eliminating l' from (54) using equations (49) and (50) gives

$$\tau_b = \frac{1}{J_B} \left[\frac{\epsilon k T_0 N_D}{2 \ln J_{ho}/J_B} \right]^{\frac{1}{2}} \tag{55}$$

Assuming the p^+ cathode is non-degenerate the saturation hole current density is given by

$$J_{ho} = \frac{N_A e \bar{v}}{4} \tag{56}$$

where N_A is the acceptor doping concentration in the p^+ region and \bar{v} is the mean thermal velocity ($\approx 10^7 \text{ cm/s}$). Putting $N_A \approx 10^{16} \text{ cm}^{-3}$ gives

$$J_{ho} \approx 10^4 \text{ A/cm}^2.$$

Anticipating what is to follow, baritts are normally operated with J_B in the range $10-100 \text{ A/cm}^2$. Thus the term $\{\ln(J_{ho}/J_B)\}^{\frac{1}{2}}$ in equation (55) is typically of order $2-2.6$. To the present degree of accuracy we can write therefore

$$\tau_b \approx \frac{0.3}{J_B} (\epsilon k T_0 N_D)^{\frac{1}{2}} \tag{57}$$

Putting $N_D \approx 10^{15} \text{ cm}^{-3}$ gives

$$\tau_b \approx \frac{10^{-9}}{J_B} \text{ seconds} \tag{58}$$

We shall see later that the ratio T/τ_b is important where T is the transit time across the depleted n region. We will define this ratio as $T/\tau_b = \zeta_b$. If the n region length is $5 \mu\text{m}$, and the saturated drift velocity is 10^7 cm/s , then $T = 5 \times 10^{-11} \text{ s}$ and

$$\frac{T}{\tau_b} = \zeta_b = \frac{5 \times 10^{-11}}{10^{-9}} J_B = 5 \times 10^{-2} J_B \tag{59}$$

Thus ratios of T/τ_b , in the range 1 to 5 say are obtainable for current densities varying between 20 and 100 A/cm^2 .

5.2 Open-Circuit Voltage Response

The field distribution at time t after the initial delta function of current $\tilde{Q}_0\delta(t)$ is shown in Fig. 21. After time t the charge on the cathode is $\tilde{Q}_0 \exp(-t/\tau_b)$. Thus the field at the cathode is $(\tilde{Q}_0/A\epsilon) \exp(-t/\tau_b)$. A hole that has travelled a distance x from the cathode must have left the cathode at a time x/v_0 earlier, i.e. at

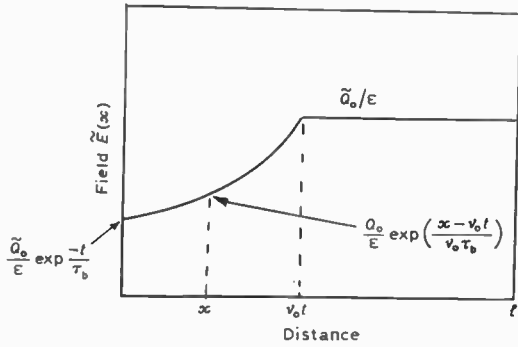


Fig. 21. Variation of field $\tilde{E}(x)$ following impulse excitation with distance.

time $t - (x/v_0)$. Thus the field at x is

$$\tilde{E}(x) = \frac{\tilde{Q}_0}{A\epsilon} \exp\left(-\frac{(t-x/v_0)}{\tau_b}\right) \quad x \leq v_0 t \quad (60)$$

For $x > v_0 t$

$$\tilde{E}(x) = \frac{\tilde{Q}_0}{A\epsilon} \quad (61)$$

The area under the field curve may be found by integrating (60) and (61) with respect to x to give the total voltage:

$$\tilde{V} = \frac{\tilde{Q}_0 l}{A\epsilon} \left\{ (1-t/T) + \frac{\tau_b}{T} \left[1 - \exp\left(-\frac{t}{\tau_b}\right) \right] \right\} \quad t \leq T \quad (62a)$$

$$\tilde{V} = \frac{\tilde{Q}_0 l}{A\epsilon} \frac{\tau_b}{T} \left\{ \exp\left(-\frac{t}{\tau_b}\right) \left[\exp\left(\frac{T}{\tau_b}\right) - 1 \right] \right\} \quad t \geq T \quad (62b)$$

Noting that $A\epsilon l = C_0$ as before, the impulse response $\tilde{V}_1 C_0$ to a unit delta function is plotted in Fig. 22 for various values of the ratio $\zeta_b = T/\tau_b$, using equations (62a) and (62b). The case $\zeta_b = \infty$ corresponds to the case $\zeta = 0$ (Fig. 8) for the t.e. amplifier. We noted in Section 2 that if the voltage response was convex upwards negative resistance was likely to result. Obviously, since the curves in Fig. 22 do not depart too much from straight lines, the amount of negative resistance, if any, might be expected to be small.

5.3 Small-signal Frequency Dependent Resistance

By taking the Fourier cosine transform of the open circuit voltage response, the device series resistance can

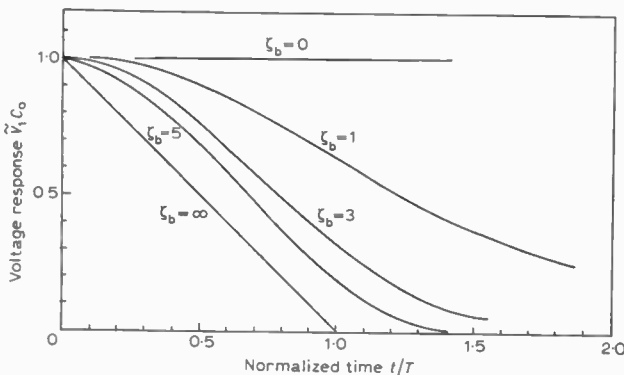


Fig. 22. Impulse response of baritt for various values of the barrier delay parameter $\zeta_b = T/\tau_b$.

be found. Performing the necessary integration gives

$$R(\omega) = \frac{T}{C_0} \frac{T}{[1+(\theta^2/\zeta_b^2)]} \left\{ \frac{1 - \cos \theta + (\theta/\zeta_b) \sin \theta}{\theta^2} \right\} = \frac{T_0}{C_0} U(\zeta_b \theta) \quad (63)$$

$U(\zeta_b \theta)$ is plotted in Fig. 23 as a function of transit angle θ for various values of the ratio ζ_b . By differentiating (63) it can be shown that the maximum negative resistance occurs when $\zeta_b = 3.024$, and the transit angle $\theta = 5\pi/3 = 300^\circ$. This maximum value is

$$R(\omega)_{\max} = \frac{0.009T}{C_0} \quad (64)$$

Since equation (59) gives $\zeta \propto J_B$, Fig. 23 shows that the maximum negative resistance increases as the bias current increases, until $\zeta_b \approx 3$, and then decreases as the bias current is further increased. This behaviour is clearly seen in experimental devices.

If the negative resistance for the baritt (Fig. 23) is compared with that for the t.e. amplifier (Fig. 7), it is clear that the baritt will only give a negative resistance which is between 1/10 and 1/20 that obtainable from a t.e. device. Therein lies one of its disadvantages.

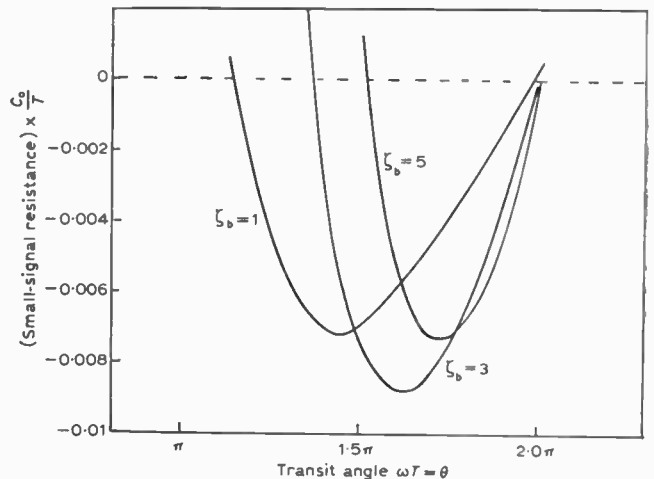


Fig. 23. Small signal resistance of baritt device as a function of transit angle θ , for various values of delay parameter ζ_b .

5.4 Noise Measure of the Baritt

The open-circuit mean square noise voltage due to diffusion noise can be calculated in just the same manner as for the t.e. amplifier having $\zeta = 0$, since velocity saturation pertains everywhere. The barrier cathode has no effect on the diffusion noise, as should be obvious by following through the derivation leading to equation (39) in the context of the present device. The barrier does produce shot noise however which we will consider briefly later.

Thus the appropriate value of the $S(\zeta\theta)$ to use for the baritt noise measure is $\zeta = 0$ in Fig. 15. The ratio $S(0, \theta)/U(\zeta_b = 3, \theta)$ is plotted in Fig. 24 for the baritt having $\zeta_b = 3$ and thus adjusted for minimum noise figure. As equation (45) shows, the noise measure is proportional to this ratio. Comparison of Figs. 17

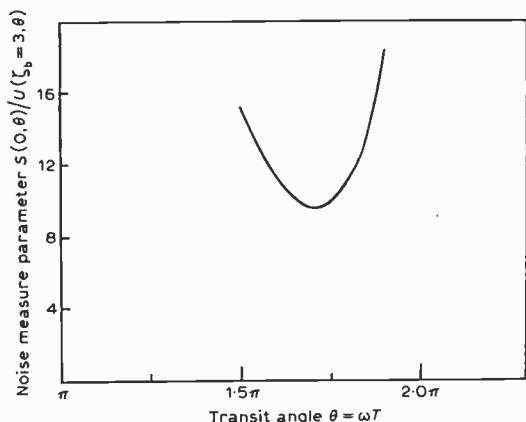


Fig. 24. Noise measure parameter $S(0, \theta)/U(\zeta_b = 3, \theta)$ as a function of transit angle θ , for optimum value of delay parameter $\zeta_b = 3$.

and 24 shows that for a given free carrier concentration (p_0 for holes in the case of the particular baritt being considered here) and diffusion coefficient, the noise figure of the baritt is some five times greater than for the t.e. amplifier. However, such a comparison is misleading since the free carrier concentration in a baritt is normally much less than for a t.e. device.

Taking the minimum value for S/U to be 10 for the baritt, the lowest noise measure may be written, using equation (45), as

$$M = \frac{p_0 e^2 D l 10}{v_0 \epsilon k T_0} \tag{65}$$

The free hole concentration p_0 is given by

$$p_0 = \frac{J_B}{e v_0} \tag{66}$$

where J_B is the bias current. Using equations (65) and (66),

$$M = \frac{10 J_B e D l}{v_0^2 \epsilon k T_0} \tag{67}$$

This value of M pertains for $\zeta_b \approx 3$; hence from equation (59), $J_B \approx 100 \text{ A/cm}^2$ for a device with $l \approx 5 \mu\text{m}$, $N_D \approx 10^{15} \text{ cm}^{-3}$.

The hot electron diffusion coefficient for holes in silicon has been measured by Sigmon and Gibbons²⁰ and appears to be only slightly dependent on field. We will take the low field value of $15 \text{ cm}^2/\text{s}$ as appropriate therefore, even under hot electron conditions.

Equation (67) gives, with these assumptions

$$M \approx 3 \text{ or } 4.8 \text{ dB.}$$

This relatively low value of noise measure for the baritt would seem to make it strongly competitive with the t.e. amplifier as far as noise performance is concerned. We have however omitted to calculate the contribution to the total noise measure that arises from shot noise generated as carriers across the barrier. Although this calculation is quite straightforward, it is beyond the scope of the present paper. Stutz *et al.*²¹ have shown that it is important at low current densities ($J_B \leq 10 \text{ A/cm}^2$) but at higher current densities it is effectively smoothed by the background of injected space charge. A further

factor that has prevented noise measures as low as the value predicted here being observed so far is probably the important degradation of negative resistance that arises from the spreading resistance of the device contacts. We have noted that the available negative resistance in a baritt is considerably less than in a t.e. amplifier; thus any added parasitic series resistance is important, particularly as the noise measure is inversely proportional to the total device series resistance.

The lowest noise figure reported to date for a silicon p^+np^+ structure having dimensions similar to those discussed here is 10 dB;^{9,22} the corresponding noise measure is 9.5 dB.

6 Conclusions

The negative resistance and noise measure of transferred-electron and baritt amplifiers have been calculated with the aid of a simple impulse model which helps to illustrate the physical mechanisms responsible for gain and noise. In particular, the InP reflexion amplifier is shown, at least in theory, to be capable of giving a lower noise than presently observed.

The validity of these calculations may be questioned since they relate to the t.e. amplifier for a situation where both the d.c. electric field and free carrier concentration are spatially uniform. Such conditions are difficult to achieve in practice because of space charge injection from the cathode contact. However, more detailed computer simulations,²³ where realistic devices are modelled, show that the simple analysis described in this paper is capable of predicting the noise measure with fair accuracy. For example, in reference 24, an InP structure is described which has an nl product of $3 \times 10^{10} \text{ cm}^{-2}$ and a computed minimum noise measure of approximately 4 dB compared to the value predicted here of just over 2 dB. The difference is caused by noise generated in the low field region near the cathode and which is not accounted for in the simple theory.

It is tempting to speculate on whether new hot electron devices having lower noise measures than those described here can be devised. The ingredients would appear to be a material with a low diffusion coefficient and a mechanism which can produce significant negative resistance without space charge growth (and consequent amplification of the noise fluctuations) and which does not involve a barrier to control injection and thereby produce shot noise.

7 Acknowledgments

I am very grateful to Mr. J. E. Sitch of this Department for many helpful discussions. The optimum nl product for minimum noise was first noted in some of his computer simulations of realistic devices.

8 References

- Baskaran, S. and Robson, P. N., 'Gain and noise figure of GaAs transferred-electron amplifiers at 34 GHz', *Electronics Letters*, 8, No. 5, pp. 109-10, 9th March 1972.
- Baskaran, S. and Robson, P. N., 'Noise performance of InP reflexion amplifiers in Q band', *Electronics Letters*, 8, No. 5, pp. 137-8, 9th March 1972.

3. Rabier, A. and Spitalnik, R., 'Diode characterization and circuit optimisation for transferred-electron amplifiers', Proc. of 1973 European Microwave Conference, Vol. 1, Paper A6.1.
4. Braddock, P. W. and Gray, K. W., 'Low noise wideband indium-phosphide transferred-electron amplifiers', *Electronics Letters*, 9, No. 2, pp. 36-7, 25th January 1973.
5. Braddock, P. W., Gray, K. W. and Hodges, R. D., 'Measurement of the noise figure and admittance of InP transferred-electron amplifying devices', Proceedings of the 1973 European Microwave Conference Vol. 1, Paper A7.5.
6. Perlamn, B. S., Upadhyayula, C. L. and Marx, R. E., 'Wideband reflection-type transferred electron amplifiers', *IEEE Trans. on Microwave Theory and Techniques*, MTT-18 No. 11, pp. 911-21, November 1970.
7. Conlon, R. F. B. and Heeks, J. S., 'Characterization of wideband supercritical transferred-electron amplifiers', Proceedings of the 1973 European Microwave Conference, Vol. 1, Paper A6.2.
8. Coleman, D. J., Jr. and Sze, S. M., 'A low-noise metal-semiconductor-metal (m.s.m.) microwave oscillator', *Bell Syst. Tech. J.*, 50, No. 5, pp. 1695-9, May-June 1971.
9. Björkman G. and Snapp, C. F., 'Small-signal noise behaviour of companion p⁺-n-p⁺, and p⁺-n-v-p⁺ punchthrough microwave diodes', *Electronics Letters* 8, No. 20, pp. 501-3, 5th October 1972.
10. Shockley, W., Copeland, J. A. and James, R. P., 'The impedance field method of noise calculation in active semiconductor devices', in 'Quantum Theory of Atoms, Molecules, Solid State' pp. 537-63 (Academic Press, New York 1966).
11. Bulman, P. J., Hobson, G. S. and Taylor, B. S., 'Transferred Electron Devices' (Academic Press, London, 1972).
12. Fawcett, W. and Herbert, D. C., 'High field transport in indium phosphide', *Electronics Letters*, 9, No. 14, pp. 308-9, 12th July 1973.
13. McCumber, D. E. and Chynoweth, A. G., 'Theory of negative-conductance amplification and of Gunn instabilities in 'two valley' semiconductors', *IEEE Trans. on Electron Devices*, ED-13, No. 1, pp. 4-21, January 1966.
14. Thim, H. W. and Barber, M. R., 'Microwave amplification in a GaAs bulk semiconductor', *IEEE Trans. on Electron Devices*, ED-13, No. 1, pp. 110-14, January 1966.
15. Fawcett, W. and Rees, H. D., 'Calculation of the hot electron diffusion rate for GaAs', *Physics Letters*, 29A, 10, pp. 578-9, 11th August 1969.
16. Hammar, C. and Vinter, B., 'Diffusion of hot electrons in indium phosphide', *Electronics Letters*, 9, No. 1, pp. 9-10, 11th January 1973.
17. Haus, H. A. and Adler, R. B., 'Circuit Theory of Linear Noisy Networks', (Wiley, New York, 1959).
18. Thim, H. W., 'Noise reduction in bulk negative-resistance amplifiers', *Electronics Letters*, 7, No. 4, pp. 106-8, 25th February 1971.
19. Maloberti, F. and Svelto, V., 'Noise spectrum and noise figure of a device with bulk negative differential mobility', *Alta Frequenza*, 40, pp. 667-73, 1971.
20. Sigmon, T. W. and Gibbons, J. F., 'Diffusivity of electrons and holes in silicon', *Applied Physics Letters*, 15, No. 10, pp. 320-2, 15th November 1969.
21. Statz, H., Pucel, R. A. and Haus, H. A., 'Velocity fluctuation noise in metal-semiconductor-metal diodes', *Proc. IEEE*, 60, No. 5, pp. 644-5, May 1972.
22. Sjölund, A., 'Small-signal noise analysis of p⁺-n-p⁺ baritt diodes', *Electronics Letters*, 9, No. 1, pp. 2-4, 11th January 1973.
23. Sitch, J. and Robson, P. N., 'The noise measure of transferred electron amplifiers', to be published.
24. Sitch, J., 'Computer modelling of low-noise indium-phosphide amplifiers', *Electronics Letters*, 10, No. 6, pp. 74-5, 21st March 1974.

9 Appendix 1: Effect of diffusion on the injected space charge

We denote all small-signal quantities by a superscript tilde. The equations governing the propagation of the injected charge density $\tilde{\rho}$ are

$$(a) \text{ Poisson } \frac{\partial \tilde{E}}{\partial x} = \tilde{\rho}/\epsilon \tag{68}$$

$$(b) \text{ Continuity } \frac{\partial \tilde{J}}{\partial x} + \frac{\partial \tilde{\rho}}{\partial t} = 0 \tag{69}$$

$$(c) \text{ Current } \tilde{J} = \rho_0 \mu \tilde{E} + v_0 \tilde{\rho} - D \frac{\partial \tilde{\rho}}{\partial x} \tag{70}$$

The first two terms in (70) are due to drift, the last term to diffusion; ρ_0 and v_0 are the d.c. carrier density and drift velocity respectively. Elimination of \tilde{J} and \tilde{E} from these give

$$D \frac{\partial^2 \tilde{\rho}}{\partial x^2} - v_0 \frac{\partial \tilde{\rho}}{\partial x} - \tilde{\rho}/\tau - \frac{\partial \tilde{\rho}}{\partial t} = 0 \tag{71}$$

where τ is the dielectric relaxation time $\epsilon/\rho_0 \mu$. The appropriate solution to (71), as may be checked by substitution, is

$$\tilde{\rho} = \frac{-\tilde{Q}_0}{A2\sqrt{(\pi Dt)}} \exp\left\{-\frac{(x-v_0 t)^2}{4Dt}\right\} \exp(+t/\tau) \tag{72}$$

if the sign of the relaxation time is negative. The total charge

$$A \int_{-\infty}^{\infty} \tilde{\rho} dx$$

is seen to be equal to the total injected charge $-\tilde{Q}_0$ at $x = 0, t = 0$, and the charge density has the form of a Gaussian delta function. The centre of gravity of the Gaussian function moves with the drift velocity v_0 . The electric field \tilde{E} is given from (68) as

$$\tilde{E} = \int_{-\infty}^x \frac{\tilde{\rho} dx}{\epsilon} \tag{73}$$

Substituting for $\tilde{\rho}$ from (72), making the substitution $s^2 = \{(x-v_0 t)^2\}/4Dt$ and performing the resulting integration gives equation (21).

10 Appendix 2: On the relationship between noise current fluctuations and diffusion coefficient

Consider that we follow the motion of a single drifting carrier over time T , which contains many collisions. Figure 25 shows how the resolved component of velocity along the direction of the field might fluctuate over this time. Obviously the distance moved in time t in the direction of the field is

$$x = \int_0^T v(t) dt \tag{74}$$

Suppose we conducted this experiment many times for different trial particles. There would be a spread in x , from trial to trial, about the ensemble average \bar{x} , where

$$\bar{x} = v_0 T \tag{75}$$

v_0 being the drift velocity. The probability density function for x would be Gaussian because of the central limit theorem; or looked at another way, if the experiment

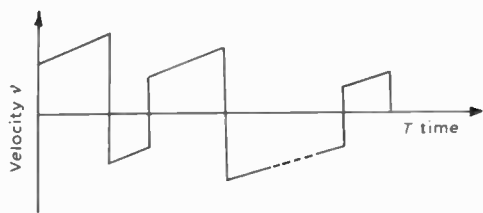


Fig. 25. Variation of the parallel component of velocity of a single electron with time in the presence of a drift field and scattering events.

starts with every particle of the ensemble at $x = 0$, $t = 0$ (i.e. a delta function), they then diffuse to give a spatial Gaussian distribution in accordance with the macroscopic diffusion equation (see eqn. (72), for example). It is readily shown that in this case

$$2DT = (\overline{x - \bar{x}})^2 \tag{76}$$

where a bar denotes an ensemble average, and D is the longitudinal diffusion coefficient. Equation (76) could be considered as defining the diffusion coefficient; it is certainly the quantity experimentally measured, for example, by Sigmon and Gibbons.²⁰

From equations (75) and (76)

$$D = \frac{1}{2T} \overline{\left[\int_0^T (v(t) - v_0) dt \right]^2} \tag{77}$$

Writing

$$v(t) - v_0 = v^1(t) \tag{78}$$

we obtain

$$D = \frac{1}{2T} \overline{\left[\int_0^T v^1(t) dt \right]^2} \tag{79}$$

Strictly D is a macroscopic concept and T should contain many collisions. Thus we could formally write (79) as

$$D = \lim_{T \rightarrow \infty} \frac{1}{2T} \overline{\left[\int_0^T v^1(t) dt \right]^2} \tag{80}$$

10.1 Noise Spectrum

The noise current induced in the external circuit by an electron charge e moving with velocity v , between electrodes spaced d apart is

$$i = \frac{ev}{d} \tag{81}$$

Using equation (78), we can write for the trial electron shown in Fig. 25:

$$i = \frac{e}{d}(v_0 + v^1(t)) \tag{82}$$

which holds over the time T . Now the Fourier transform of this waveform $F(f)$ say, is given by

$$F(f) = \frac{e}{d} \int_0^T (v_0 + v^1(t)) \exp(-j\omega t) dt \tag{83}$$

The energy spectral density on a 1Ω basis is $|F(f)|^2$, and the average power spectral density is $|F(f)|^2/T$. The ensemble long time average power spectral density

$\overline{G(f)}$ is then, from (83),

$$\begin{aligned} \overline{G(f)} &= \lim_{T \rightarrow \infty} \frac{e^2 \left| \int_0^T (v_0 + v^1(t)) \exp(-j\omega t) dt \right|^2}{d^2 T} \tag{84} \\ &= \lim_{T \rightarrow \infty} \left\{ \frac{e^2 \left| \int_0^T v_0 \exp(-j\omega t) dt \right|^2}{d^2 T} + \right. \\ &\quad \left. + \frac{e^2 \left| \int_0^T v^1(t) \exp(-j\omega t) dt \right|^2}{d^2 T} + 0 \right\} \tag{85} \end{aligned}$$

The last term in brackets is zero because $\overline{v^1(t)} = 0$. The first term in brackets in (85) can be evaluated to give

$$\lim_{T \rightarrow \infty} \frac{e^2 v_0^2 T \left\{ \frac{\sin(\omega T/2)}{\omega T/2} \right\}^2}{d^2} = \frac{e^2 v_0^2}{d^2} \delta(f) \tag{86}$$

from a definition of the unit delta function $\delta(f)$.

The total number of electrons, per unit cross section area, in the volume length d is $n_0 d$, where n_0 is the free electron density. The power spectral density or mean square current spectral density $\overline{J_n^2(f)}$ is therefore using (85) and (86)

$$\overline{J_n^2(f)} = \frac{n_0 e^2}{d} \left\{ \lim_{T \rightarrow \infty} \frac{2}{T} \overline{\left[\int_0^T v^1(t) \exp(-j\omega t) dt \right]^2} \right\} + n_0^2 e^2 v_0^2 \delta(f) \tag{87}$$

The factor 2 in equation (87) arises since spectral components at negative and positive frequencies have to be taken into account. The delta function in the spectral density just gives the mean square current density due to the d.c. component of current and is seen to be correct. The noise away from d.c. is just the first term on the r.h.s. of (87). In particular for low frequencies, we can assume $\omega \rightarrow 0$, and thus (87) gives

$$\overline{J_n^2} = \frac{n_0 e^2}{d} \left\{ \lim_{T \rightarrow \infty} \frac{2}{T} \overline{\left[\int_0^T v^1(t) dt \right]^2} \right\} \tag{88}$$

The r.h.s. in curly brackets is just $4D$, from equation (80). Thus we have

$$\overline{J_n^2} = \frac{4n_0 e^2 D}{d} \tag{89}$$

which is the formula we require for computing the noise in t.e. devices. Equation (89) shows that if the longitudinal diffusion coefficient is calculated correctly by say a Monte-Carlo technique¹⁵ where the free flights of many individual electrons are computed, it serves also to specify the mean square noise current fluctuations per unit bandwidth. This is a very general result and holds presumably at any drift field and also if inter-valley transfer takes place.

Manuscript received by the Institution on 1st April 1974 (Paper No. 1610jCC214)

LETTERS

From: O. Fr Harbek

Professor J. C. Anderson, D.Sc(Eng.),
Ph.D., F.Inst.P., C.Eng., M.I.E.R.E.

and F. W. Stephenson, B.Sc., Ph.D.

Electrical Conduction in Thin Lubrication Oil Films — An Explanation of the Coherer?

I have with interest read the paper by J. C. Anderson and W. G. Fiennes on the above subject.* I have for years been interested in, and intrigued by the 'coherer', used for detection of electromagnetic transmissions in wireless spark telegraphy at the beginning of this century.

A satisfactory explanation of how these devices worked has, to my knowledge, never been given, and now it has of course long ceased to be of interest.

There seems to me, however, to be a fundamental similarity between the arrangement reported in the above paper and the 'coherer' made by Oliver Lodge and A. Muirhead.† This consisted of a small steel disk, rotated by a motor and dipping into a pool of mercury. The mercury was covered with a drop or film of mineral oil.

The device was normally non-conducting, but when it was 'hit' by transient voltages picked up by a suitable aerial it became conducting and could operate a relay from a local current source. The transient nature of the received, heavily damped, wave trains from the spark transmitter seemed to be a requirement to make the device work.

This suggests a barrier break-down due to electron injection caused by localized field emission. The sensitive non-conducting state is re-established as a fresh oil film is drawn in by the rotation of the steel disk.

O. FR. HARBEK

Norwegian Defence Research Establishment,
P.O. Box 115, N-3191 Horten,
Norway.

19th August 1974

Mr. Harbek has raised a most interesting question in connection with the coherer. I think he is absolutely right and that the coherer depended upon space-charge limited current in the oil film in the same way as the oil film in our experiments.

In the article in *The Electrician*, in which Lodge and Muirhead describe the device, a d.c. voltage of 0.03 to 0.5 V is quoted as being applied to the coherer and it is stated that, 'at moderate speed' 1 V is sufficient to break down the film of oil and establish 'coherence'. From our results it is not

unlikely that 1 V would be sufficient to initiate current run-away of the type shown in Fig. 7 of our paper. From the same Figure I think one can understand the reason why a continuous wave train does not work. After the film reaches the trap-filled limit and becomes highly conducting, reduction of the voltage does not immediately reduce the current, because the space charge in the film itself acts as a source of current. There is thus a recovery time before the film again becomes non-conducting. I would therefore expect a continuous wave of sufficient amplitude to cause the coherer to remain in a conducting state.

There is a second point in this connection; the transient due to a spark, having a rapid rise, may well produce a large inductive voltage in the receiving coil, which is sufficient to initiate conduction. A continuous sine wave of low amplitude may not produce a sufficient voltage and so the coherer would never conduct.

There is one further feature worth noting. The coherer incorporated a felt pad in contact with the disk. This is said to wipe off dust and dirt picked up from contact with the mercury. No doubt this is its primary function, but it would also tend to wipe off charge-conditioned oil and help to re-establish the non-conducting state.

J. C. ANDERSON

Department of Electrical Engineering,
Imperial College of Science and Technology,
Exhibition Road,
London SW7 2BT

3rd September 1974

Design Tables for Active R C Networks

I would like to draw attention to certain errors in my paper 'Design tables for low-pass equal-valued capacitor active RC networks' which was published in Vol. 44, No. 5, May 1974 (pp. 250-256).

The Chebyshev approximating functions in the above paper have been ascribed the wrong coefficients. The examples given thus refer to functions *A*, *B*, *C*, *D* rather than to Chebyshev 0.5 dB, 1 dB, 2 dB and 3 dB ripple.

The general form of solution for the Chebyshev function is the same as indicated in the text and the error in no way affects any of the theoretical aspects of the paper.

A new set of tables has been prepared to take into account the correct coefficients and will be sent on request.

F. W. STEPHENSON

Department of Electronic Engineering,
The University of Hull
Hull HU6 7RX

4th October 1974

* *The Radio and Electronic Engineer*, 44, No. 3, p. 141, March 1974.

† *The Electrician*, 50, p. 930, 1903.

IERE News and Commentary

Institution Christmas Cards

Due to unavoidable circumstances it has not been possible to produce new designs for IERE Christmas Cards for 1974. Limited stocks of the two designs supplied last year are still available at the same prices. (See September and October 1973 Journals for illustrations of these cards). The special order form on page (vii) of this issue must be used.

International Award for Solid State Physics

The Secretariat of the European Physical Society (EPS) in Geneva has announced the establishment of the Hewlett-Packard Europhysics Award for outstanding achievement in Solid State Physics. This prize of 20,000 Swiss Francs (about £3,000) will be awarded each year by EPS to one or several physicists, without restriction as to nationality, thanks to an annual donation made to the Society by Hewlett-Packard S.A., the European headquarters organization of the Hewlett-Packard Company, Palo Alto, California.

According to the charter 'the award shall be given in recognition of a recent work by one or more individuals in the area of physics of condensed matter, specifically work leading to advances in the fields of electronic, electrical and materials engineering which, in the opinion of the Society's selection committee, represents scientific excellence. Recent work is defined to mean completed within 5 years prior to the award. The award may be given for either pure or applied research at the discretion of the Society'.

The Selection Committee for the award has been appointed by the Executive Committee of the EPS and the first award will be made on the occasion of the Third EPS General Conference in Bucharest in September 1975.

IEE Conference Publications

Members of the IERE may purchase single copies at reduced rates of the following volumes of papers read at conferences for which the Institution was a co-sponsor:

'Precision Electromagnetic Measurements', London, July 1974 (IEE Conference Publication 113), £8.80 (normal price £12.40).

'Frontiers in Education', London, July 1974 (IEE Conference Publication 115), £10.00 (normal price £15.00).

Orders for members wishing to take advantage of these special rates should be placed through the IERE Publications Department, 9 Bedford Square, London WC1B 3RG.

The August Journal

The attention of members was drawn in a 'stop press' announcement in the September issue to the urgent requirement for copies of the August 1974 issue of *The Radio and Electronic Engineer*. An error in the computer controlled addressing process for this issue has meant that some members have been sent two copies. As a result, stocks have been completely exhausted and it would be greatly appreciated if those members who did in fact receive an extra copy of the August issue would return it to the Institution as soon as convenient.

Fellowship for Operational Research

There has been in existence for a number of years an Operational Research Society which has provided a forum for those interested in the many aspects of operational research to meet and discuss the technical aspects of this wide field.

The Fellowship for Operational Research Limited, which has recently been formed, has the objective of supporting operational research as a profession by establishing standards of practice on competence and ethical conduct. It co-operates with the Operational Research Society and seeks to establish professional standing by electing Fellows who have experience and qualifications of assessed standing. The grade of Associate also exists for those who are not yet qualified to be Fellows.

Further information about the Fellowship may be obtained from 3 Field Court, Grays Inn, London WC1 5EN.

International Engineers Meetings

The next meeting of the Commonwealth Engineering Conference (CEC) is expected to be held in Accra, Ghana, in the week starting 16th June 1975. This will be the first time that the Conference has met in Africa. The Chairman of the CEC is Sir Angus Paton and its Secretary is Mr. M. W. Leonard.

The next General Assembly of the World Federation of Engineering Organisations (WFEO) will be held in Tunis in the week starting 23rd June 1975. It is planned that there will be one day for business meetings and two or three days for discussion of themes of concern to the engineering profession. CEI is the UK national member of WFEO. Its Secretary General is Dr. G. F. Gainsborough, Secretary of the Institution of Electrical Engineers.

Institution Representatives

It is regretted that there were certain omissions and inaccuracies in Appendices to the Annual Report for 1973-74, published in the August issue of the Journal.

In Appendix 3, the Institution's Representative at Watford College of Technology should have been shown as F. P. Thomson (*Member*).

In Appendix 5, the Institution Representatives at the City and Guilds of London Institute should have included the following entry: *Advisory Committee for Communication Technical Information*
F. P. Thomson (*Member*).

The Clerk Maxwell Lodge

Mr. R. T. Webb, B.Sc., M.I.W.M., has been elected as the 20th Master of the Clerk Maxwell Lodge for the year 1974-75.

The Lodge is supported by a number of members of the Institution and information regarding Lodge Meetings can be obtained from the Secretary, Mr. S. J. H. Stevens, B.Sc., C.Eng., F.I.E.R.E., The Birches, Park Close, Fetcham, Leatherhead, Surrey.

Membership of the Annan Committee

The membership of the Committee of Inquiry into the Future of Broadcasting which is being set up by the Government was announced in the House of Commons in a written answer by the Home Secretary, Mr. Roy Jenkins, in June just before the Parliamentary Recess.

The Chairman is Lord Annan, Provost of University College London, and the fifteen other members of the Committee who are representative of political and social affairs, the arts, local government, the trades unions and education, include Professor Geoffrey Sims (Fellow), Head of the Department of Electronics at the University of Southampton for the past eleven years. Professor Sims became Vice Chancellor of the University of Sheffield on September 1st, and a note on his career was published in the August Journal.

The Committee's terms of reference, announced by the Home Secretary on April 10th, are:

'To consider the future of the broadcasting services in the United Kingdom, including the dissemination by wire of broadcast and other programmes and of television for public showing; to consider the implications for present or any recommended additional services of new techniques; and to propose what constitutional, organizational and financial arrangements and what conditions should apply to the conduct of all these services.'

Speaking at a press conference following the first meeting of the Committee, Lord Annan said that they would be making recommendations about the broadcasting services in the 1980s, but before doing this the services which had been provided in the last ten years would need to be reviewed.

He continued:

'We are bound to receive evidence from many organizations and individuals with an interest in broadcasting. But in the first instance, we want viewers and listeners to write to us to let us know what they think of the present services, what they like and what they dislike and—if they care to—why.'

(Announcements inviting evidence have recently appeared in the advertisement columns of several national newspapers).

Lord Annan believed that technological developments would obviously affect very considerably the future of broadcasting and the cost of new advances would influence their acceptance.

It is expected that the Committee will take about two and a half years to report and that a similar period of time will be needed for consultation on the Committee's recommendations and for any legislation that may be necessary. To allow the necessary time for the Committee to complete its task and for consideration of its proposals the Government have extended the Independent Broadcasting Authority Act 1973 to July 1979; it would otherwise expire in July 1976. The Charter of the BBC has been extended for a similar period.

In 1961 the IERE, through the Technical Committee and the Television Group Committee, presented evidence on a number of technical matters to the 'Pilkington' Committee on Broadcasting and the question of whether evidence should be submitted to the Annan Committee is being considered by the Executive and Professional Activities Committees.

National Centre of Systems Reliability

The establishment of the National Centre of Systems Reliability has been authorized by the Department of Industry. The Centre will be based on the reliability expertise

developed by the Safety and Reliability Directorate of the United Kingdom Atomic Energy Authority. It will extend the UKAEA's existing services to industry in the assessment of the reliability and safety of commercial plant which will continue to be operated as the Systems Reliability Services (SRS).

The commercial and data bank activities of the SRS will be complemented by an Applied Research Unit which will undertake research and development of systems reliability technology in the national interest. The R and D programme will be directed to the solution of reliability and availability problems that arise in industry.

The Centre will be at Culcheth, near Warrington, under the control of the Authority's Director of Safety and Reliability. In addition to Authority staff from Culcheth, Harwell and Risley, the Centre will also have attached staff from a number of universities that are actively participating in this work. The Centre will be able to draw on the resources of all establishments of the Authority.

Reliability assessments have been performed by SRS over the years on a very wide range of industrial plants including mass production engineering plants, oil refineries, chemical plants, ships and protective systems, any of which can be regarded as an assembly of components liable to periodic breakdown. From information on the failure characteristics of various components, it is possible, by applying the techniques developed by the UKAEA, to forecast quantitatively the likely reliability and/or availability of a plant. Most plants include potential hazards, e.g. flammable materials, and these hazards may be reduced to acceptable levels by the analysis of the modes and effects of individual failures and by the provision of preventative or warning systems.

Enquiries concerning the work of the Centre should be addressed to the National Centre of Systems Reliability, UKAEA, Wigshaw Lane, Culcheth, Warrington, WA3 4NE. Telephone No.: Warrington 31244, Exts. 213, 214 and 212.

Export Awards for Smaller Manufacturers

Each year five 'Export Awards' are made to mark the contributions which have been made by small firms to British exports. These awards are sponsored by British Airways (Overseas Division), the British Overseas Trade Board and the Association of British Chambers of Commerce who administer the scheme.

Any independent manufacturing company or group of companies employing fewer than 200 people, whose exports exceeded £50,000 in the year ending 31st March 1973 and £100,000 in the year ending 31st March 1974 and which has not won the Award before will be eligible to apply.

An unusual feature is that the Award is intended to recognize not only the achievement of management but of the staff as well. For the management of each winning firm a trophy and certificate will be awarded. The main prize, however, goes to the employees and is the only award of its kind to do so. Each winning firm will have the opportunity to nominate an employee from the shop floor or office, and spouse, to participate in a two-weeks' group tour of Kenya, including a visit to a Game Reserve.

Application forms and fuller details of the Award may be obtained from the Associations of British Chambers of Commerce, 75 Cannon Street, London EC4N 5BB (Tel. No. 01-248 7211). The closing date for entries is 2nd December 1974. For further information contact John im Thurn, ABCC Director International Affairs at the above address.

Obituary

The Council has learned with regret the deaths of the following members:

Raymond Hubert Garner, B.Sc.(Eng), (Fellow 1958, Member 1947) died on 16th July 1974 aged 65. He leaves a widow.

Ray Garner will be best known to members of this Institution for his great contribution to its educational work over many years of active membership. He served for 8 years as Chairman of the Education Committee, and during this period the Committee worked under his inspiration to bring the Institution's Graduateship Examination up to the ever increasing demands of a profession whose technological requirements were becoming continually more complex. When he finally stepped down from office the educational requirements for membership of the Institution were such as to make comparatively smooth the transition to the CEI examination. He was always very much aware of the importance of technicians to the engineering profession and forcefully advocated their closer association with the Institution.

Born and educated in Leicester, Mr. Garner attended the then University College and obtained the B.Sc. External Degree in Engineering of London University in 1936. His early industrial experience was gained with Leicester engineering firms: Gent and Company and the Midland Dynamo Company. However, his inclinations had always been towards teaching and after a number of part-time appointments, he went to Paddington Technical Institute in 1935 as Lecturer in Electrical Engineering. A period at Walsall Technical College followed and in 1936 he was appointed Head of the Engineering Department at Shrewsbury Technical College. Here he remained for ten years organizing its great expansion for the training of service men and women made necessary by the war, and in 1946 he moved to Blackpool Technical College as Head of the Engineering and Science Department.

For the remainder of his professional life Ray Garner's appointments were in Scotland. In 1948 he undertook the challenging post of Principal of the new School of Engineering, Burnbank, Lanarkshire and seven years later he was appointed Principal of Coatbridge Technical College where he remained until a severe stroke in 1971 led to premature retirement. His work load had not merely been that of a College Principal: for many years he worked closely with the Lanarkshire County Council in setting up new Technical Colleges in the area, notably at Motherwell and Hamilton.

In the midst of his educational administrative duties, he found time to write a textbook on 'Mechanical Design for Electrical Engineers', published in 1956.

In addition to his service on the Education and Training Committee, Ray Garner was an elected member of the Council for some

seven years and for three years he was a Vice President. He served on the Executive Committee from 1964 to 1967 and he took a very active part for many years in the work of the Scottish Section, serving as Chairman and as Secretary. He represented the Institution at many meetings with Government Departments, with other institutions and with industry, and he was an IERE representative on the Joint Committees for National Certificates and Diplomas in Electrical and Electronic Engineering.

Technical education in Scotland, in particular, has surely missed Ray Garner's enthusiasm and drive during the last three years and his passing will be greatly regretted in that country as well as among his numerous friends and colleagues in this Institution.

Alfred Maxwell Keeling, O.B.E., T.D. (Member 1962) died on 23rd June 1974 aged 68. He leaves a widow.

Educated privately, Maxwell Keeling entered the GEC Telephone and Radio Works in 1925 and during the pre-war years was concerned with a wide range of communications work for the company; from 1938 to 1939 he was Sales Engineer for special systems. He was commissioned in the Royal Corps of Signals, Territorial Army, in 1937 and served throughout the war with the Corps, his later appointments including G.S.O. 2 to the Signal Officer in Chief, Home Forces (with the rank of Major) and Officer in charge of the Secretariat of British Signals Communications Board in Germany.

In November 1945 Mr. Keeling joined the Department of the Director of Electrical Engineering, Admiralty, as Electrical Engineer in charge of development work concerned with ships' communications systems, a post which he filled with distinction until his retirement in 1970. In the New Year Honours List for 1967 he was appointed O.B.E.

In retirement Maxwell Keeling continued his active work with the Royal British Legion and other charitable bodies. This gave full scope for his fine organizing ability and his real concern for those in trouble. He will be sadly missed by a wide circle of friends.

A.J.B.N.

Arthur William Mews (Member 1953) died on 3rd June, 1974, aged 54 years. He leaves a widow, one son and two daughters.

Arthur Mews was educated at Bedlington Grammar School and he served for four years during the war as a wireless operator with the Royal Corps of Signals. He was invalided out in 1943 and joined Rediffusion (North-East) Limited as a shift engineer. He continued with this company for the next 13 years, ultimately becoming Assistant Chief Engineer. During this period he gained City and Guilds qualifications by part-time study at Rutherford College of

Technology and for some years lectured on Radio Service work at the College.

In 1956 he went to live in Cheshire and took up an appointment as Chief Engineer with Rediffusion (Merseyside) Limited at Bootle.

Mr. Mews took an active part in the Institution's affairs, serving on the Committees of both the North-East Section and the Merseyside Section as Programme Secretary, and for several years until 1964 he was Chairman of the Merseyside Section.

P.F.

Kenneth Walmsley (Member 1973, Graduate 1970) died on 4th September, 1974. He was 35 years of age and leaves a widow.

Kenneth Walmsley received his early technical training as a craft apprentice with English Electric at Accrington, and after a period outside the industry, he joined the Capacitor Division of Standard Telephones and Cables at Paignton in 1961. He remained with this company as a Measuring Equipment and Standards Engineer in the test house where he was responsible for design, development and construction of measuring equipment and calibration of divisional primary standards. During this period he studied at South Devon Technical College and Plymouth Polytechnic to complete his Higher National Certificate in Electrical Engineering with endorsements in electronic subjects.

Raymond Herbert George Salkilld (Member 1968) died on 23rd May 1974; he was 49 years of age and leaves a widow.

Educated at Christ's College, Finchley, Mr. Salkilld obtained his technical education at Enfield Technical College and Northern Polytechnic. From 1941 to 1946 he was with A.C. Cossor Limited as Junior Test Engineer and he subsequently went into REME serving as telecommunications mechanic with responsibility for radar installations. From 1948 to 1953 he was in business on his own account and he then joined GEC Electronics with whom he remained until his death. In 1962 he was promoted to Principal Engineer and led a project team working on defence equipment.

Anthony John Aylward (Graduate 1967) died on 15th January 1974 aged 44 years. He leaves a widow and one daughter.

Mr. Aylward was educated in the Training Ship *Arethusa* and in 1945 entered Boy's Service in the Royal Navy in H.M.S. *Ganges*. He remained in the Navy until 1956 when he was invalided out of the Service in the rank of Petty Officer; his last appointment was in H.M.S. *Collingwood* as an Instructor on radar equipments. Mr. Aylward joined the then Ministry of Civil Aviation with whom he continued until his sudden death. From 1967 onwards he was Senior Instructor at the Civil Aviation Department's Training School at Bletchley.

Conferences in 1975

Antennas for Aircraft and Spacecraft

An international conference on 'Antennas for Aircraft and Spacecraft' will take place at the Institution of Electrical Engineers, Savoy Place, London WC2R 0BL, between 3rd-6th June 1975.

This conference will consider both the military and civil applications of antenna systems, and should be of interest to those responsible for the design, installation and use of radio and radar antenna systems in aircraft and spacecraft.

Subject areas to be covered in the conference programme will include: design problems for antennas for aeronautical and satellite systems; environmental problems; radomes; electronic scanning; aerials with built-in electronics; multi-purpose antennas; special problems of antennas for helicopters and light aircraft; antennas for v.l.f. navigational aids; design of h.f. antennas in aircraft; fixed and scanning radar systems; antennas for millimetre surveillance devices; homing and direction finding from aircraft; methods of testing antennas on the ground and in flight; the calculation of the performance of aerials installed in aircraft and spacecraft; antenna systems components (e.g. phase shifters and circulators); problems of commissioning and maintenance.

The conference is being organized by the Electronics Division of the Institution of Electrical Engineers in association with the IERE, the Institute of Electrical and Electronics Engineers (United Kingdom and Republic of Ireland Section), the Institute of Mathematics and its Applications, and the Royal Aeronautical Society.

The organizing committee invite offers of contributions of not more than 6 A4 pages, which allows for 3000 words of text (or less if illustrations are included) which will be considered for inclusion in the conference programme. Those intending to make an offer should submit a synopsis (of approximately 250 words) immediately to the Conference Department. Full transcripts will be required for assessment by 27th January 1975.

Registration forms and further programme details will be made available a few months before the event from the Conference Department, IEE, Savoy Place, London WC2R 0BL.

Quantum Electronics Conference

The Quantum Electronics Group of The Institute of Physics, in association with the IERE, the IEE and the Chemical Society, is organizing a Second National Quantum Electronics Conference which will be held at St. Catherine's College, Oxford from the 2nd to 4th September 1975.

The aims of the Conference are to provide a national forum for the interchange of information in the field of Quantum Electronics. Contributions from young research workers will be especially welcomed. Topics covered in the conference will include laser physics and laser design, non-linear optics, scattering and spectroscopy, industrial and scientific applications of lasers including laser fusion and isotope separation, optical communications, and related topics in theoretical and experimental quantum electronics.

Offers of contributions—200 words—should be sent to the Conference Secretary, Mr. I. J. Spalding, UKAEA, Culham Laboratory, Abingdon, Oxfordshire OX14 3DB (Telephone: Oxford 41721, Ext. 6253). The provisional deadline for papers is the end of May 1975. Further information may be obtained from the Meetings Officer, The Institute of Physics, 47 Belgrave Square, London SW1X 8QX.

Electrical Methods of Machining, Forming and Coating

'Electrical Methods of Machining, Forming and Coating' is the title of a conference which is being organized by the Institution of Electrical Engineers, and will be held at the IEE, Savoy Place, London WC2 between 18th-20th November 1975.

It is envisaged that the conference will have a strong practical bias for which papers are sought from users, suppliers of equipment and research organizations working in the fields of the various techniques. Reviewing application current practice, process limitations and economic comparisons with conventional methods of potential development.

The scope of this conference, which is the third in the series, will be concerned with machining, cutting, welding, surface treatment and coating of materials utilizing techniques such as particle beam techniques; laser beam techniques; electrical discharge machining; electro-chemical machining and forming; electro-magnetic/electro-hydraulic forming; and electro-phoresis/electro-static coating.

The conference is being organized by the Science, Education and Management Division of the IEE in association with other learned and technical societies and associations.

The organizing committee invite offers of contributions of approximately 3500 words (or less if illustrations are included). Those intending to make an offer should submit, without delay a 250-word synopsis to the IEE Conference Department, Savoy Place, London WC2R 0BL. The authors whose papers are selected will be invited to develop the material to a full contribution for submission by 23rd June 1975.

Electrical Safety in Hazardous Environments

A conference on 'Electrical Safety in Hazardous Environments' has been organized by the Institution of Electrical Engineers to be held at the IEE, Savoy Place, London WC2R 0BL between 9th-11th December 1975.

The conference is the second in a series which aims to examine the various techniques developed, to achieve safety in electrical equipment in industries such as mining, oil petrochemical, and other industries on and off shore, where there is a potential hazard due to explosive mixtures of gases, vapour, mist or dust.

The areas under consideration will include power systems, control, instrumentation, communication and electro-statics. These will be presented within the scope of the following: headings of philosophy of risk assessment; statutory requirements; research and testing; standards; apparatus, design and construction including new materials; the need for certification; codes of practice; installation of apparatus and systems; safety procedure; maintenance and environmental suitability.

The conference has been organized by the Power and Control and Automation Divisions of the IEE, in association with the Institute of Electrical and Electronics Engineers (UK and Republic of Ireland Section), the Institute of Petroleum and the Institute of Physics.

The Organizing Committee invite offers of contributions of approximately 2500 words (or less if illustrations are included) which will be considered for inclusion in the Conference programme. Those intending to make an offer should submit a 250 word synopsis to the IEE Conference Department as soon as possible.

Registration forms and further programme details will be available a few months before the conference from the IEE Conference Department, Savoy Place, London WC2R 0BL

Members' Appointments

CORPORATE MEMBERS

Capt. R. F. Burvill, RN (Fellow 1973) has been appointed to the National Defence College, Kingston, Ontario, Canada to be a member of the 1974/5 Canadian National Defence Course. He was previously in the Ministry of Defence as Assistant Director (Policy), Defence Signals Staff.

Mr. S. L. H. Clarke, B.A. (Fellow 1964, Member 1959) was appointed Technical Director (Automation) of G.E.C. Marconi Electronics Limited in April this year and is now based at the Great Baddow Research Laboratories. He joined Elliotts after graduating in 1951 and subsequently became



Head of the Computer Research Laboratory of Elliott Automation. He has recently been appointed to the Board of Process Peripherals Limited. Mr. Clarke served on the Institution's Instrumentation and Control Group Committee and was its Chairman from 1969 to 1971. He has also served on the Membership Committee and has contributed several papers to the Journal.

Mr. J. S. Sansom, O.B.E. (Fellow 1974, Member 1959, Graduate 1954) has been appointed Director of Studios and Engineering with Thames Television. Mr. Sansom joined independent television in 1957 from industry and worked initially for



TWW, then with ABC Television where he was Chief Engineer from 1966 until the formation of Thames Television in 1968 when he became Chief Engineer of that Company. He was appointed Technical Controller in 1970. Mr. Sansom has served on various national and international

technical committees including the Technical Sub-Committee of the Television Advisory Committee and UK Study Group XI of the CCIR. In 1970 he presented a paper on 'Television Studio Measurements' at the IERE Conference on Television Measuring Techniques.

Mr. N. Wheatley (Fellow 1973, Member 1970, Associate 1961) has been appointed Manager of International Relations with Cable and Wireless at Hong Kong. He went to Hong Kong in 1973 as Manager of Overseas Services having previously held the appointment of Regional Engineer for the company in the Arabian Gulf. In 1970 Mr. Wheatley contributed a paper to the Journal on the planning and commissioning of the communications satellite Earth station at Bahrain.

Mr. B. W. Barnes (Member 1973, Graduate 1966) who has been with the East African Posts and Telecommunications Corporation since 1970 has been transferred from the Uganda Regional Headquarters to the Corporation's Telecommunications Headquarters in Nairobi. Before going to East Africa, Mr. Barnes was with the British Post Office; from May 1967 to September 1969 he was seconded to Cable and Wireless to establish a telephone training school.

Mr. P. D. H. Cobham, B.Sc. (Member 1968, Graduate 1963) who has been on the teaching staff of Twickenham College of Technology since 1968, has been promoted to Senior Lecturer in Electrical and Electronic Engineering. In 1967 he contributed a paper to the Journal on Karnaugh map techniques for designing data interfaces.

Sqn. Ldr. T. C. Davies, B.Sc., RAF (Member 1971) has been posted from RAF Wattlesham as Elect. Eng. 2 at the Headquarters of Training Command RAF Brampton.

Mr. A. V. T. Dike (Member 1958, Associate 1955) has been appointed Director and General Manager of Clarke Instruments Limited at Camberley. He was previously with Marconi Space and Defence Systems, latterly as Manager of the Naval and Ocean Engineering Division.

Mr. I. G. Frith (Member 1971, Graduate 1968) is now Electronic Process Control Supervisor with Senior Service Limited. He was previously a Project Engineer with Dewrance Controls Limited, Skelmersdale.

Sqn. Ldr. R. G. Hatcher, RAF (Member 1973, Graduate 1967) who has been on the staff of Headquarters RAF Germany since 1972, has returned to the UK and is now with the Procurement Executive of the Ministry of Defence, Military Aircraft Projects/1 *Phantom*.

Mr. H. F. Kearney (Member 1968, Associate 1965) has taken up an appointment with the Overseas Development Administration in Brazil. He was previously on the teaching staff of Borehamwood College of Further Education.

Major F. T. Kuwornoo (Member 1971, Graduate 1967) has been appointed Officer Commanding Engineering Wing, Ghana Air Force Station at Accra.

Capt. P. A. Law (Member 1957, Graduate 1952) has been appointed Assistant Controller of Operations at the Headquarters of the Defence Communications Network. He was previously with the NATO Integrated Communication System Management Agency.

Lt. Col. J. M. N. Lyons, R Sigs (Member 1968, Graduate 1962) has taken up the appointment of GSO 1 (Weapons) at the Headquarters 2 Signal Group, Aldershot. He was previously on the staff of the School of Signals, Blandford.

Mr. G. May (Member 1968, Associate 1951) is now a Group Leader in the Communications Division of the Radio Department at the Royal Aircraft Establishment, Farnborough. From 1970 to August of this year Mr. May was with the Directorate of Research Avionics Space and Air Traffic, Ministry of Defence.

Mr. J. A. Nash (Member 1974, Associate 1971) has been appointed Project Leader at the Bahrain Automatic Telex Exchange of Cable and Wireless Limited. For the past three years he has been on the Head Office staff of the Company, latterly as a senior development engineer.

Mr. J. D. Munday (Member 1969, Graduate 1967) has been appointed to the post of Manager of Cable and Wireless Limited in the Yemen Arab Republic. He has been with the Company since 1955 and his previous post was in Qatar.

Mr. J. P. Osborn (Member 1964, Graduate 1963) who has been at the University of Bath School of Education for the past two years, has been appointed senior lecturer in further education at Huddersfield Polytechnic College of Education (Technical).

Mr. V. H. Piddington (Member 1955) is now Principal Post Design Engineer with Rank Radio International, Plymouth. He was previously at the Company's works in Chiswick.

Mr. L. A. Rioual, B.Sc. (Member 1961) who was Marketing Director with Forges d'Alleward S.A. has taken up an appointment as an engineer with the French Atomic Energy Commission at Saclay. In 1963 he contributed a paper to the Journal on the use of magnetic amplifiers for submarine telegraph signals.

Mr. C. P. Rourke (Member 1973, Graduate 1970) who was a Research Technologist with SIRA Institute, is now a Development Engineer at the University of Sussex.

Mr. B. G. Roberts (Member 1967, Graduate 1962) who joined the British Broadcasting Corporation in 1958 and was latterly Assistant Engineer in charge of Studio Engineering at the Television Centre, has taken up an appointment with the New Zealand Broadcasting Corporation in Head Office (Operations) Wellington.

Mr. D. R. A. Steadman, B.Sc.(Eng.) (Member 1968) who was Manufacturing Manager of the Marine Systems Division of the Plessey Company at Ilford, has been appointed Manufacturing Director with Cossor Electronics Limited at Harlow.

Mr. P. S. Sumanatillede, Dip.El. (Member 1970, Graduate 1962) formerly Senior Electrical Engineer with the State Fertilizer Manufacturing Corporation in Sri Lanka, is now a Lecturer in the Department of Electrical and Electronic Engineering at the Ngee Ann Technical College, Singapore.

Mr. D. R. Willis (Member 1969, Graduate 1967) has taken up the appointment of Technical Director at Tesla Engineering Limited, Storrington, Sussex where he is particularly concerned with electromagnets and particle guidance systems. He was previously Technical Manager at Lintott Engineering and concerned with ion implantation and semiconductor processing.

Mr. T. J. Wright (Member 1973, Graduate 1970) is now an Assistant Electrical Engineer with the Directorate General, Ships, Ministry of Defence, Bath.

NON-CORPORATE MEMBERS

Mr. C. L. Hung, B.A.Sc. (Graduate 1959) is now Engineer in charge of Engineering Support at the Air Traffic Control Simulation Centre, Ministry of Transport, Ottawa. He was previously a Test Set Design Engineer for computer applications with Northern Electric.

Mr. J. F. Purchase (Graduate 1972) who went to Messerschmitt-Bolkow-Blohm, Munich, as a Space Craft Systems Engineer two years ago, has now joined ESTEC, Noordwijk, as an E.M.C. Engineer.

Staff Sgt. P. J. Selby, R. Signals (Graduate 1970) has been posted to 4th Division Headquarters Signal Regiment BAOR on completing a course at the School of Signals, Blandford Camp.

Mr. R. L. Shelley (Graduate 1969), who was with Smiths Industries as Production Superintendent with the Access Systems Unit, has been appointed Head of Production Engineering with Chubb Integrated Systems Ltd., St. Albans.

Mr. D. C. L. Thomas (Graduate 1969) is now a Project Engineer with the Procurement Executive at the Ministry of Defence.

Mr. A. L. Unthank (Graduate 1968) is now a Site Construction Engineer, Electrical, with Kennedy and Donkin, consulting engineers, at Whitehead, Co. Antrim, Northern Ireland.

Mr. M. R. Weaver (Graduate 1969) who joined Instrumentation Laboratory (UK) Ltd. as Area Sales and Service Manager for South East England, has been appointed United Kingdom Service Manager with the Company.

Mr. C. J. Leal (Associate Member 1974, Associate 1971) is now a First Engineer (Communications) with the System Operations Branch, Chief Engineer's Office, London Electricity Board.

Mr. E. E. Muro (Associate Member 1974) has completed a British Council scholarship for study at Norwood Technical College and the University of Wales Institute of Science and Technology and has returned to Kenya as Assistant Engineer Instructor at the East African Posts and Telecommunications Corporation's Training School.

STANDARD FREQUENCY TRANSMISSIONS—August 1974

(Communication from the National Physical Laboratory)

| Aug. 1974 | Deviation from nominal frequency in parts in 10^{10} (24-hour mean centred on 0300 UT) | | | Relative phase readings in microseconds NPL—Station (Readings at 1500 UT) | | Aug. 1974 | Deviation from nominal frequency in parts in 10^{10} (24-hour mean centred on 0300 UT) | | | Relative phase readings in microseconds NPL—Station (Readings at 1500 UT) | |
|--------------|--|---------------|----------------------|--|----------------|--------------|--|---------------|----------------------|--|----------------|
| | GBR 16 kHz | MSF 60 kHz | Droitwich 200 kHz | *GBR 16 kHz | †MSF 60 kHz | | GBR 16 kHz | MSF 60 kHz | Droitwich 200 kHz | *GBR 16 kHz | †MSF 60 kHz |
| 1 | 0 | 0 | -0.2 | 699 | 599.2 | 17 | 0 | 0 | -0.2 | 699 | 599.4 |
| 2 | 0 | 0 | -0.2 | 699 | 599.2 | 18 | 0 | 0 | -0.2 | 699 | 599.6 |
| 3 | 0 | 0 | -0.2 | 699 | 599.2 | 19 | 0 | 0 | -0.2 | 699 | 599.8 |
| 4 | 0 | 0 | -0.2 | 699 | 599.4 | 20 | 0 | 0 | 0 | 699 | 599.8 |
| 5 | 0 | +0.1 | -0.1 | 699 | 598.7 | 21 | 0 | 0 | 0 | 699 | 600.1 |
| 6 | 0 | +0.1 | -0.1 | 699 | 597.9 | 22 | 0 | 0 | -0.1 | 699 | 599.7 |
| 7 | 0 | -0.1 | -0.2 | 699 | 598.4 | 23 | 0 | 0 | -0.1 | 699 | 599.8 |
| 8 | 0 | 0 | -0.2 | 699 | 598.7 | 24 | 0 | 0 | -0.1 | 699 | 599.3 |
| 9 | 0 | 0 | -0.2 | 699 | 598.5 | 25 | 0 | 0 | -0.1 | 699 | 599.9 |
| 10 | 0 | 0 | -0.2 | 699 | 598.7 | 26 | 0 | 0 | -0.1 | 699 | 600.0 |
| 11 | 0 | 0 | -0.2 | 699 | 598.6 | 27 | 0 | 0 | -0.1 | 699 | 600.1 |
| 12 | 0 | 0 | -0.2 | 699 | 598.7 | 28 | 0 | 0 | -0.1 | 699 | 600.1 |
| 13 | 0 | 0 | -0.2 | 699 | 599.0 | 29 | 0 | 0 | -0.1 | 699 | 600.5 |
| 14 | 0 | 0 | -0.2 | 699 | 599.2 | 30 | -0.1 | 0 | -0.1 | 700 | 600.5 |
| 15 | 0 | 0 | -0.2 | 699 | 599.0 | 31 | 0 | 0 | -0.2 | 700 | 600.8 |
| 16 | 0 | 0 | -0.2 | 699 | 599.2 | | | | | | |

All measurements in terms of H-P Caesium Standard No. 334, agrees with the NPL Caesium Standard to 1 part in 10^{11} .

* Relative to UTC Scale; $(UTC_{NPL} - Station) = + 500$ at 1500 UT 31st December 1968.

† Relative to AT Scale; $(AT_{NPL} - Station) = + 468.6$ at 1500 UT 31st December 1968.

Correction. In the table of Standard Frequency Transmissions for June which was published in the August 1974 Journal (page 406) there is an error in the column showing Deviations from Nominal Frequency for GBR. The figure for 27th June should read 0 and not 0.1.

IERE Library

A Bulletin for Members

Do YOU ever use the Library ?

As a member of the IERE, this is one of the services for which you pay your subscription. Even if you do already use the Library, you may nevertheless not be aware of all the services which are offered by it.

Existing Services for Members

In order to keep abreast of the ever-swelling flood of relevant published information which threatens to engulf him, the electronic engineer needs to make full use of an extensive collection of recent material, arranged for ease of reference and retrieval.

This is where the IERE Library can help you. The existing services include:

1. Books for loan (in the U.K.) by personal call or by post. All except reference books are available on loan to members, normally for 4 weeks, renewable on application to the Librarian.

2. Telephone and postal enquiries of all kinds can be dealt with when a personal visit is not possible.

3. Lists of recent additions to the Library are printed in *The Radio and Electronic Engineer*.

4. Select bibliographies on specific subjects can be compiled on request for researchers, and information searches carried out.

5. Inter-library lending brings the stock of numerous other libraries, including the British Library, within reach of users. Most books and periodical articles not in stock can be borrowed for the use of members.

6. Photo-copies of articles in journals held in the Library can be made on request, in accordance with the Copyright regulations. A charge of 5p per sheet is made to cover the cost of this service.

New Librarian

Appointed in July, Mrs. S. A. Clarke is engaged in reorganizing existing materials, increasing the stock, and trying to encourage a greater use of the Library.

Reorganization

You may be interested to know about some of the projects currently in progress for the reorganization of the Library:

(a) Compilation of a list of periodicals holdings, with details of length of files. Copies will be available to members on request when it is completed.

(b) Reorganization of the books on the shelves and of the card catalogue.

(c) Construction of a new subject index to the collection, to facilitate reference to the catalogue.

(d) A general reference collection is being built up.

The completion of these and other necessary modernizations will take about two years.

Comments

Your comments about the Library, and any suggestions you may have for additional services which it may be useful to develop, will be welcomed by the Librarian.

Archives of Science and Technology

The National Archive for Electrical Science and Technology (NAEST) was founded in November 1973 by the Council of the Institution of Electrical Engineers. It aims to fulfil the need for a national information centre to aid the electrical and electronics industry and profession in its concern to preserve, record and, where necessary, store material of historic interest. The National Archive with its panel of experts, selected from eminent academic and professional organizations, will locate existing material judged by them to be of future archival value within the sphere of electrical science and technology. This material will be available for the use of IEE members, scholars and the public.

Another body concerned with the preservation of documents is the Contemporary Scientific Archives Centre at Oxford. In 1967 the Royal Society and the Royal Commission

on Historical Manuscripts established a Joint Committee on Scientific and Technological Records under the Chairmanship of the late Sir Harold Hartley. Subsequently, it was recognized that a need existed for a centre to locate, preserve and make accessible the personal papers of contemporary scientists and technologists. A generous grant, from the Wolfson Foundation supplemented by further grants from other bodies, including the MacRobert Trusts and CEI, made it possible to launch the project for, in the first instance, three years. Mrs. M. M. Gowing, who was appointed Professor of History of Science at Oxford University in 1972, is the Centre's Director. Work at the Centre is supervised by a small Management Committee but all major policy decisions are referred to the full Joint Committee on which CEI is represented by its Secretary, Mr. M. W. Leonard.

Recent Accessions to the Library

This list of additions to the Library covers the month of August 1974. With the exception of titles marked 'REF', which are for reference in the Library only, these books may be borrowed by members in the British Isles by personal call or by post. Information on loan conditions can be obtained from the Librarian, Mrs. S. A. Clarke. The dates shown in brackets refer to reviews or shorter notices which have appeared in *The Radio and Electronic Engineer*.

New Periodical Subscriptions

'Aslib Monthly Book List'. Started with January 1974 issue. (12 issues p.a.) REF.

'Her Majesty's Ministers and Senior Staff in Public Departments'. Started with July 1974 issue. (5 issues p.a.) REF.

General Reference Works

'International list of periodical title word abbreviations.' *A.N.S.C. for UNISIST/ICSU-AB Working Group on bibliographical descriptions*, 1970. REF.

Shiers, George

'Bibliography of the history of electronics.' *Scarecrow Press, USA*, 1972. REF.

'Non-book materials cataloguing rules.' *Council for Educational Technology for the United Kingdom, with the Library Association*, 1974. 2nd ed. REF.

'Whitaker's Almanack.' *J. Whitaker & Sons*, 1974. REF.

'BLL Conference Index 1964-1973.' *British Library Lending Division*, 1974. REF.

Gowers, Sir Ernest

'The complete plain words.' (Revised by Sir Bruce Fraser). *HMSO*, 1973. 2nd ed. REF.

Collins, F. Howard

'Authors and printers dictionary,' revised by Stanley Beale. *Oxford University Press*, 1973. REF.

'Hart's Rules for Compositors and Readers at the University Press, Oxford.' *Oxford University Press*, 1970. REF.

'Publishers' International Year Book.' World directory of book publishers. *A. P. Wales*, 1973. 6th ed. REF.

'World Directory of Booksellers.' *A. P. Wales*, 1970. REF.

'Concise Oxford Dictionary of Quotations.' *Oxford University Press*, 1972. (Paperback). REF.

Mathematics

Vajda, S.

'Theory of linear and non-linear programming.' *Longman*, 1974.

Engineering

'The Engineer Buyer's Guide.' *Morgan-Grampian (Publishers) Ltd.*, 1974 ed. REF.

Control Theory

Towill, D. R.

'Transfer function techniques for control engineers.' *Iliffe*, 1970.

Electrical Engineering

Kay, L.

'The design and evaluation of a sensory aid to enhance spatial perception of the blind.' Department of Electrical Engineering, University of Canterbury, Christchurch, New Zealand. (Electrical engineering report no. 21, January 1973).

'Guide to the repair of printed board assemblies.' *Electronic Engineering Association*, 1961.

'The International system of units (SI).' National Physical Laboratory. *HMSO*, 1973. Ed. Chester H. Page and Paul Vigoureux. REF.

'Capacitor guide.' *Electronic Engineering Association*, no date.

Electronics

Long, William E. and Evans, Paul L.

'Electronic principles and circuits: an introduction to electronics for the technician.' *Wiley*, 1974.

Bannister, B. R. and Whitehead, D. G.

'Fundamentals of digital systems.' *McGraw-Hill*, 1973. [April 1974].

'A solid state of progress.' (Illustrations). *Fairchild Camera and Instrument Corporation*, 1974.

'Product guide.' *Electronic Engineering Association*, 1974. REF.

McCray, James A. and Cahill, Thomas A.

'Electronic circuit analysis for scientists.' *Wiley*, 1973.

Sinclair, Ian R.

'Understanding electronic circuits.' *Fountain Press*, 1973.

Sinclair, Ian R.

'Understanding electronic components.' *Fountain Press*, 1972.

Semiconductor Devices

'Linear integrated circuit D.A.T.A. book.' *D.A.T.A., Inc.*, Spring 1974 ed. REF.

'Digital integrated circuit D.A.T.A. book.' *D.A.T.A., Inc.*, Spring 1974 ed. REF.

'Semiconductor application notes D.A.T.A. book.' *D.A.T.A., Inc.*, Autumn 1974 ed. REF.

'Semiconductor diode D.A.T.A. book.' *D.A.T.A., Inc.*, Autumn 1974 ed. REF.

'Semiconductor heat sink, socket and associated hardware D.A.T.A. book.' *D.A.T.A., Inc.*, 1974-75 ed. REF.

'Thyristor D.A.T.A. book.' *D.A.T.A., Inc.*, Spring 1974 ed. REF.

'Transistor D.A.T.A. book.' *D.A.T.A., Inc.*, Spring 1974. REF.

'MSI-LSI Memory D.A.T.A. book.' *D.A.T.A., Inc.*, Spring 1974 ed.

'Guide to the servicing and testing of electronic equipment containing semiconductor devices.' *Electronic Engineering Association*, 1962.

Jowett, C. E.

'Semiconductor devices: testing and evaluation.' *Business Books*, 1974.

Electronic Tubes

'Microwave tube D.A.T.A. book.' *D.A.T.A., Inc.*, Spring 1974 ed. REF.

INSTITUTION OF ELECTRONIC AND RADIO ENGINEERS

Applicants for Election and Transfer

THE MEMBERSHIP COMMITTEE at its meetings on 28th December 1973, 19th September and 8th October 1974 recommended to the Council the election and transfer of 27 candidates to Corporate Membership of the Institution and the election and transfer of 20 candidates to Graduateship and Associateship. In accordance with Bye-law 23, the Council has directed that the names of the following candidates shall be published under the grade of membership to which election or transfer is proposed by the Council. Any communication from Corporate Members concerning those proposed elections must be addressed by letter to the Secretary within twenty-eight days after the publication of these details.

Meeting: 28th December 1973 (Membership Approval List No. 195)

GREAT BRITAIN AND IRELAND

CORPORATE MEMBERS

Transfer from Graduate to Member

CAUL, Desmond James. *Canterbury, Kent.*
COLLINS, Edwin Thomas. *Maidstone, Kent.*
HARPER, John Martin. *Hitchin, Herts.*
HUNTER, Kenneth George. *Prenton, Birkenhead.*
MANNION, Michael Halford. *Surbiton, Surrey.*
O'HARA, Kenneth Alwyn. *Southfields, London SW18.*
OWEN, William Charles. *Weston, Bath.*

SNOXELL, Michael Peter. *Nr. Luton, Beds.*
SOAMES, Michael Richard. *Fulbourn, Cambridge.*
SORENTI, Gino. *Welwyn, Herts.*
STEVENS, Denis James. *Reading, Berks.*
SWAIN, Michael Charles. *Chelmsford, Essex.*
TAYLOR, Jack. *Chelmsford, Essex.*
TAYLOR, Michael John. *Slough, Bucks.*
UDALL, Brian. *Chester, Cheshire.*
WALLACE, Graham Robert. *Bromley, Kent.*
WOOD, John Michael. *Bournemouth, Hants.*

Transfer from Associate to Member

ROGERS, Roy Percy. *Bexleyheath, Kent.*

OVERSEAS

CORPORATE MEMBERS

Transfer from Graduate to Member

CHEESEBROUGH, John Sydney. *Rotterdam, Holland.*
OKINE, Godfrey Omani. *Accra, Ghana.*
OLUBAJO, Lawrence Olusesam. *Lagos, Nigeria.*
PATEL, Govindbhai Parbhuhai. *California, U.S.A.*
STREATER, Barry Brangwyn. *Brussels, Belgium.*

Direct Election to Member

CORNISH, Leonard Southward. *Hong Kong.*

Meeting: 19th September 1974 (Membership Approval List No. 196)

GREAT BRITAIN AND IRELAND

NON-CORPORATE MEMBERS

Transfer from Student to Graduate

WELLS, John Robert. *Warrington, Cheshire.*
WILSON, Paul Frederick. *Lowestoft, Suffolk.*

Direct Election to Graduate

MAHMOOD, Fazal Akber. *Glasgow.*
WANSTALL, Geoffrey Patrick. *Deal, Kent.*

STUDENT REGISTERED

AYLING, Stephen David. *Littlehampton, Sussex.*

OVERSEAS

NON-CORPORATE MEMBERS

Direct Election to Graduate

CHIMNI, Ranjit Singh. *Karnataka, India.*
CHUA, Thai Nguan. *Singapore 12.*
NG, Ho Shing. *Hong Kong.*

Direct Election to Associate

CHOW, Ying Poi. *Singapore.*

Transfer from Student to Associate Member

HOR, Kean Beng. *Sabah East Malaysia.*

Direct Election to Associate Member

FALCONAKIS, John. *Athens, Greece.*

STUDENTS REGISTERED

CHAN, Kam Tong. *Kowloon, Hong Kong.*
HO, Wing Leung. *Hong Kong.*
VANGALA, Krishnamachari. *Trimulgherry, Secunderabad.*

Meeting: 8th October 1974 (Membership Approval List No. 197)

GREAT BRITAIN AND IRELAND

CORPORATE MEMBERS

Transfer from Graduate to Member

FREE, Charles Edward. *Leighton Buzzard, Beds.*
BAL, Suwanna (Mrs.) *London.*

Direct Election to Member

STEVENSON, John Kenneth. *Wembley, Middlesex.*

NON-CORPORATE MEMBERS

Transfer from Student to Graduate

CARVER, John Ernest Llewellyn. *Bridgend, Glam.*

Transfer from Graduate to Associate Member

SMITH, Bryan Ernest. *Winscombe, Avon.*

Direct Election to Associate Member

GALLEY, Robert Douglas. *Slough, Bucks.*
OLAOYA, Abimbola. *London.*
PARRY, Leslie John. *Bracknell, Berks.*

STUDENTS REGISTERED

BURGIN, Roger Arthur. *Middlesex.*
CANN, Christopher Stuart. *Esher, Surrey.*
LAZENBURY, Michael Philip Andrew. *Weston-Super-Mare, Avon.*
SIBBALD, Alastair. *Newcastle-upon-Tyne.*
TABNER, William Michael. *Camberley, Surrey.*
ZAURO, Mohammed Umar. *London W.5.*

OVERSEAS

NON-CORPORATE MEMBERS

Transfer from Student to Graduate

ALABI, Gabriel Adewumi. *Lagos, Nigeria.*
NGU, Anthony Tung Woo. *Sarawak, Malaysia.*

Direct Election to Graduate

FONSEKA, Manannaidelage, Mark Antony Leo. *Negombo, Sri-Lanka.*

Transfer from Graduate to Associate Member

RODNEY, Eric Phoenix. *Guyana, South America.*

Direct Election to Associate Member

CALLIS, Anthony John. *Mufulira, Zambia.*

STUDENTS REGISTERED

CHENG, SUM (Samuel). *Kowloon, Hong Kong.*
CHEUNG, Shiu Keung. *Kowloon, Hong Kong.*
CHEW, Teng Seng. *Singapore.*
DISSANAYAKE, Tissa. *Sri-Lanka.*
GOH, Poh Heng. *Singapore.*
HUI, Wai Keung. *Kowloon, Hong Kong.*
JAYASURIYA, Dangalla Appuhamilage Harisinghe Abhayasekera. *Sri-Lanka.*
LEUNG, Sheung Ming. *Hong Kong.*
LEUNG, Shing Tak. *Kowloon, Hong Kong.*
LEUNG, Hau-Kin. *Kowloon, Hong Kong.*
MUTHUGALA, Shanta Laksman Pushpakumar. *Sri-Lanka.*
NG, Stephen Cho-Leung. *Kowloon, Hong Kong.*
SILVA, Chandramarakkhalage Lucas Anthony Emmanuel. *Sri-Lanka.*
SO, Ka Wing Jackson. *Kowloon, Hong Kong.*

Addendum

Meeting: 7th May 1974, List No. 184 published June 1974

OVERSEAS

CORPORATE MEMBERS

Direct Election to Member

FIGARADO, Father Paul. *Kerala, India.*

Corrigendum

Meeting: 9th July 1974, List No. 190 published August 1974

GREAT BRITAIN AND IRELAND

NON-CORPORATE MEMBERS

Direct Election to Associate

COOPER, Anthony Henry George. *Southend on Sea, Essex.*

Forthcoming Institution Meetings

London Meetings

Wednesday, 27th November

AEROSPACE, MARITIME AND MILITARY SYSTEMS GROUP

The US Navy Navigation Satellite System
By W. F. Blanchard (*Redifon Telecommunications*)

IERE Lecture Room, 6 p.m. (Tea 5.30 p.m.)
The lecture commences with a description of the *Transit* Satellite System and then considers the use of these satellites in respect of marine navigation. A demonstration of equipment working direct from a satellite will be given.

Thursday, 28th November

AUTOMATION AND CONTROL SYSTEMS GROUP
CAD of Type 2 Phase Lock Loops

By P. Atkinson and A. J. Allen (*University of Reading*)

IERE Lecture Room, 6 p.m. (Tea 5.30 p.m.)
The practical advantages of type 2 phase-locked loops compared with type 1, and digital as opposed to continuous are well known. Although such devices find great application in the instrumentation and telecommunications fields, little attention has been paid to their design methodology, because conventional forms of analysis are apparently of little value in this connection. The lecture will review the problem from a fundamental viewpoint taking a typical commercial digital phase-locked loop as an example. The study shows that stable operation of the loop over its operating range may be achieved using small-signal frequency response techniques which allow for both the effect of sampling and the expected changes in loop gain. A new universal chart will be described which allows the rapid determination of the optimum loop gain and filter characteristics required to meet a given specification. It will be shown how the performance may be verified using a specialized time-domain computer simulation which allows large signal step responses and ultimate settling time to be determined. A numerical design example will be described in detail showing how the actual circuit component values are determined. The connection between system bandwidth and ultimate settling time for the digital phase-locked loop will also be briefly discussed.

Wednesday, 11th December

EDUCATION AND TRAINING GROUP

Colloquium on THE GRADUATE ELECTRONIC ENGINEER IN BRITAIN AND EUROPE POSTPONED—New date to be announced

Wednesday, 18th December

AEROSPACE, MARITIME AND MILITARY SYSTEMS GROUP

Colloquium on ELECTRONICS AND THE MOTOR VEHICLE

IERE Lecture Room, 10 a.m.
Advance registration necessary. For further details and registration forms, apply to Meetings Secretary, IERE.

Wednesday, 8th January

AUTOMATION AND CONTROL SYSTEMS GROUP

Train Control Developments on British Rail
By J. W. Birkby (*British Railways Board*)

IERE, Lecture Room, 6 p.m. (Tea 5.30 p.m.)

Monday, 13th January

JOINT IEE/IERE MEDICAL AND BIOLOGICAL ELECTRONICS GROUP

A Review of Electron Microscopy

By Dr. V. E. Cosslett, F.R.S. (*University of Cambridge*)

IEE, Savoy Place, London WC2, 5.30 p.m. (Tea 5 p.m.)

Wednesday, 15th January

JOINT MEETING OF AEROSPACE, MARITIME AND MILITARY SYSTEMS GROUP AND ROYAL INSTITUTE OF NAVIGATION

Colloquium on ADVANCES IN AIRBORNE EQUIPMENT FOR NAVIGATION AND FLIGHT CONTROL

Royal Aeronautical Society, 4 Hamilton Place, London W1, 10.30 a.m.

Advance registration necessary. For further details and registration forms apply to Royal Institute of Navigation, 1 Kensington Gore, London SW7.

Topics to be considered include trends in the design of flight control equipment, effects of miniaturization in airborne computers, the question of the boundary between hardware and software in such computers, and some aspects of the present state of the art of inertial and associated equipment.

Wednesday, 15th January

COMMUNICATIONS GROUP

Good Quality Reception from Medium-wave Broadcasting

By Dr. R. C. V. Macario (*University College of Swansea*)

IERE Lecture Room, 6 p.m. (Tea 5.30 p.m.)

Following an introductory background to the present and predicted state of the m.f. broadcast band, techniques for improving the quality of reception of the transmitted broadcasts will be described and demonstrated:

(1) Synchronous detection of local broadcasts. (2) Synchronous detection of all broadcasts. (3) PICOR systems of bandwidth improvements. (4) Stereo possibilities.

Tuesday, 21st January

JOINT IEE/IERE COMPUTER GROUPS

Designing Machines for People

By Dr. C. R. Evans (*NPL*)

IEE, Savoy Place, London WC2, 5.30 p.m. (Tea 5 p.m.)

Wednesday, 29th January

JOINT IEE/IERE MEDICAL AND BIOLOGICAL ELECTRONICS GROUP

Sensing, Sizing and Sorting of Cells: the Laser Sorter

By D. F. Capellaro (*University College London*)

IEE, Savoy Place, London WC2, 5.30 p.m. (Tea 5 p.m.)

Wednesday, 29th January

COMMUNICATIONS GROUP

Speech Engineering

By Dr. A. J. Fourcin (*University College London*)

Haldane Theatre, Wolfson House, Stephenson's Way (off Euston Street), London NW1, 6 p.m. (Tea 5.30 p.m.)

Kent Section

Wednesday, 27th November

Problem Solving and Decision Making in Management

By P. J. Curra

Lecture Theatre 18, Medway and Maidstone College of Technology, Maidstone Road, Chatham, at 7 p.m.

Tuesday, 21st January

Quadraphonics

By Dr. K. Barker (*University of Sheffield*)

Lecture Theatre 18, Medway and Maidstone College of Technology, Maidstone Road, Chatham, 7 p.m.

Thames Valley Section

Thursday, 5th December

JOINT MEETING WITH IEE

The Application of Electronics in Telephone Exchange Switching

By F. W. Croft (*Post Office*)

J. J. Thomson Physical Laboratory, University of Reading, Whiteknights Park, Reading, 7.30 p.m.

The lecture will give an outline of the Post Office electronic telephone exchange widely used in public service, and touch briefly on a new system for large electronic exchanges. Electronic equipment systems used to steer calls over the electro-mechanically stored program control processors will also be covered.

Thursday, 23rd January

Optoelectronics Devices

By M. Miller (*Texas Instruments*)

J. J. Thomson Physical Laboratory, University of Reading, Whiteknights Park, Reading, 7.30 p.m.

Southern Section

Wednesday, 4th December

JOINT MEETING WITH IEE

Application of New Bipolar Integrated Circuits

By P. Krebs (*Ferranti*)

Lanchester Theatre, Southampton University, 6.30 p.m.

Wednesday, 11th December

Recent Advances in Digital Circuit Fault Diagnosis

By Dr. R. G. Bennetts (*Southampton University*)

Southampton College of Technology, East Park Terrace, 7.30 p.m.

South Western Section

Wednesday, 11th December

JOINT MEETING WITH IEE

Computation of Courses for Sailing Yachts

By J. Elliot (*EMI Electronics*)

No. 4 Lecture Theatre, School of Chemistry, University of Bristol, 7 p.m. (Tea 6.30 p.m.)

This presentation will be based on the paper published in the December 1973 Journal which gained the author the Institution's Wheatstone Premium.

Tuesday, 14th January

JOINT MEETING WITH IEE

Electronic Techniques in Archaeology

By Dr. E. T. Hall (*Department of Archaeology, Oxford University*)

The College, Regent Circus, Swindon, 6.15 p.m.

Wednesday, 22nd January

Mobile Radio in the Era of Spectrum Congestion

By Professor W. Gosling (*University of Bath*)

Room 4 E 3.10, University of Bath, 7 p.m.

South Midland Section

Thursday, 5th December

High Fidelity Sound Reproduction

By R. L. West (*Polytechnic of North London*)

The Foley Arms, Malvern, 7.30 p.m.

This meeting will be a lecture/demonstration and will trace the development of the subject from early beginnings, highlighting important landmarks en route. It will include demonstrations of some of the most recent equipment and techniques.

Monday, 13th January

JOINT MEETING WITH IEE

Sound Control

By G. A. C. Watts (*Neve Electronic Laboratories*)

B.B.C. Club, Evesham, 7.30 p.m.

South Wales Section

Wednesday, 11th December

Reed Relay Telephone Exchanges

By A. N. Harris (*Wales Telecommunications Board*)

Department of Applied Physics and Electronics, UWIST, Cardiff, 6.30 p.m. (Tea 5.30 p.m.)

Wednesday, 15th January

Training of the Euro-Engineer

By F. R. J. Langridge (*Engineering Employers' Federation*)

Department of Applied Physics and Electronics, UWIST, Cardiff, 6.30 p.m. (Tea 5.30 p.m.)

West Midland Section

Monday, 2nd December

JOINT MEETING WITH IEE

Sonar and Underwater Acoustic Communications

By V. G. Welsby (*University of Birmingham*)

PO Training Centre, Duncan Hall, Stone, 7 p.m.

A review of modern techniques based on the use of sound waves in the sea and in lakes, rivers, etc. is given and systems for diver communication and navigation are described. High resolution sonars, sometimes using focused acoustic arrays, have uses which range from the study of the behaviour of fish shoals to aiding police searches in muddy canals. Acoustic telemetry is used to control submersible vehicles and to channel collected information back to the surface. Acoustic waves are used to count migrating fish in rivers.

Wednesday, 15th January

JOINT MEETING WITH ROYAL TELEVISION SOCIETY

Status of British Broadcasting

By C. B. Wood (*B.B.C.*)

ATV Centre, Birmingham, 7 p.m.

East Midland Section

Wednesday, 4th December

Computer Recognition of Handwritten Numbers

By Dr. D. J. Quarmby (*Loughborough University*)

Lecture Theatre 'A', Physics Block, Leicester University, 7 p.m. (Tea 6.30 p.m.)

Thursday, 16th January

Digital and Computer Control of Industrial and Research Robots

By Dr. A. Pugh (*Nottingham University*)
Nottingham University, 7 p.m. (Tea 6.30 p.m.)

Merseyside Section

Wednesday, 11th December

Electronics in Motor Vehicles

By L. Phoenix (*Lucas Electrical*)

Department of Electrical Engineering and Electronics, University of Liverpool, 7 p.m. (Tea 6.30 p.m.)

Electronics may replace existing vehicle equipment but perform with greater reliability and longer life or may make possible completely new functions.

North Western Section

Thursday, 12th December

JOINT MEETING WITH IEE

The Development of Measurements in Radio

By D. E. Waddington (*Marconi Instruments*)

Lecture Theatre R/H10, UMIST, 6.15 p.m. (Tea 5.45 p.m.)

Thursday, 16th January

Quadraphonics

By Dr. K. Barker (*University of Sheffield*)

Renold Building, UMIST, 6.15 p.m.

North Eastern Section

Tuesday, 17th December

Noise: Some Problems Solved and Unsolved

By Professor D. A. Bell (*University of Hull*)

Main Lecture Theatre, Ellison Building, Newcastle Upon Tyne Polytechnic, Ellison Place, 6 p.m. (Tea 5.30 p.m.)

Wednesday, 15th January

Electronic Aids for Medical and Biological Studies

By Dr. E. T. Powner (*UMIST*)

Y.M.C.A., Ellison Place, Newcastle-upon-Tyne, 6 p.m. (Tea 5.30 p.m.)

Yorkshire Section

Wednesday, 4th December

Electronics Instrumentation for Respiratory Monitoring

By C. L. Smith (*Glamorgan Polytechnic*)

Barnsley College of Further Education, 6.30 p.m. (Tea 6 p.m.)

Scottish Section

JOINT MEETING WITH IEE

Mini-Computers—wherever next?

M. Judd (*Data General*)

Monday, 9th December

Whitehall Restaurant, 59 Renfield Street, Glasgow, at 7 p.m.

Tuesday, 10th December

South of Scotland Electricity Board Showrooms, 130 George Street, Edinburgh at 6 p.m.

Technical News

Waveguides for X-Rays

An X-ray version of a basic component in 'integrated' optics technology—the thin-film waveguide—has been reported by Eberhard Spiller and Armin Segmuller of International Business Machines Corporation's Thomas J. Watson Research Centre. The new device offers diverse possibilities for exploiting the extremely short wavelengths and high energy characteristics of the X-ray region of the electromagnetic spectrum. Among the potential applications that have been suggested are 'lightpipes' to guide X-rays to needed locations, X-ray focusing devices in miniaturized systems, and resonant cavities for X-ray lasers.

The X-rays sent through the new device have a wavelength of only $1/54$ angstroms in contrast to ordinary red light, which has wavelengths ranging from about 6500 \AA to 7500 \AA . Thus, the 0.3 millimetre-long waveguides so far achieved are equivalent, in wavelength terms, to red-light waveguides a metre or more in length.

One of the reasons why integrated optics were not previously extended to shorter wavelengths was that, as the wavelength decreases through the visible spectrum and into the ultraviolet (beginning at about 3800 \AA), potential waveguide materials absorb radiation more and more strongly. Increasing absorption does not continue indefinitely, however. Beyond an absorption maximum at about 1000 \AA in the ultraviolet, absorption tends to grow progressively smaller—particularly in materials of low atomic weight—even though the refractive index increases. (This situation is in marked contrast to that which is found in the visible and long-wave ultraviolet region, where absorption losses tend to increase with higher indices of refraction.)

In building waveguides a relatively high index of refraction is important because the guiding material must have a higher index than that of the surrounding 'cladding' material. It is this condition which allows total internal reflexion at the film/cladding boundary and permits the light to zig-zag down the film in one or more different patterns or 'modes'. The experimental waveguides are constructed by sandwiching a layer of boron nitride 300 to 500 \AA thick between a substrate and cover layer of sapphire. A raised, thicker region of the cover layer defines the length of the boron nitride acting as a waveguide, the thinner regions on either side serving as areas for input and output of the X-rays.

Although the incident X-ray beam strikes the sapphire cover layer at such a shallow angle that it is reflected, the wave nature of X-rays allows a certain fraction of energy to penetrate the cover layer (if it is not too thick) and excite a waveguide mode in the boron nitride film. Under present conditions, one or the other of the two lowest modes can be excited, depending on the precise angle at which the X-ray beam is aimed at the sapphire cover layer.

Experimentally, the excitation is recognized by a dip in the intensity of the reflected beam when the angle of the incident beam is varied—by tiny fractions of a degree—and measured by a computer-controlled X-ray diffractometer. Experimental and theoretically calculated curves for intensity show a high degree of agreement.

To show actual propagation—not simply excitation—a series of experiments was performed in which peaks of X-ray emission from the output region of the sapphire cover layer were shown to correspond to dips in the intensity curve reflected from the input region. A fraction of the energy coupled into the boron nitride layer had evidently been

propagated through it, i.e. the layer had acted as a waveguide. (Critical beam angles and device dimensions are such that special precautions were required to shield the output region from the reflected part of the input beam, so that the output would not be swamped by the far more intense reflexion.)

Spiller and Segmuller state that an order-of-magnitude increase in propagation length is theoretically possible by using other materials, and that moderately flexible guidance of X-rays over several metres might be achieved by using capillary waveguides, fibres in which a tube of cladding would surround a long 'thread' of guiding material. In addition, by going to still shorter wavelengths, for which absorption losses are even smaller, guidance over yet greater distances should be possible.

Details of the X-ray waveguide are published in Spiller and Segmuller's paper in *Applied Physics Letters* for 15th January.

Photovoltaics and Solar Cells

The United Kingdom section of the International Solar Energy Society is preparing a report on the potential of solar energy in the country. In this connexion it is intended to give an account of present scientific, technical and production activities in the U.K. which cover the area of photovoltaic-effect solar cell investigations. In order that any significant sections of such work shall not be omitted, those engaged in it are requested to contact Professor P. T. Landsberg, Department of Mathematics, University of Southampton, giving a brief note on their activities.

Sound Subcarrier Signalling from Unattended Transmitters

The BBC have recently concluded satisfactory field-trials of a new method of transmitting digital monitoring information from unmanned transmitter sites. The system, developed by the Designs Department, uses differential phase modulation of an existing low-level subcarrier pilot signal which is radiated by the television sound transmitter for continuity monitoring. The system occupies a very narrow band of frequencies above the useful audio range and the mode of transmission, coupled with error protection in the transmitted message, provides a very rugged system which can operate even when the signals are degraded to the point where the vision and sound channels as such are unusable.

Israel's Need for Engineers

Far from having too many engineers, Israel must have still more if it is to become an industrial nation; and it cannot depend on immigrants to supply the need. This warning was sounded by the President of Technion, Amos Horev, who noted with concern the recent public debate over the high cost of advanced education, and stressed that the issue affected the very fate of the country. 'We are far, far away from having any surplus of technological skills. For defence, for industry and for the economy we must invest in advanced training of our youth, for immigrants, however welcome and valuable, are no alternative', he said.

Israel, with an average of only 1.5% of engineers in its industrial work force, was a long way from the saturation point in technical man-power. For the metals industry, to be sure, the proportion of engineers varied between 5 and 8% and in electronics it reached 12% .

Amos Horev cited as examples the Technion's Faculty of Aeronautical Engineering, which had enabled the aircraft industry to grow beyond expectation. However, industry on the whole had not grown nearly fast enough. An equally vital function of advanced training was research. 'If we reduce our investment in training, we'll be cutting off the branch we are sitting on.'